GNSS, SBAS essentials and Ionospheric Monitoring in detail

Based and updated from presentations prepared and performed by M. Hernández-Pajares

UPC-IonSAT res. group

[contact e-mail : manuel@ma4.upc.edu]

https://scholar.google.es/citations?user=Tm-DcsMAAAAJ&hl=en

(Colloquium On Atmospheric Remote Sensing Using The Global Positioning System, Boulder, CO, USA, June 20-July 2, 2004; Satellite Engineering Summer School, UPM, La Granja, Segovia, Spain, July 16, 2009; 40th COSPAR Scientific Assembly 2014, August 2-10, 2014, Moscow, Russia, and contributions from M. Hernández-Pajares, J.M.Juan, J.Sanz, M. García-Fernández, R. Orús-Pérez, P.Ramos, A. Aragón-Ángel, D.Salazar, A.García-Rigo, G. Olivares, among others)

UNIVERSITAT POLITÈCNICA DE CATALUNYA
BARCELONATECH

IonSAT

Outline

(1) Thin-shell model, local model, global model

(2) L4 linear combination, parameter estimation

(3) Result examples, Errors / Quality

UNIVERSITAT POLITÈCNICA
DE CATALUNYA
BARCELONATECH

Outline

- Introduction
- The Ionosphere
- Ionospheric effects on GPS.
- From Ionosphere First principles to GPS preprocessing
- Obtaining the electron content
  - ✓Using ground-based GNSS data (VTEC)
  - ✓Using space-based GNSS data as well (Ne)
    - Space-based and ground-based GNSS data
    - Ground-based GNSS and Ionosonde data.
- Ionospheric determination at regional/continental scale
- Determining the electron content at global scale
- Application Example: WARTK and WARTK-3
- Conclusions

UNIVERSITAT POLITÈCNICA DE CATALUNYA
BARCELONATECH

IonSAT

1. Global Navigation Satellite Systems essentials

"GNSS: All time, all weather, anywhere, passive electromagnetic trilateration; supported by many recent advances of Telecommunications, Mathematics and Physics"

How does GPS work?”

One of the solutions is not on the Earth surface.

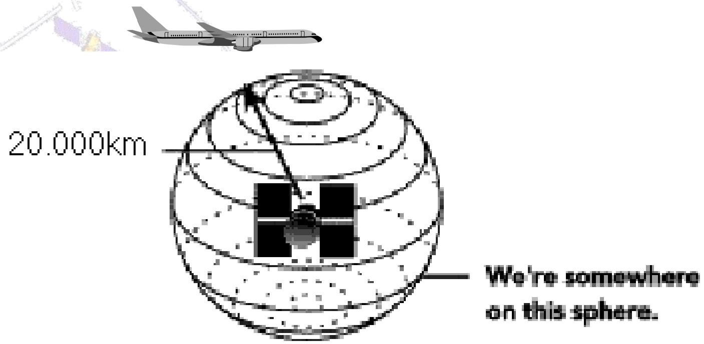

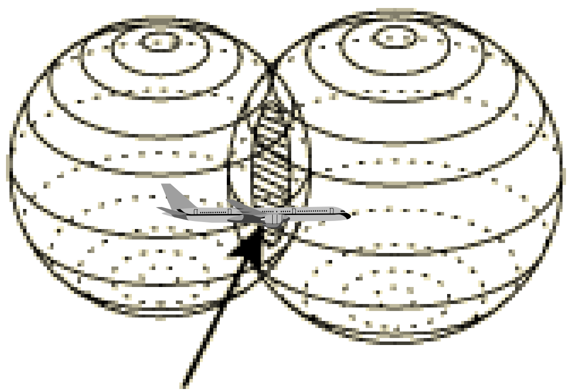

Two measurements puts us somewhere on this circle

Three measurements puts us at one of two points

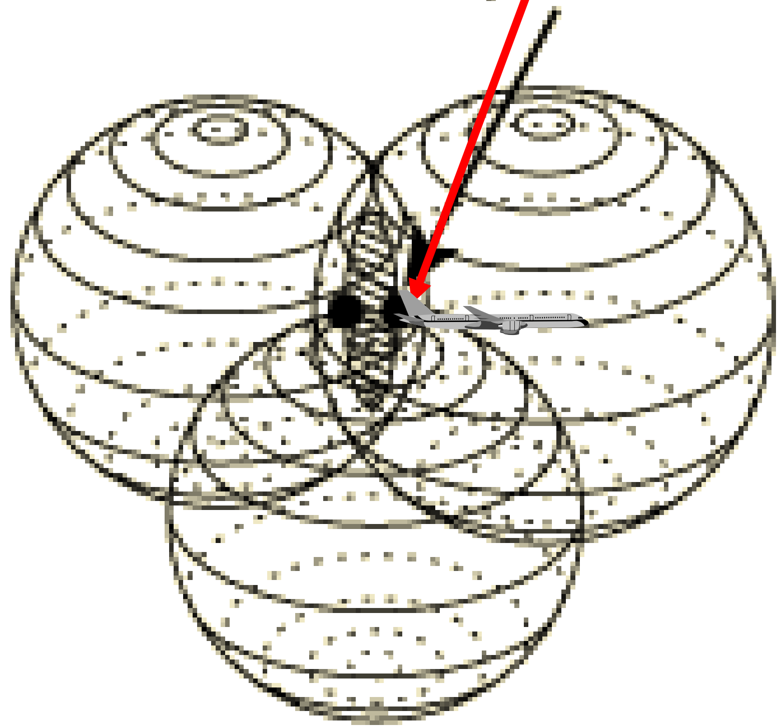

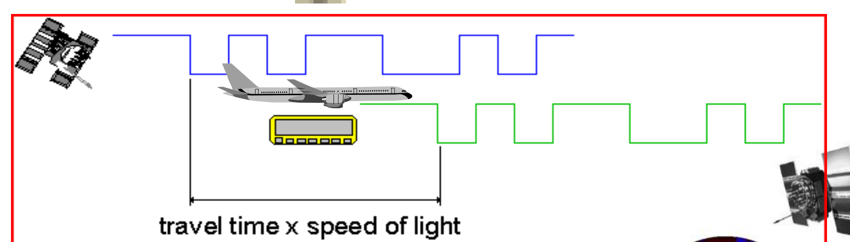

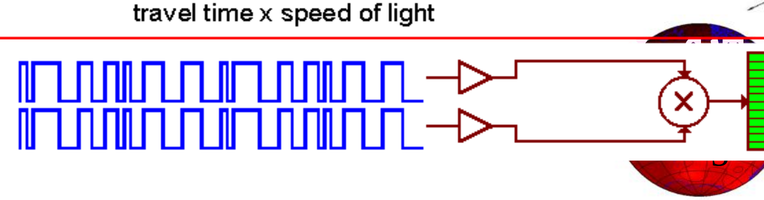

UNIVERSITAT POLITÈCNICA DE CATALUNYA
BARCELONATECH

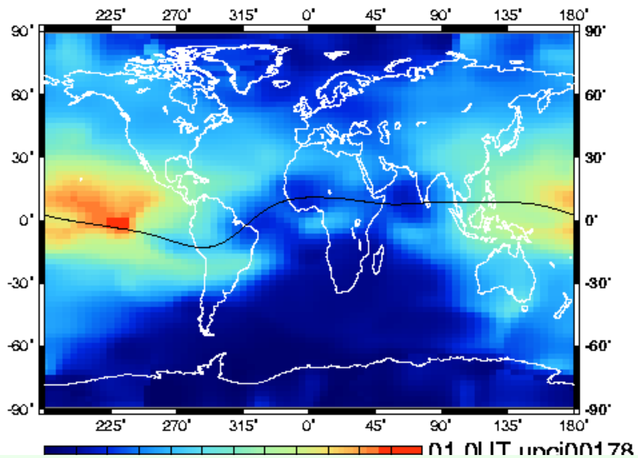

Atmospheric propagation: IONO, TROPO

Relativistic effects

MODEL:

Atmospheric propag., relativistic effects, clocks and instrum. delays are modeled and removed.

And the navigation equations are built

Main error sources

- GPS clocks << 300 km
- Relativistic effect <13m
- Instrumental delays ~1m
- Ionospheric delay 2-50m
- Tropospheric delay 2-10m
- Multipath <5m
- Thermal noise <2m

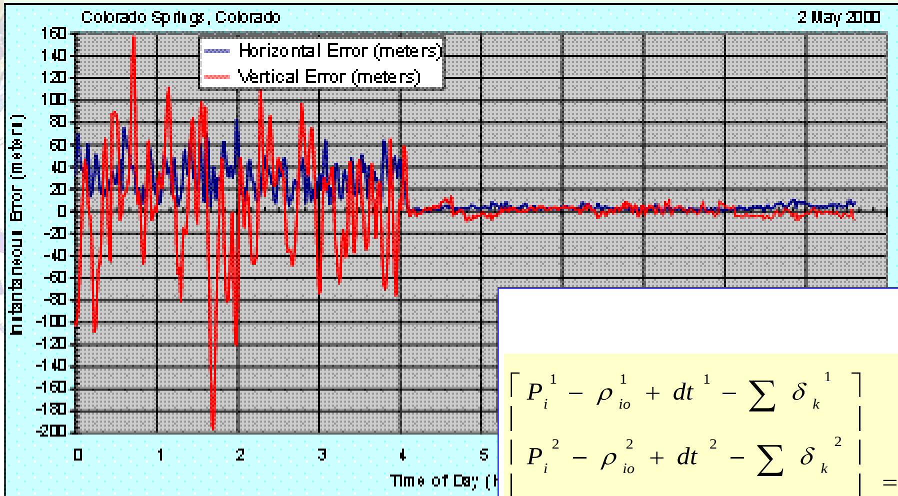

$$\begin{bmatrix} P_i^1-\rho_{io}^1+dt^1-\sum\delta_k^1 \\ P_i^2-\rho_{io}^2+dt^2-\sum\delta_k^2 \\ \cdots\cdots \\ P_i^n-\rho_{io}^n+dt^n-\sum\delta_k^n \end{bmatrix} = \begin{bmatrix} \frac{x_{io}-x^1}{\rho_{io}^1} & \frac{y_{io}-y^1}{\rho_{io}^1} & \frac{z_{io}-z^1}{\rho_{io}^1} & 1 \\ \frac{x_{io}-x^2}{\rho_{io}^2} & \frac{y_{io}-y^2}{\rho_{io}^2} & \frac{z_{io}-z^2}{\rho_{io}^2} & 1 \\ & \cdots\cdots\cdots & & \\ \frac{x_{io}-x^n}{\rho_{io}^n} & \frac{y_{io}-y^n}{\rho_{io}^n} & \frac{z_{io}-z^n}{\rho_{io}^n} & 1 \end{bmatrix} \begin{bmatrix} \Delta x_i \\ \Delta y_i \\ \Delta z_i \\ cdt_i \end{bmatrix}$$

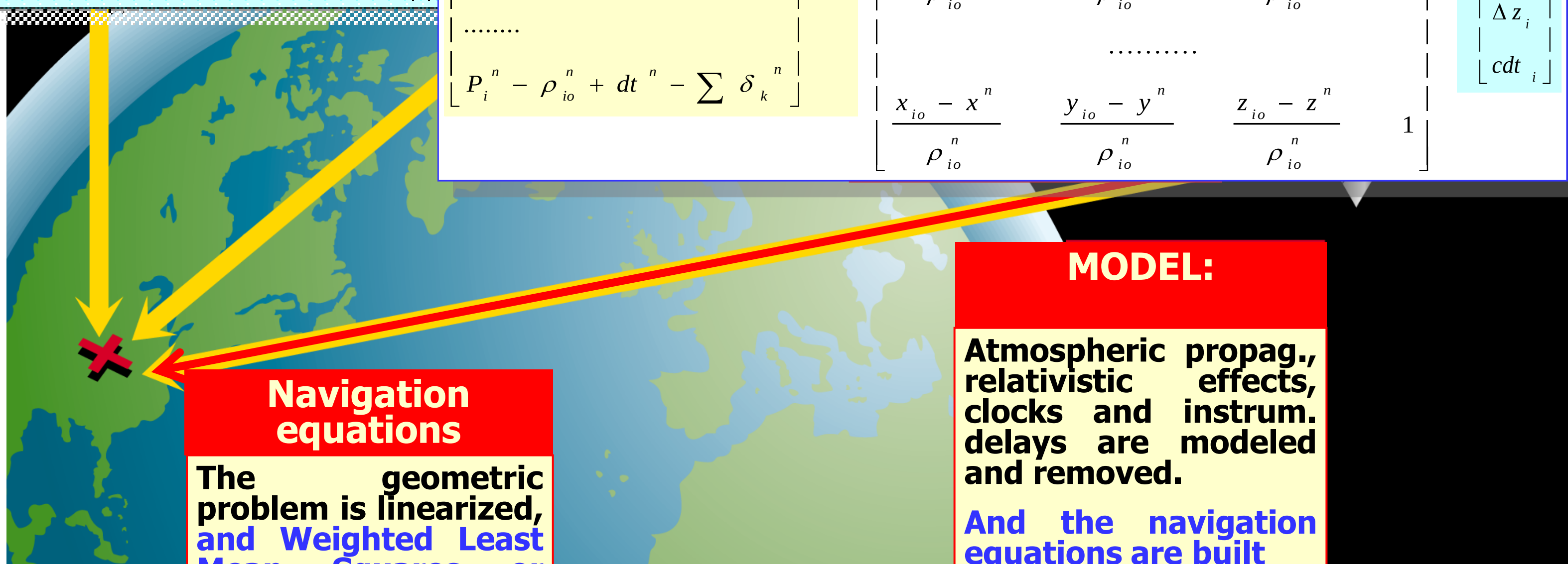

Navigation equations

The geometric problem is linearized, and Weighted Least Mean Squares or Kalman filter are used to compute the solution.

MODEL:

Atmospheric propag., relativistic effects, clocks and instrum. delays are modeled and removed.

And the navigation equations are built

UNIVERSITAT POLITÈCNICA DE CATALUNYA BARCELONATECH

IonSAT

How satellite navigation systems work

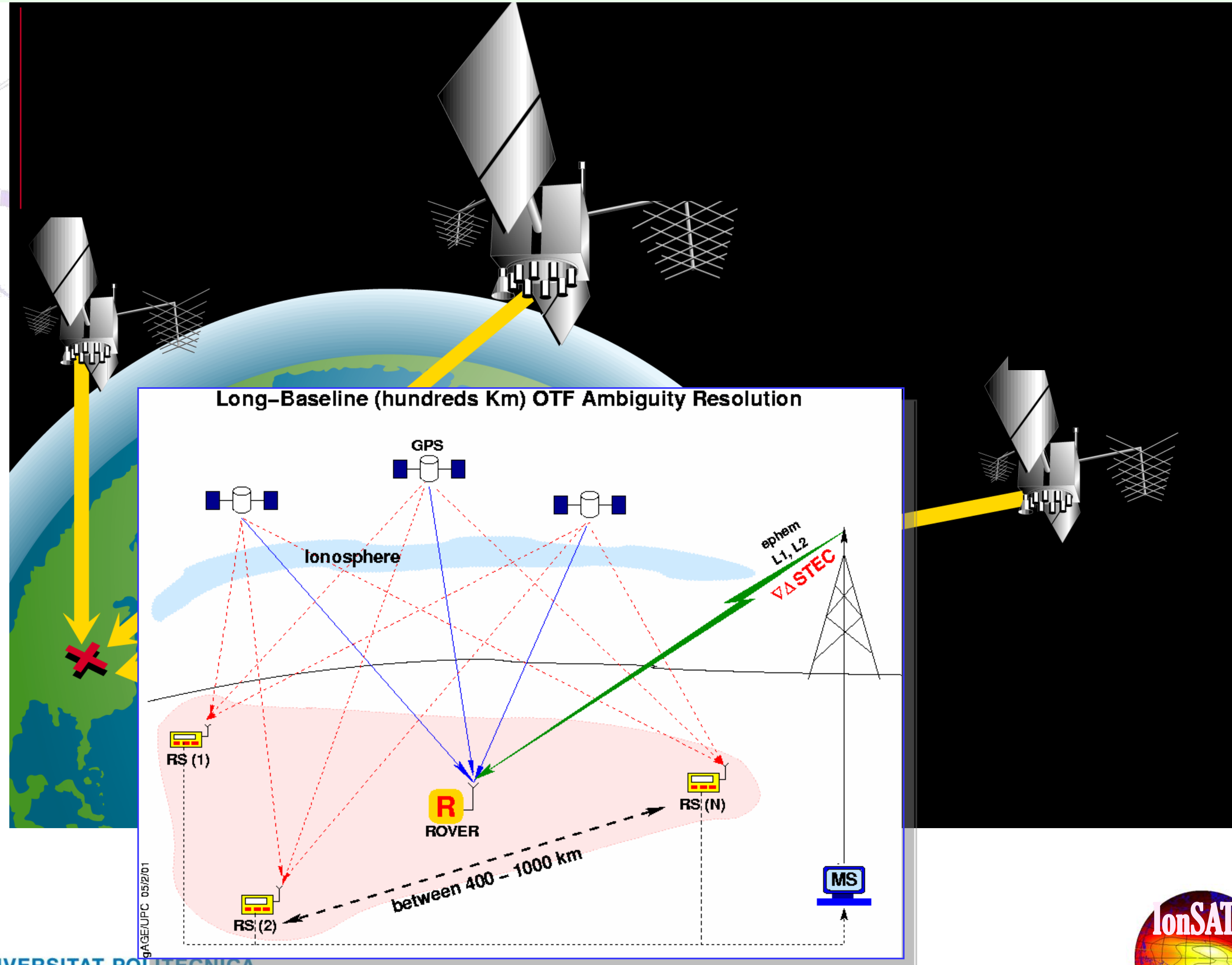

GPS segments

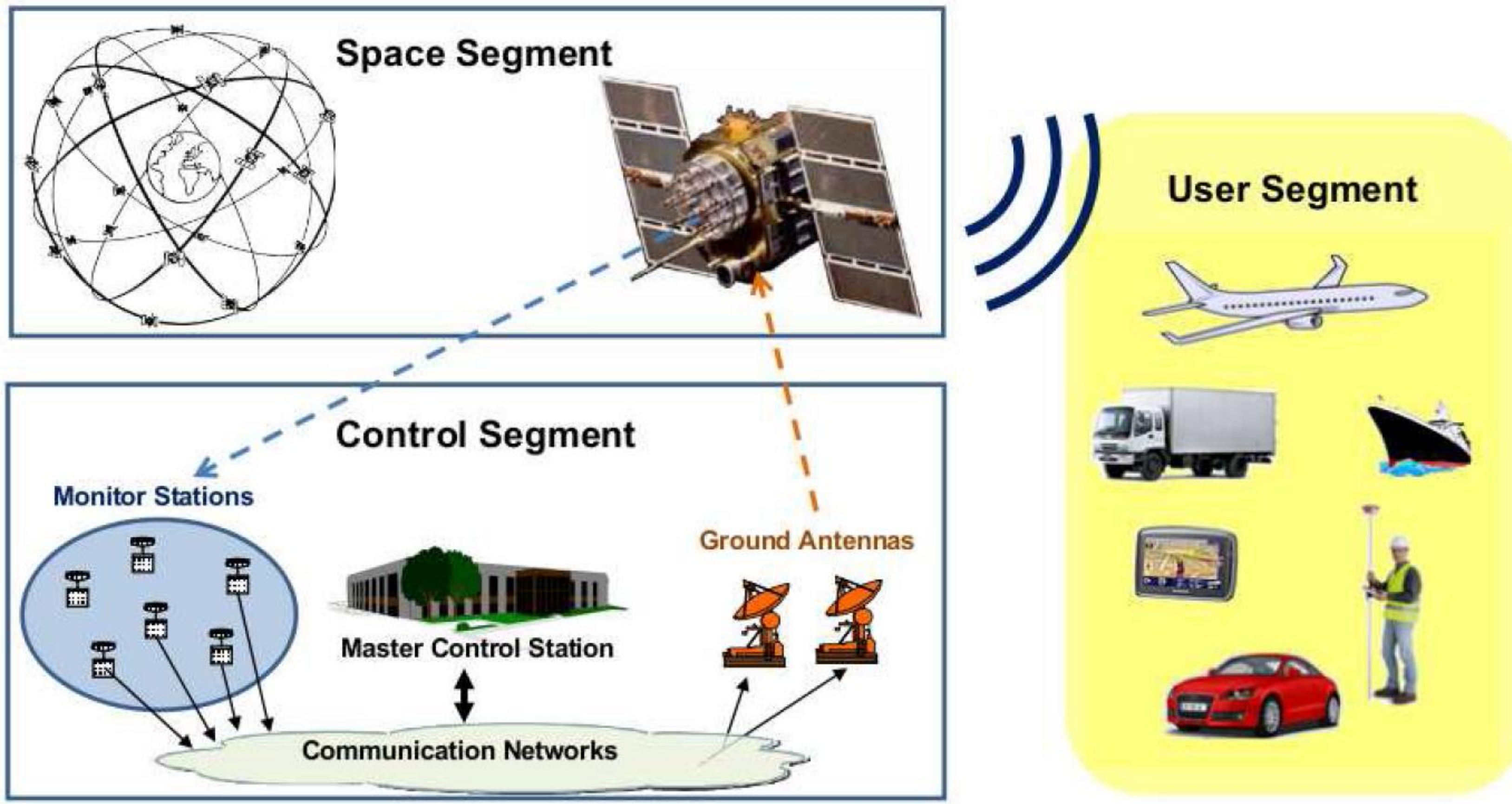

Space segment: Transmitting GPS satellites as excellent reference points (the orbits are highly predictable)

Control segment: Space State representation (providing clocks and orbits to the users, instead of raw data of the control segment stations –more suitable for worldwide usage-)

User segment: receivers from single-frequency code to dual-frequency phase and code measurements.

2. Essentials of the GNSS Augmentation concept, including EGNOS

"Giving navigation <u>integrity</u> , at civil aviation standards, by means of a control segment improved at continental scale"

UNIVERSITAT POLITÈCNICA DE CATALUNYA
BARCELONATECH

IonSAT

Augmentation concept

- To enhance the performance of the current GNSS (GPS) with additional information to:
  - Improve INTEGRITY via real-time monitoring
  - Improve ACCURACY via differential corrections
  - Improve AVAILABILITY and CONTINUITY

- Satellite Based Augmentation Systems (SBAS)
  - E.g., WAAS, **EGNOS**, MSAS
- Ground Based Augmentation Systems (GBAS)
  - E.g., LAAS
- Aircraft Based Augmentation (ABAS)
  - E.g., RAIM, Inertials, Baro Altimeter

UNIVERSITAT POLITÈCNICA DE CATALUNYA BARCELONATECH

IonSAT

Why Augmentation Systems?

- Current GPS/GLONASS Navigation Systems cannot met the Requirements for All Phases of Flight:
  - Accuracy
  - Integrity
  - Continuity
  - Availability

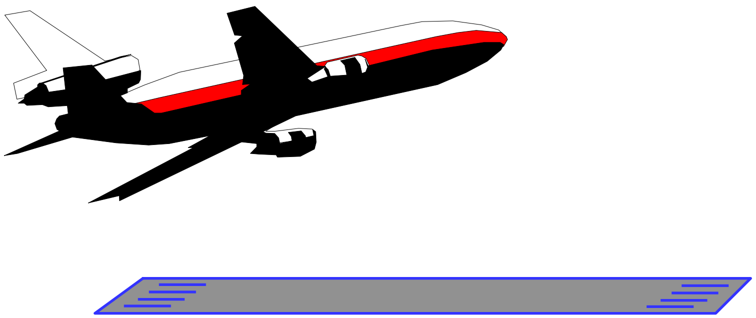

- Marine and land users will also require some sort of augmentation for improving the GPS/ GLONASS performances.

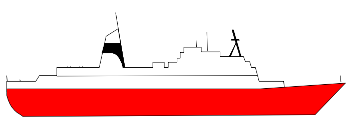

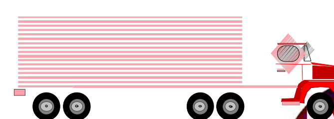

INTEGRITY

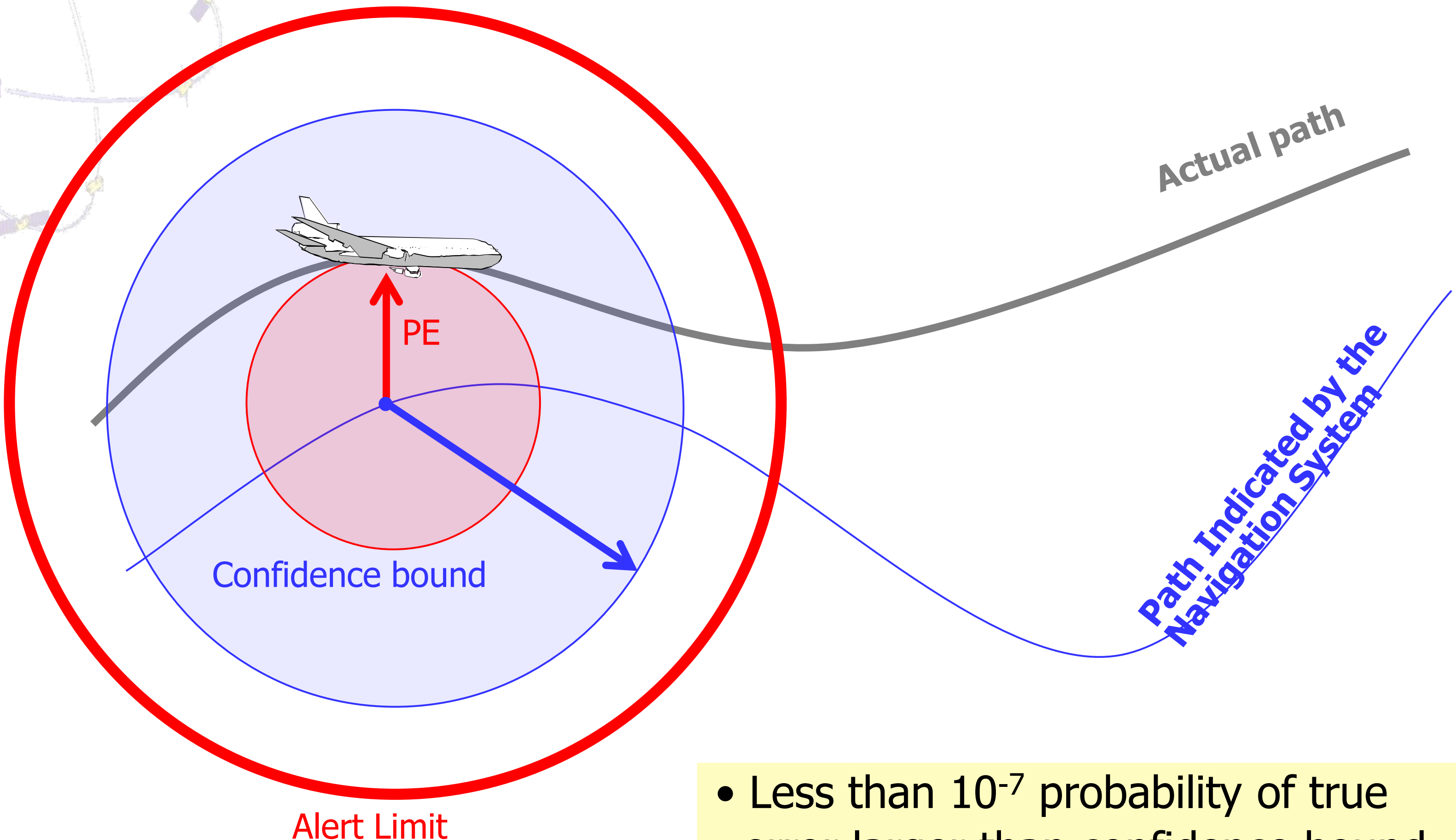

- Less than 10^{-7} probability of true error larger than confidence bound.
- Time to alarm 6 s

WHY GPS NEEDS AN AUGMENTATION ?

GPS Only

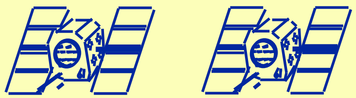

Civil Aviation

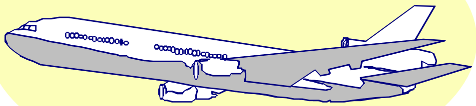

PERFORMANCE

CATEGORY I Requirements

H. 13 m V. 22m	ACCURACY (95%)	H 16.0 m V 4.0 m
99% (RAIM)	AVAILABILITY	99% to 99.990%
?	INTEGRITY RISK	2.10^{-7}/ approach Time to alarm 6 s
?	CONTINUITY OF SERVICE	Risk: 10^{-5} / approach (10^{-6} / 15 s)

UNIVERSITAT POLITÈCNICA DE CATALUNYA
BARCELONATECH

ERRORS on the GNSS Signal

- Space Segment Errors:
  - Clock errors
  - Ephemeris errors
- Propagation Errors
  - Ionospheric delay
  - Tropospheric delay
- Local Errors
  - Multipath
  - Receiver noise

Common

Strong spatial correlation

Weak spatial correlation

No spatial correlation

SBAS Concept

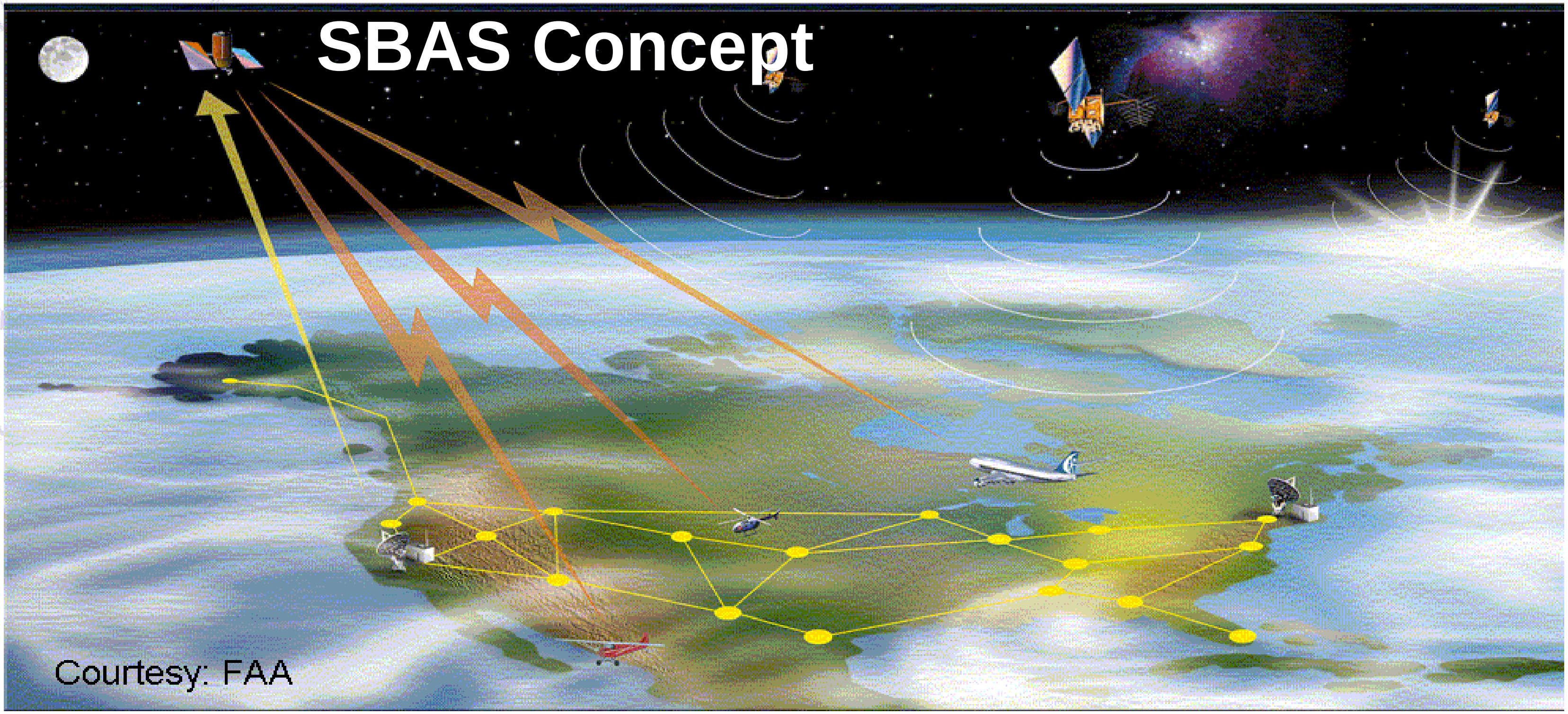

Algorithms improvement (ensuring integrity) and augmented control segment in SBAS area (such as WAAS in USA, EGNOS in Europe, MSAS in Japan, GAGAN in India).

The pseurorange error is splitted in its components.

Clock error

Ephemeris error

Ionospheric error

Local errors (troposphere, multipath, receiver noise)

Uses a network of receivers to cover broad geographic area

What is EGNOS?

- EGNOS is the European component of a Satellite Based Augmentation to GPS and GLONAS.
- EGNOS has been developed under the responsibility of a tripartite group:
  - The European Space Agency (ESA)
  - The European Organization for the Safety of Air Navigation (EUROCONTROL)
  - The Commission of the European Union.

UNIVERSITAT POLITÈCNICA
DE CATALUNYA
BARCELONATECH

IonSAT

The European Geoestationary Navigation Overlay SERVICE (EGNOS)

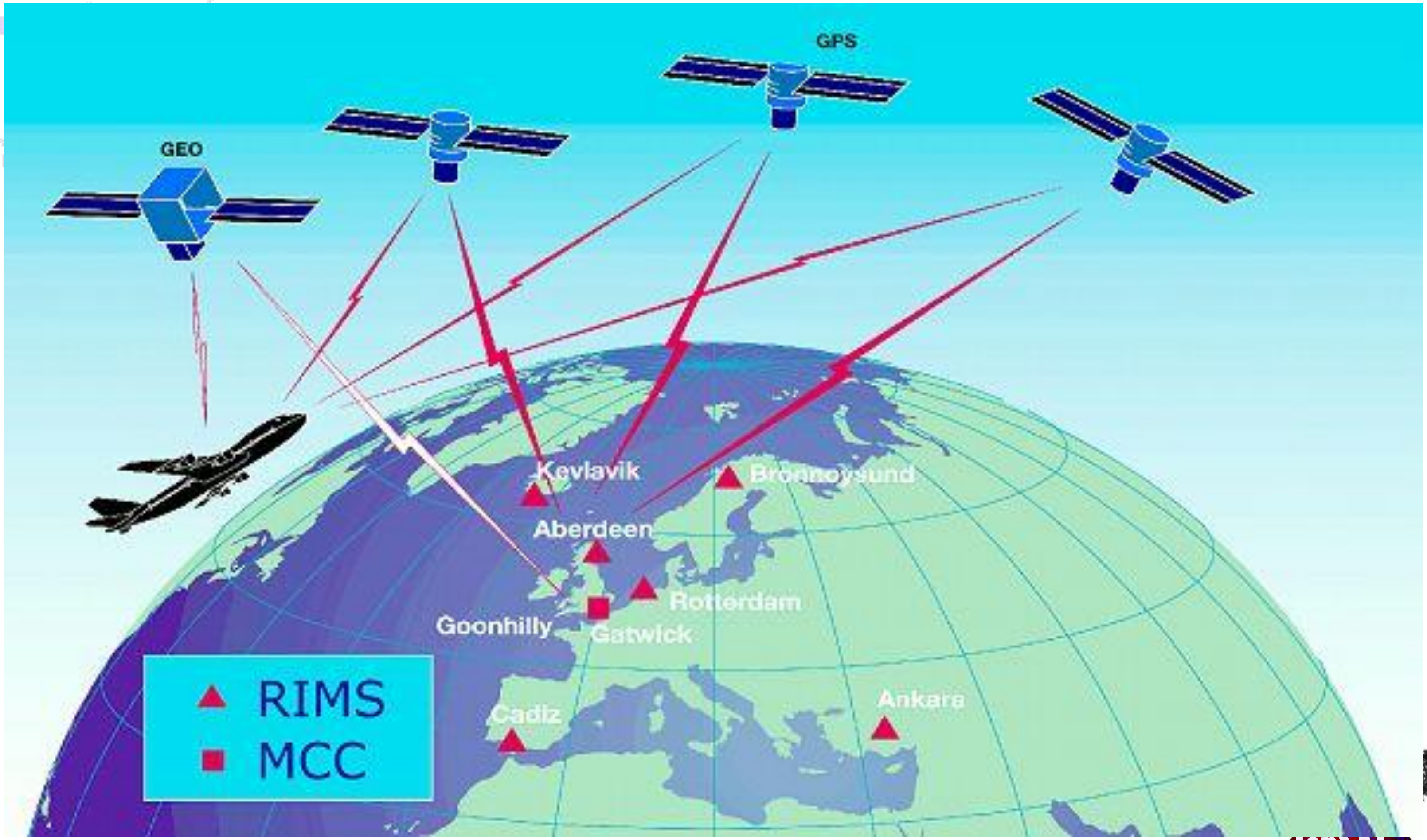

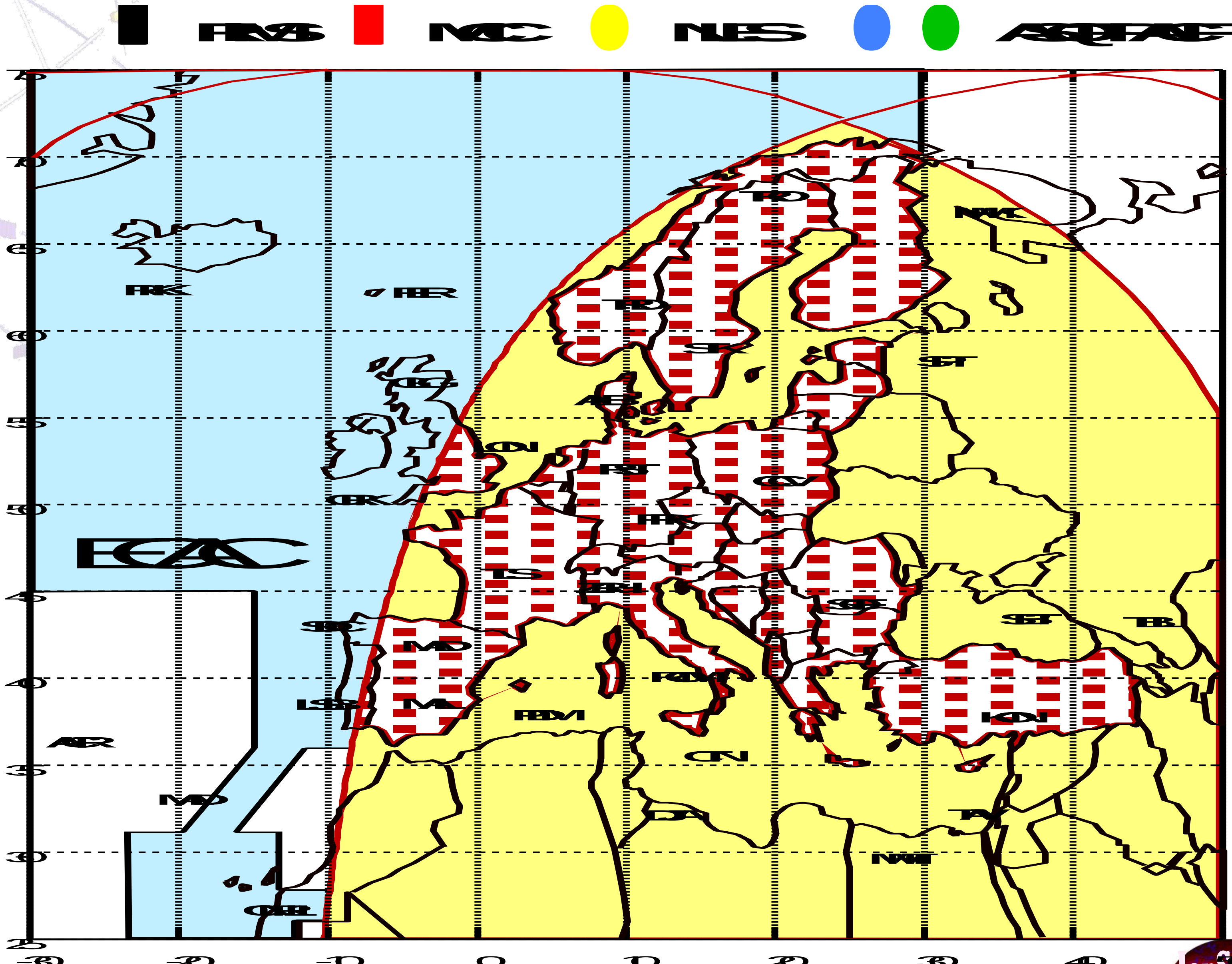

UNIVERSITAT POLITÈCNICA
DE CATALUNYA
BARCELONATECH

IonSAT

Users know the receiver-satellites geometry and can compute bounds on the horizontal and vertical position errors.

These bounds are called Protection Levels (HPL and VPL). They provide good confidence (10^{-7}/hour probability) that the true position is within a the corresponding cylinder/ellipsoid around the computed position.

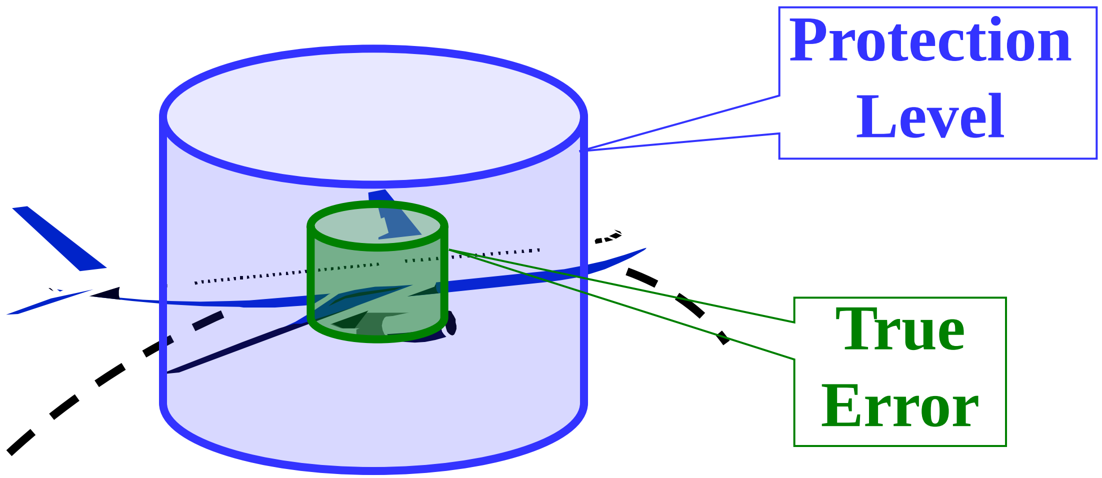

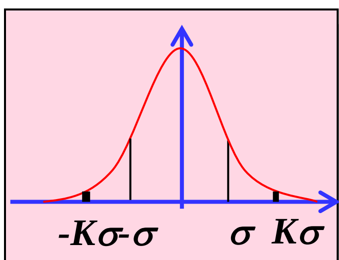

Tail area Probability

P(VPE>VPL) < 10^{-7} /sample

$$VPL = K_V \sqrt{\sum_{i=1}^{N} s_{V_i}^2 \sigma_i^2}$$

$$\sigma_i^2 = \sigma_{i,flt}^2 + \sigma_{i,UIRE}^2 + \sigma_{i,air}^2 + \sigma_{i,tropo}^2$$

GEOMETRY

UNIVERSITAT POLITÈCNICA DE CATALUNYA BARCELONATECH

IonSAT

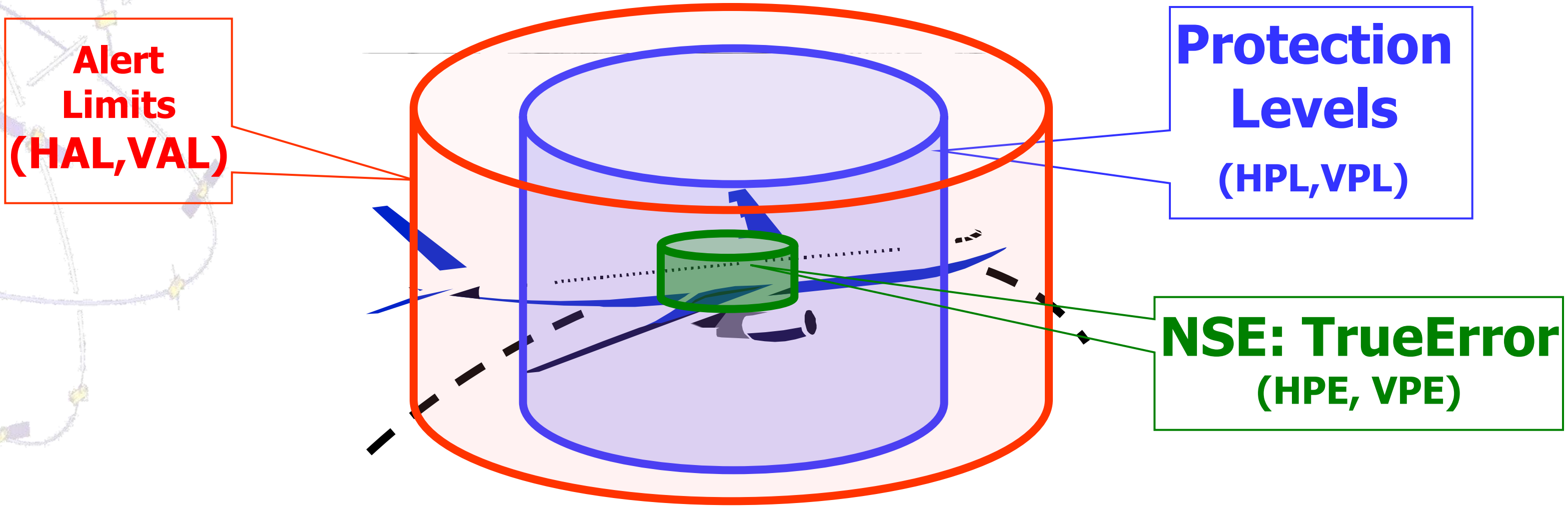

- Each epoch, HPL/VPL are compared with the Alert Limits (HAL/VAL) defined for the operation mode:
  - Hazardously Misleading Information (HMI): XPE > XAL > XPL
    ➔ INTEGRITY RISK
  - Misleading Information (MI): XPE > XPL > XAL
    ➔Out-Of-Tolerence cond.
- The system is set unavailable when XPL > XAL
- Nominal operation: XAL > XPL > XPE

UNIVERSITAT POLITÈCNICA
DE CATALUNYA
BARCELONATECH

IonSAT

STANFORD PLOTS

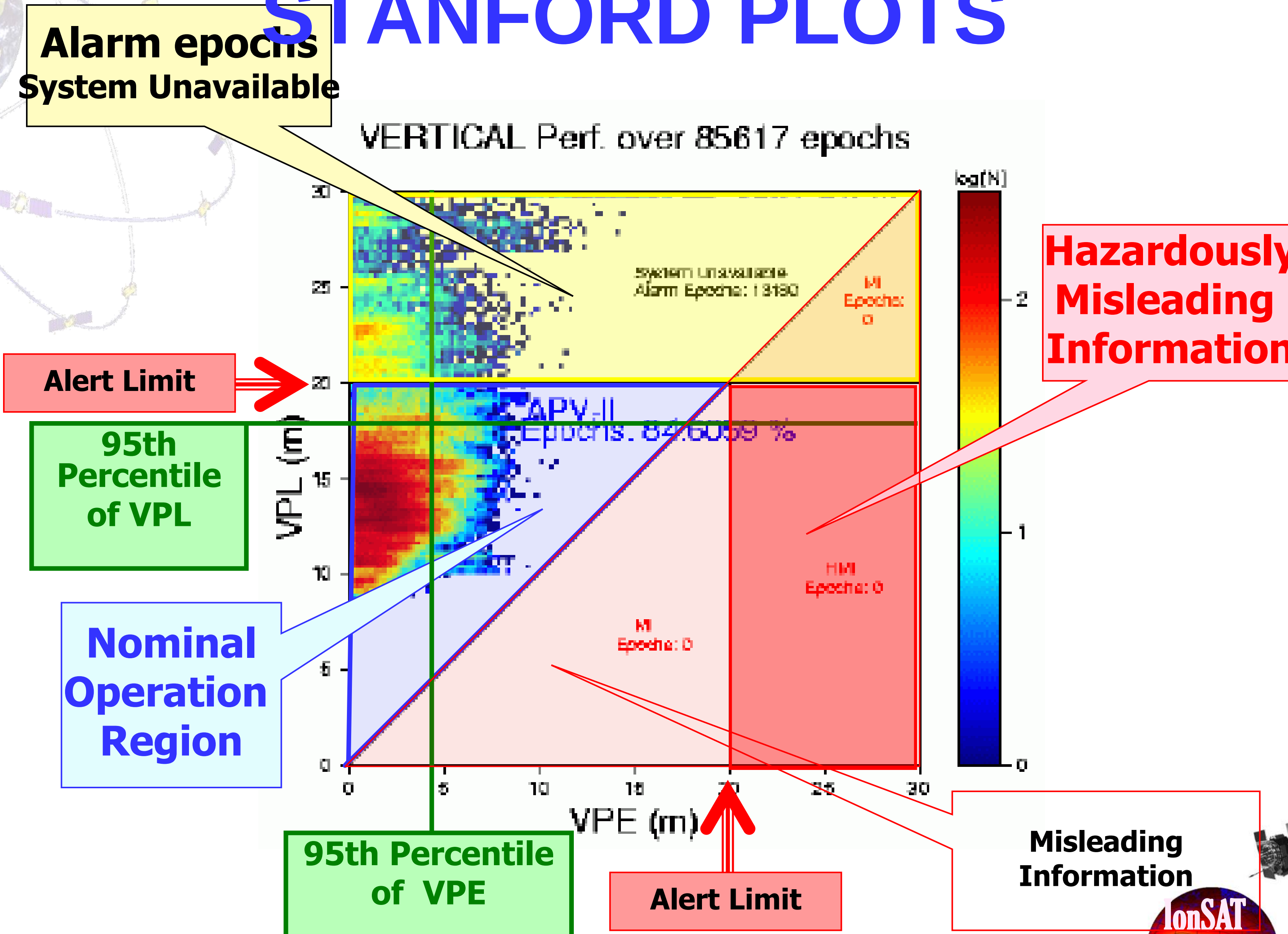

UNIVERSITAT POLITÈCNICA DE CATALUNYA
BARCELONATECH

IonSAT

3. Ionospheric monitoring with GNSS

"Determining in real-time the electron content distribution with an unprecedent spatial and temporal resolution thanks to GNSS"

UNIVERSITAT POLITÈCNICA DE CATALUNYA
BARCELONATECH

IonSAT

- Introduction

Global Positioning System, GPS

- Constellation with 24 or more satellites orbiting at 20200km height.
- GPS satellites emit at 2 L-Band frequencies (1.6 and 1.2 GHz approx.)

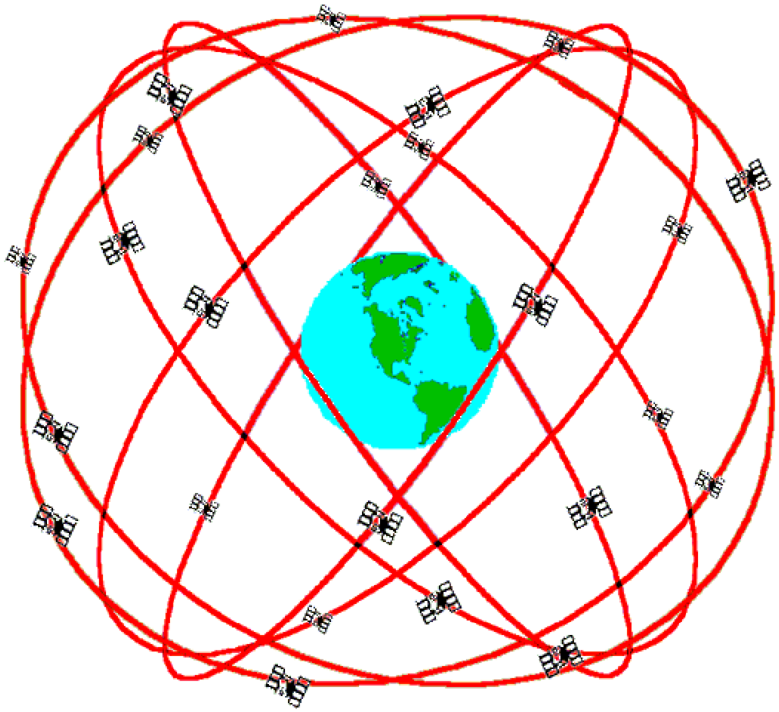

Ionosphere is dispersive →

Ionospheric effect: signal delay/advance observed from a receiver, proportional to STEC

UNIVERSITAT POLITÈCNICA DE CATALUNYA BARCELONATECH

International GPS Service, IGS

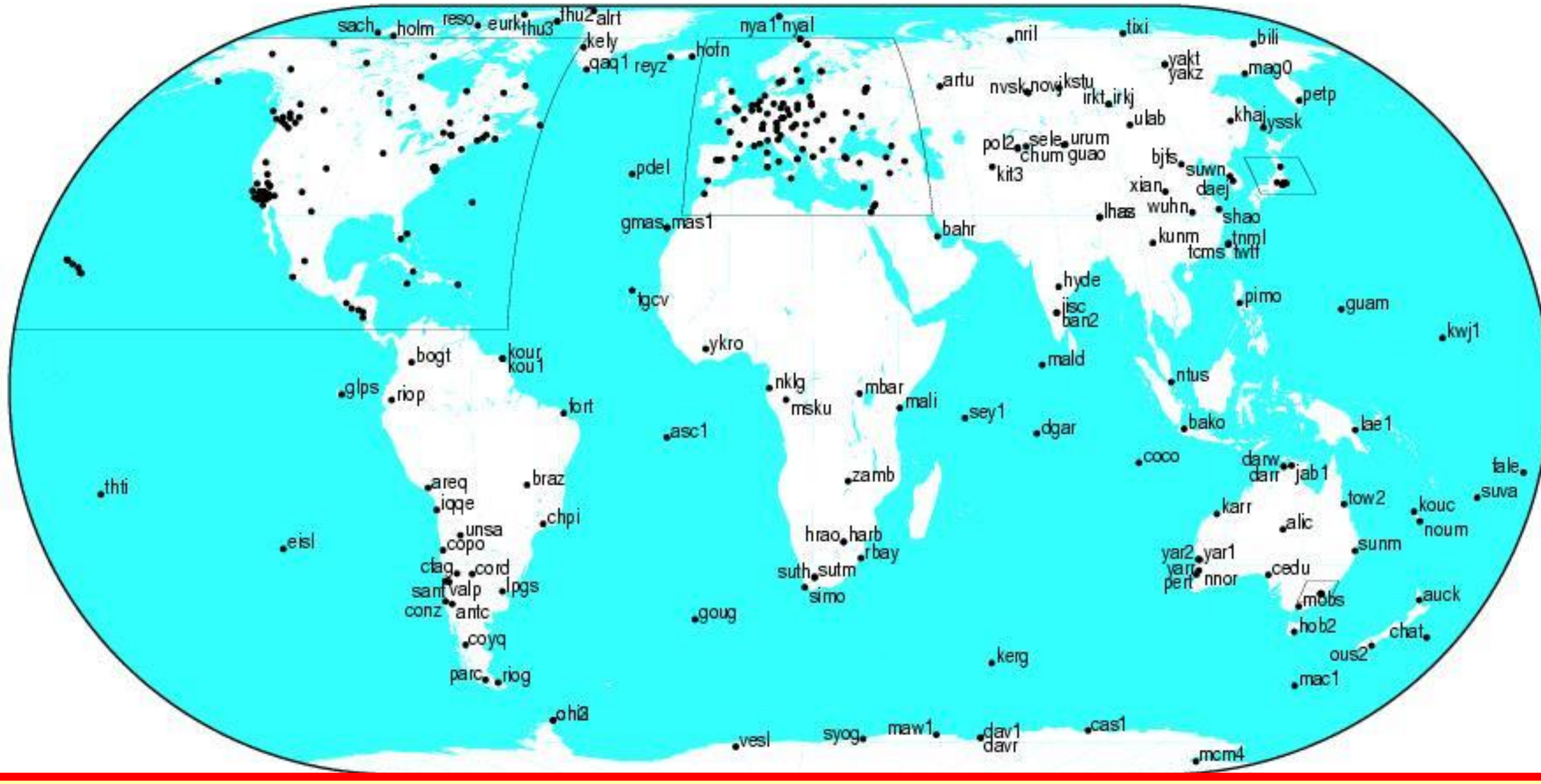

IGS directly manages more than about 350 permanent GPS stations, observing some 4-10 satellites at 30 sec rate: more than 250,000 STEC worldwide observations/hour

UNIVERSITAT POLITÈCNICA DE CATALUNYA
BARCELONATECH

GPS+ IGS: Global Iono. scanner

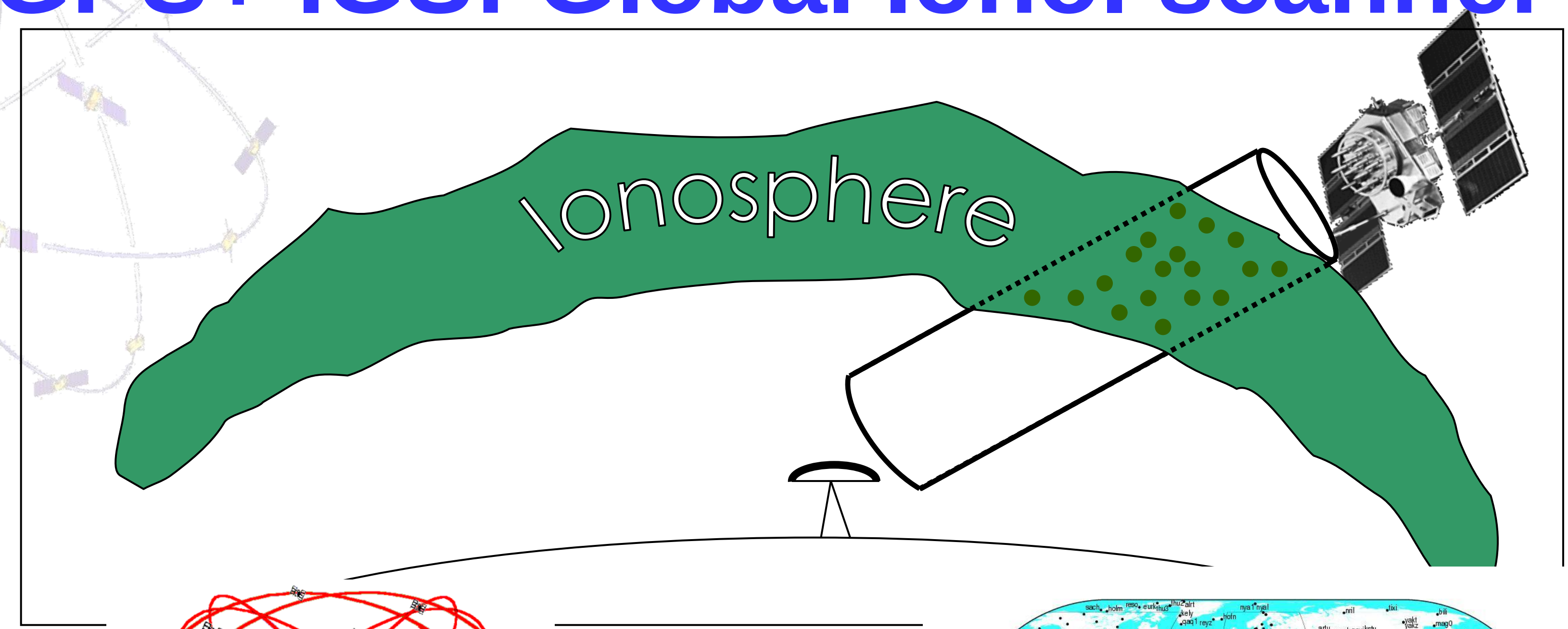

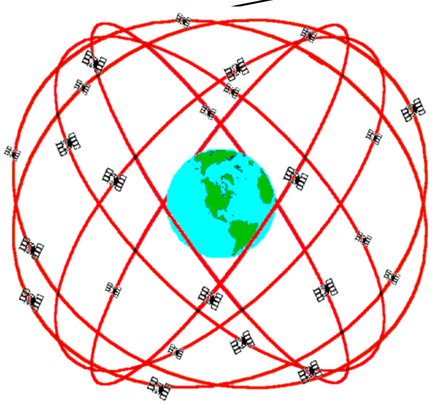

GPS+ IGS

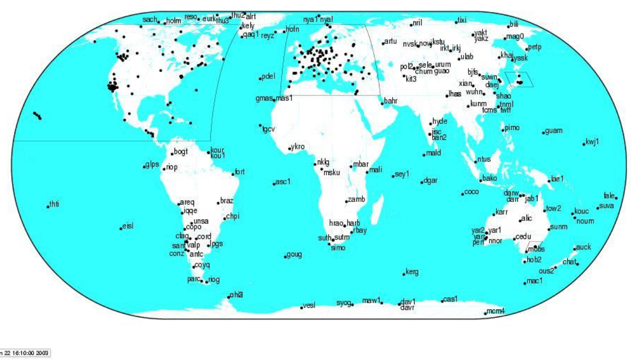

Worldwide *scanner* of the Ionosphere that can be used to generate global VTEC maps

UNIVERSITAT POLITÈCNICA DE CATALUNYA
BARCELONATECH

- The Ionosphere

Ionosphere morphology (viewed by GPS)

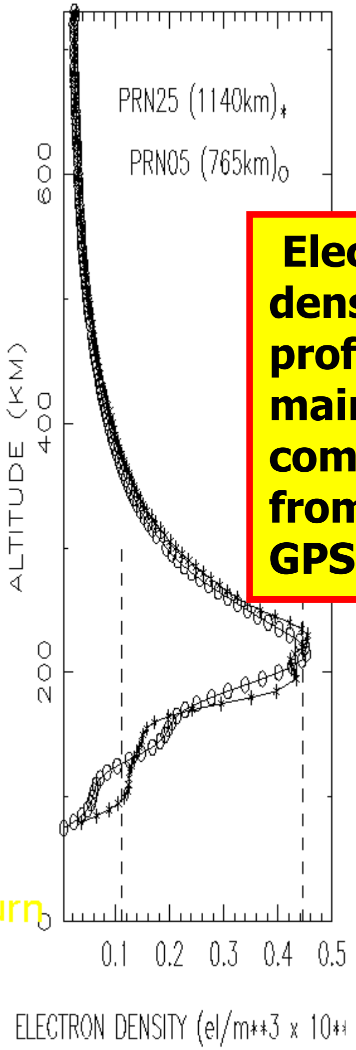

Electron density profile mainly computed from LEO GPS data.

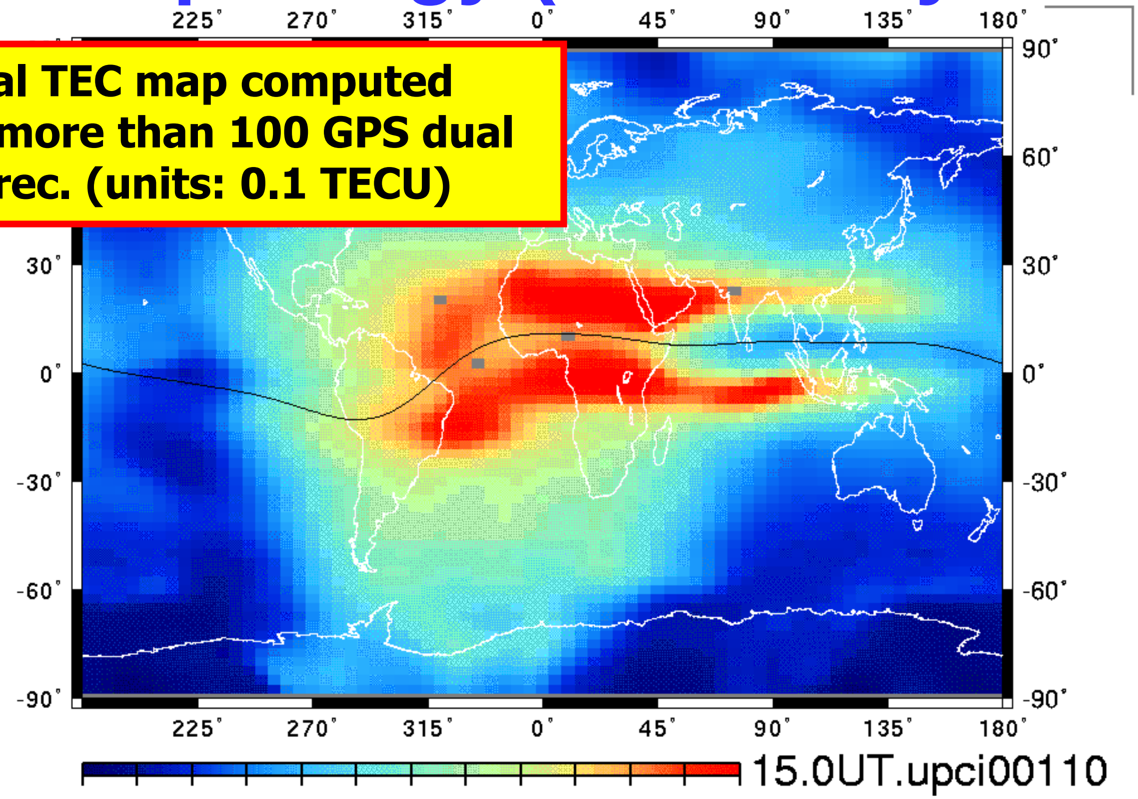

Global TEC map computed from more than 100 GPS dual freq. rec. (units: 0.1 TECU)

- **GPS signal is very sensitive to free electron distribution, which respond to the EM field, oscilating and generating a secondary EM wave which overimposes and change the velocity of the GPS signals (main iono. efect on GPS code and phase).**
- **Vertical: Maximum density height at 200-400 km.**
- **Horizontally: Maximum density at both sides of the geomagnetic equator (equatorial anomalies).**

UNIVERSITAT POLITÈCNICA DE CATALUNYA
BARCELONATECH

The photoionization and the Ionosphere

Table 5.4. Typical reaction rates relevant for ionospheric processes as indicated

Processes	Reaction rates (m^3/sec)
Dissociative recombination	
$NO^+ + e \longrightarrow N + O$	$\alpha_1 = 2.1 \times 10^{-13}\ (T_e/300)^{-0.85}$
$O_2^+ + e \longrightarrow O + O$	$\alpha_2 = 1.9 \times 10^{-13}\ (T_e/300)^{-0.5}$
$N_2^+ + e \longrightarrow N + N$	$\alpha_3 = 1.8 \times 10^{-13}\ (T_e/300)^{-0.39}$
Rearrangement	
$O^+ + N_2 \longrightarrow NO^+ + N$	$k_1 = 2 \times 10^{-18}$
$O^+ + O_2 \longrightarrow O_2^+ + O$	$k_2 = 2 \times 10^{-17}\ (T_r/300)^{-0.4}$
$O_2^+ + NO \longrightarrow NO^+ + O_2$	$k_3 = 4.4 \times 10^{-16}$
$O_2^+ + N_2 \longrightarrow NO^+ + NO$	$k_4 = 5 \times 10^{-22}$
$N_2^+ + O \longrightarrow NO^+ + NO$	$k_5 = 1.4 \times 10^{-16}\ (T_r/300)^{-0.44}$
$N_2^+ + O_2 \longrightarrow N_2 + O_2^+$	$k_6 = 5 \times 10^{-17}\ (T_r/300)^{-0.8}$
Radiative recombination	
$O^- + e \longrightarrow O + h\nu$	$\alpha_r = 7.8 \times 10^{-14}\ (T_e/300)^{-0.5}$
Electron attachment	
$O_2 + M + e \longrightarrow O_2^- + M$	$\beta_1 = 10^{-43}\ (300/T_e)e^{-600/T_e}\ [N_2]$
	$\beta_2 = 10^{-41}\ [O_2]$
$O + e \longrightarrow O^- + h\nu$	$\beta_r = 10^{-21}$
Electron detachment	
$O_2^- + h\nu \longrightarrow O_2 + e$	$\rho = 0.33\ sec^{-1}$
$O_2^- + N_2 \longrightarrow O_2 + N_2 + e$	$\gamma_1 = 2 \times 10^{-18}\ (T_r/300)^{1.5} \exp(5 \times 10^{-3}/T_r)$
$O_2^- + O_2 \longrightarrow O_2 + O_2 + e$	$\gamma_2 = 3 \times 10^{-16}\ (T_r/300)^{0.5} \exp(6 \times 10^{-3}/T_r)$
$O_2^- + O \longrightarrow O_3 + e$	$\gamma_3 = 5 \times 10^{-16}$
$O^- + O \longrightarrow O_2 + e$	$\gamma_4 = 3 \times 10^{-16}$
Ion–ion recombination	
$O_2^+ + O_2^- \longrightarrow O_2 + O_2$	$\alpha_{i1} = 2 \times 10^{-13}$
$O_2^+ + O_2^- + M \longrightarrow O_2 + O_2 + M$	$\alpha_{i2} = 3 \times 10^{-31}\ (T/300)^{-2.5}\ [M]$

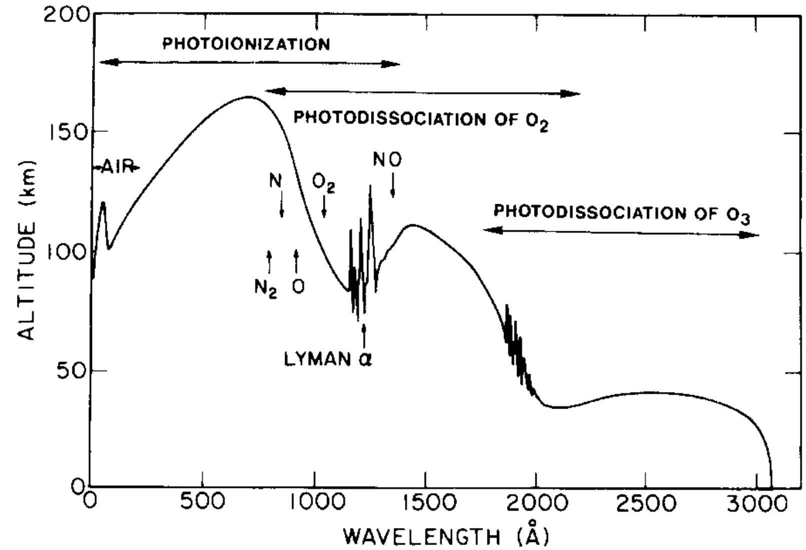

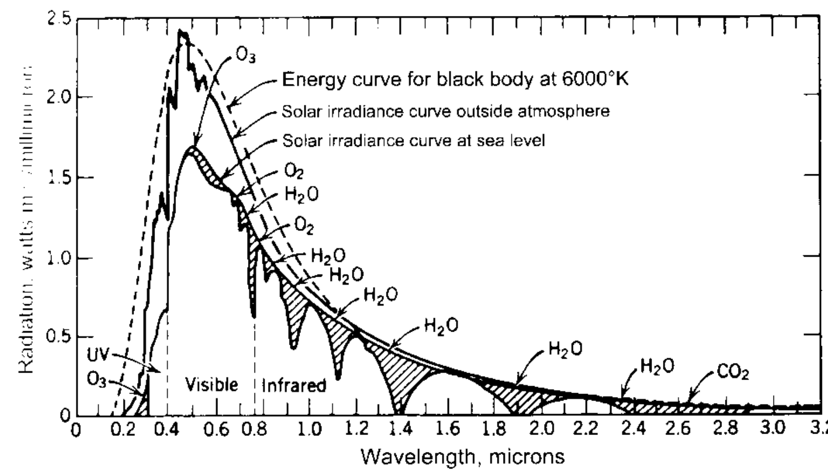

UNIVERSITAT POLITECNICA DE CATALUNYA BARCELONATECH

IonSAT

The generation of free electrons

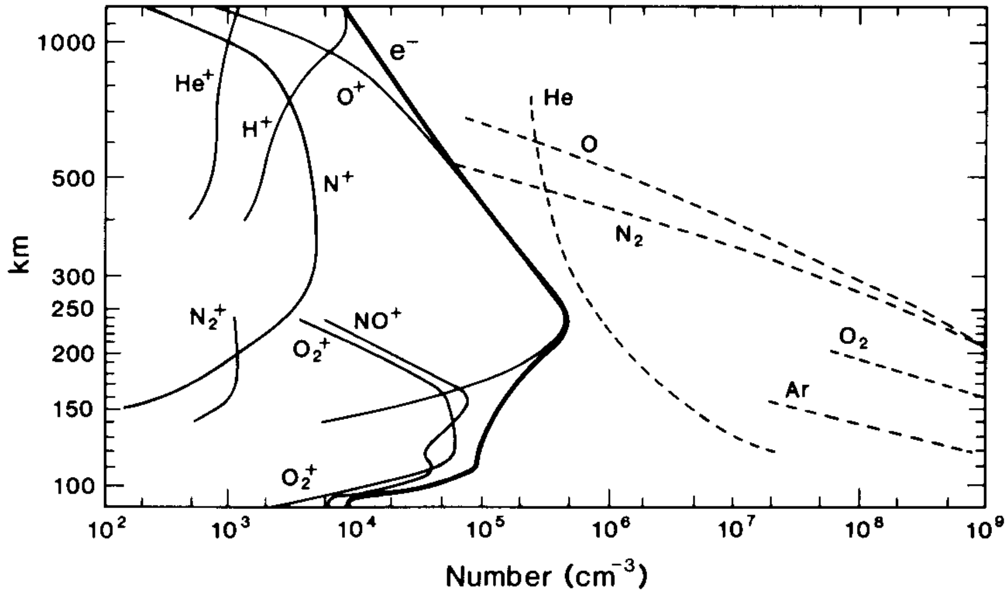

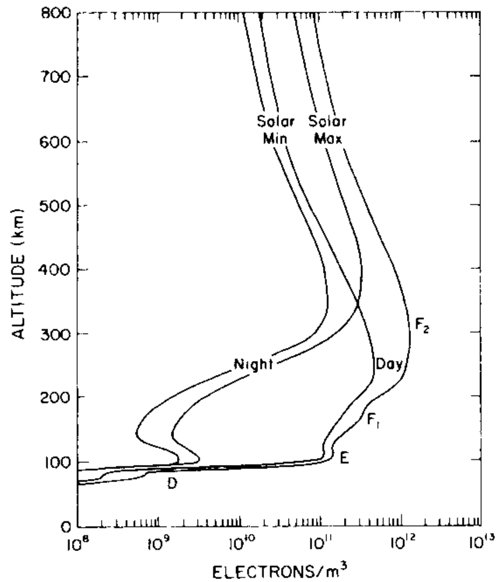

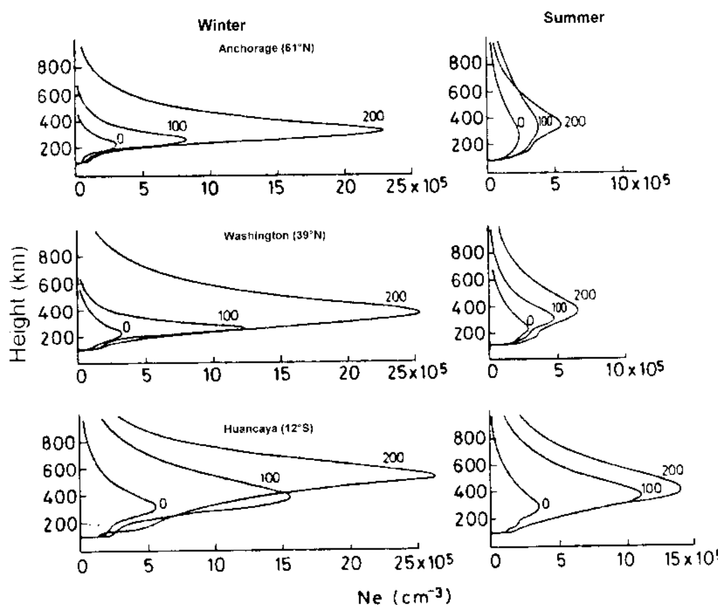

UNIVERSITAT POLITECNICA
DE CATALUNYA
BARCELONATECH

Ionosphere & photoionization: Chapman model

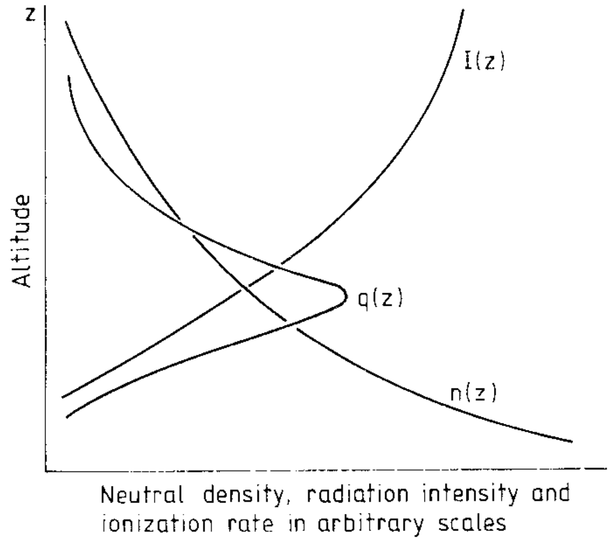

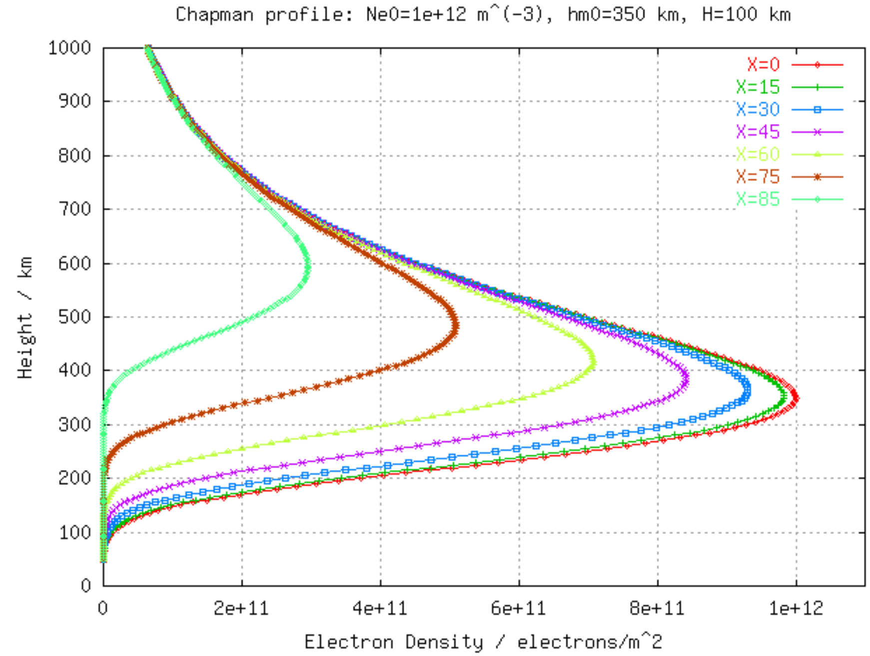

Under hydrostatic equilibrium (with pressure height scale smaller than the temperature one), assuming an ideal gas, a monochromatic beam acting on the lower part of the atmosphere, and considering photochemical equilibrium, it can be demonstrated that:

$$N_e(h,\chi) = N_{e,0}\, e^{\frac{1}{2}\left(1-\frac{h-h_{m,0}}{H}-\sec(\chi)\, e^{-\frac{h-h_{m,0}}{H}}\right)}$$

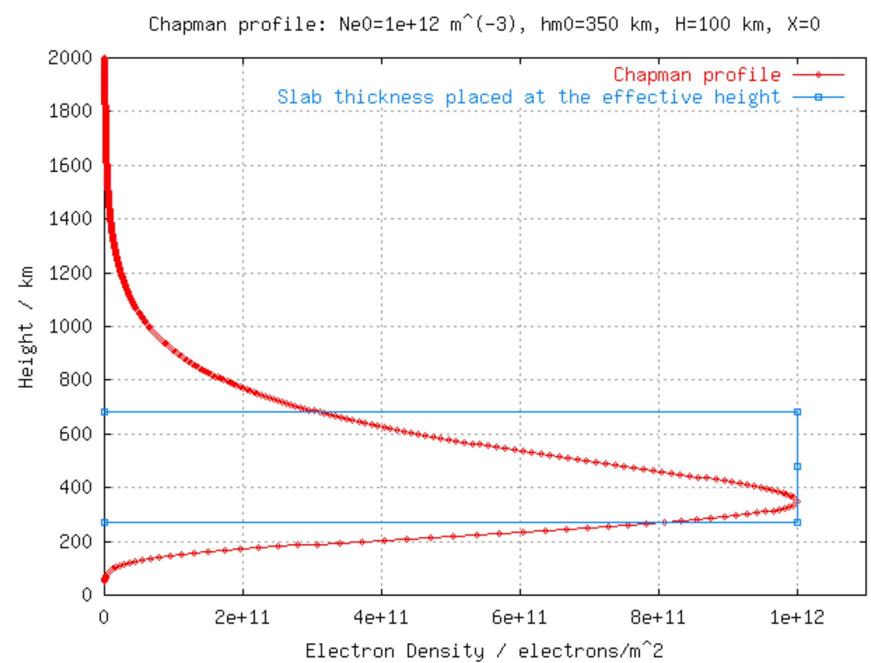

Being $N_{e,0}$ and $h_{m,0}$ the electron density peak and corresponding height, and being H the scale height.

UNIVERSITAT POLITÈCNICA DE CATALUNYA BARCELONATECH

The Solar Cycle, the Solar Wind, the Geomagnetic Storms

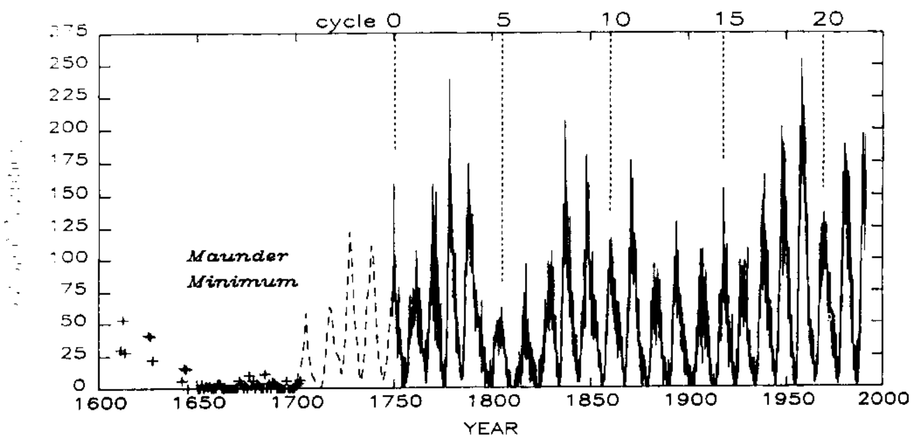

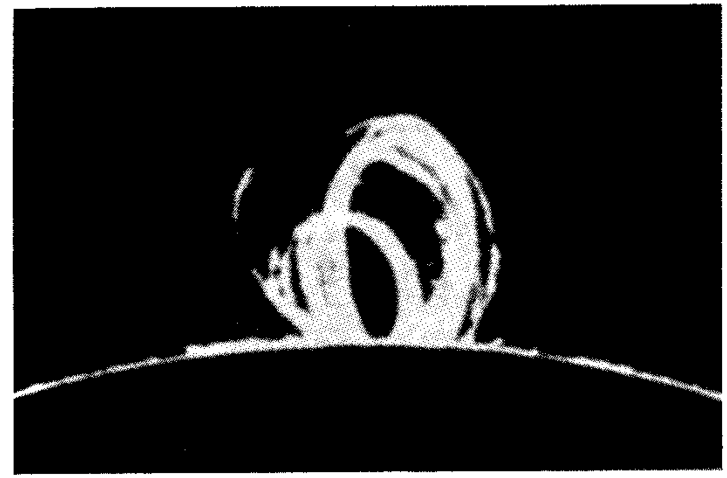

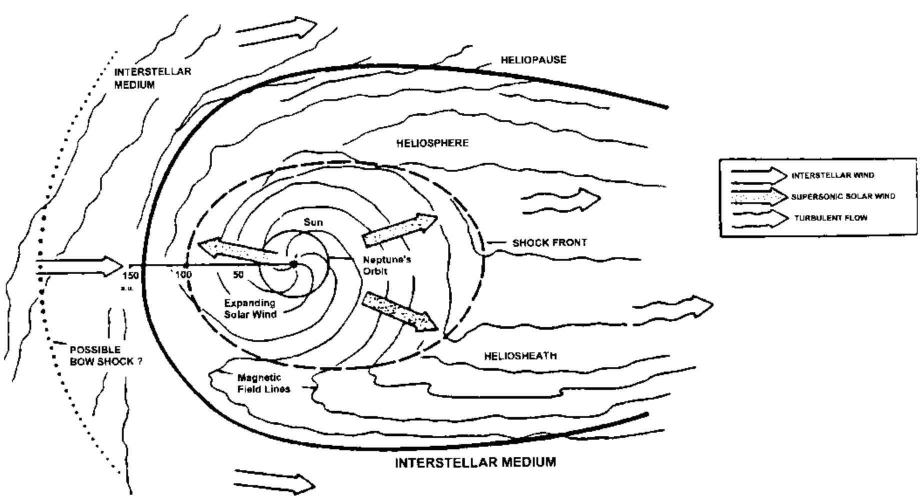

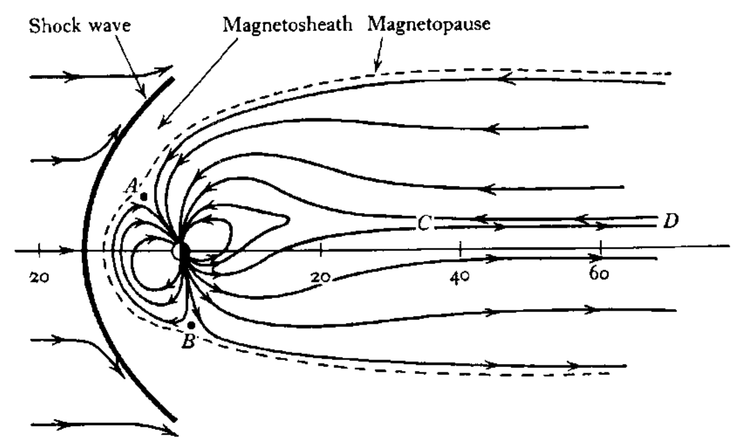

Physical background: Maxwell equations, Lorentz and Electrostatic forces

$$\vec{\nabla} \cdot \vec{D} = \rho$$

Poisson's equation (Gauss law)

$$\vec{\nabla} \cdot \vec{B} = 0$$

Divergenceless B, there are not magnetic monopoles

$$\vec{\nabla} \times \vec{H} = \vec{J} + \frac{\partial \vec{D}}{\partial t}$$

Ampère's law

$$\overline{\nabla} \times \vec{E} = -\frac{\partial \vec{B}}{\partial t}$$

Being D=εE in and B=μH in normal and homogeneous media, representing E and B to the electric and magnetic fields.

$$\hat{n} \cdot \left(\vec{D}_{+} - \vec{D}_{-}\right) = \sigma$$
$$\hat{n} \times \left(\vec{E}_{+} - \vec{E}_{-}\right) = \vec{0}$$
$$\hat{n} \cdot (\vec{B}_{+} - \vec{B}_{-}) = 0$$
$$\hat{n} \times (\vec{H}_{+} - \vec{H}_{-}) = \hat{K}$$

Being σ the surface charge density and K the surface density of current

$$m \ddot{\vec{r}} = q \vec{E} + q \vec{v} \times \vec{B} - \gamma m \dot{\vec{r}}$$

Electrostatic, Lorentz and collision forces

Being m, q and v the mass, charge and velocity of the particle (i.e. electrons)

UNIVERSITAT POLITÈCNICA DE CATALUNYA BARCELONATECH

IonSAT

Equatorial anomalies and E cross B drift

Assuming only electric and magnetic fields acting on the charged particled, the component of E along B will vanish (it is the only force acting in this direction, generating a polarized field which suppress the external one).

$$\underbrace{\left\langle m\,\dot{\vec{v}}\right\rangle = q\vec{E} + q\,\vec{u}_E \times \vec{B} = \vec{0}}_{\times \vec{B}}$$

$$\vec{0} = q\vec{E}\times\vec{B} + q\left[\underbrace{\left(\vec{u}_E\cdot\vec{B}\right)}_{0}\vec{B} - B^2\,\vec{u}_E\right]$$

$$\vec{u}_E = \frac{1}{B^2}\,\vec{E}\times\vec{B}$$

Being u_E the displacement velocity generated by the E cross B drift. For a general force F:

$$\vec{u}_F = \frac{1}{qB^2}\,\vec{F}\times\vec{B}$$

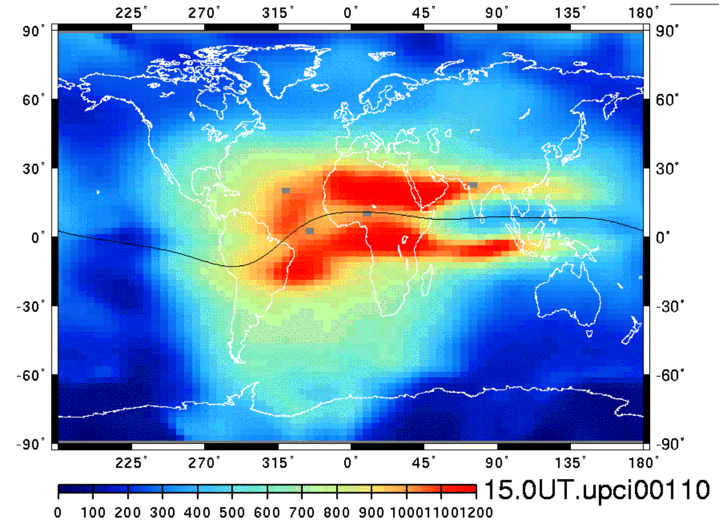

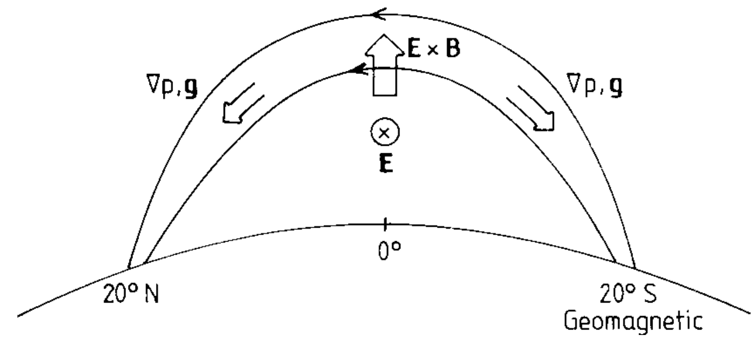

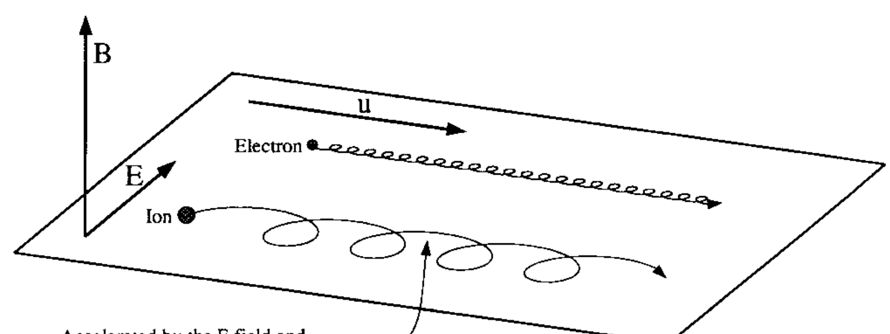

UPC UNIVERSITAT DE CATALUNY BARCELONATE

- Ionospheric effects on GPS

11-years Solar cycle

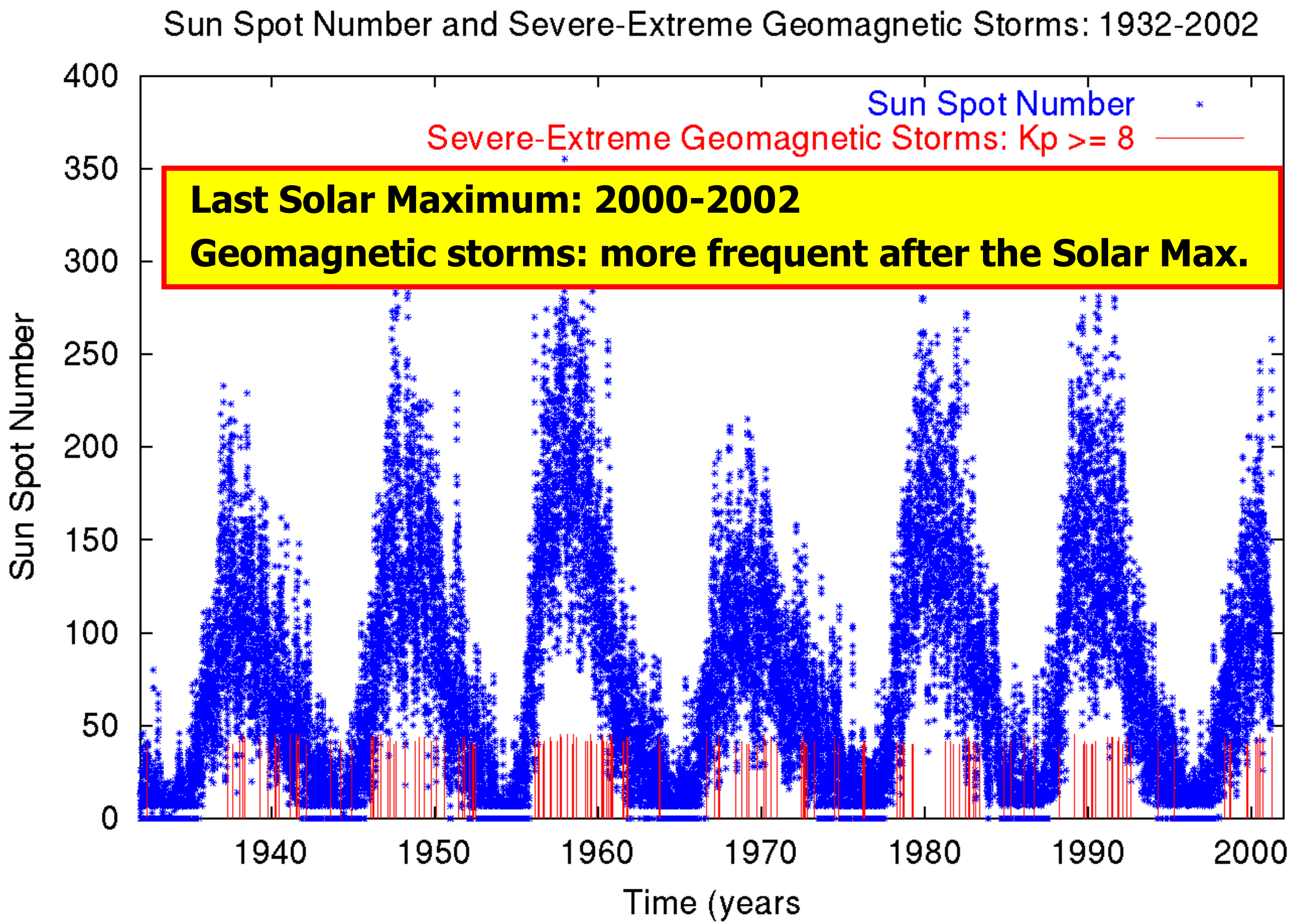

Last Solar Maximum: 2000-2002

Geomagnetic storms: more frequent after the Solar Max.

VTEC: Modulated by the Solar Cycle

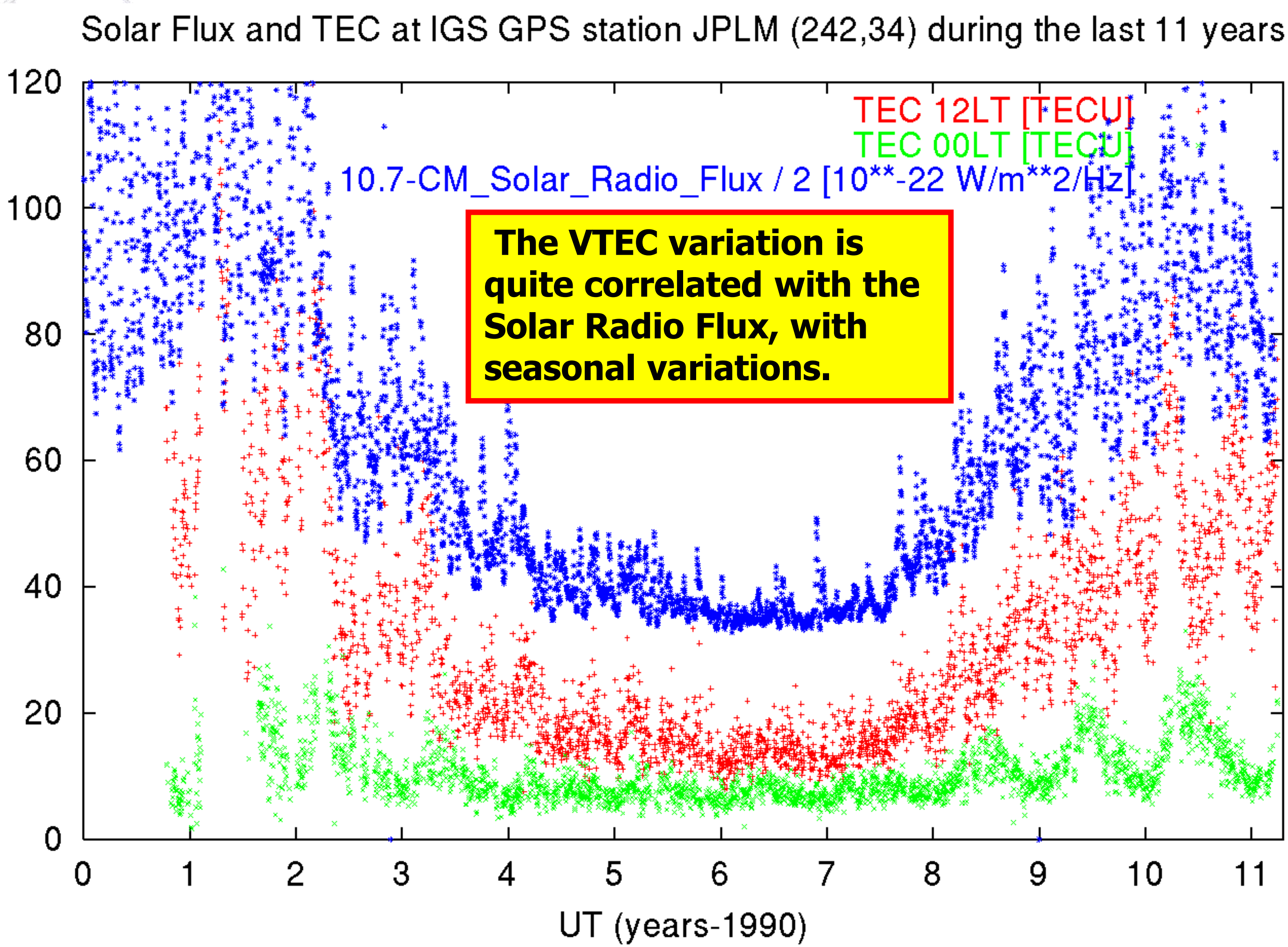

VTEC modulated by the Season

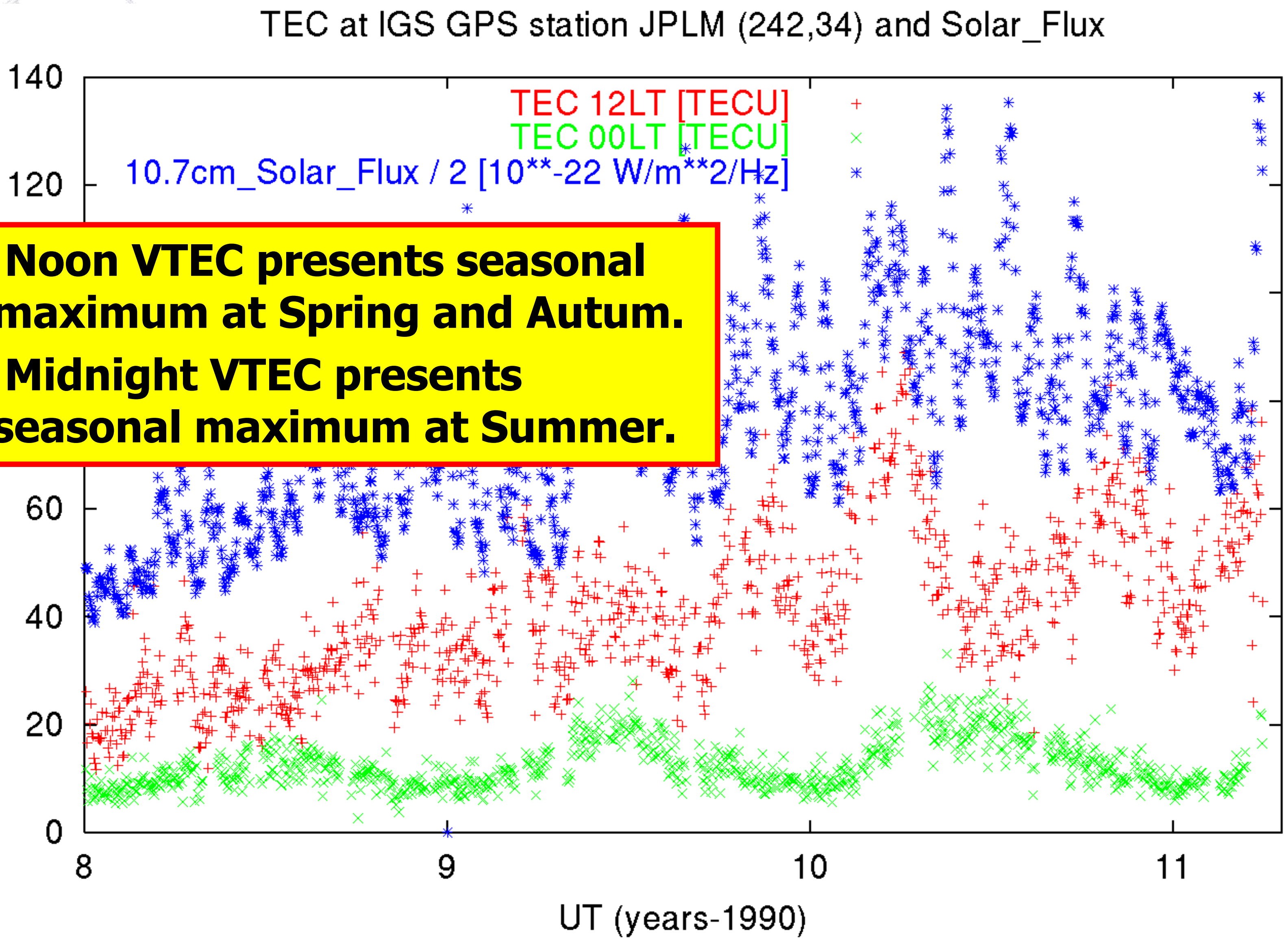

Noon VTEC presents seasonal maximum at Spring and Autum.

Midnight VTEC presents seasonal maximum at Summer.

UNIVERSITAT POLITÈCNICA DE CATALUNYA
BARCELONATECH

VTEC can change during geomagnetic storms

During geomagnetic storms the VTEC can experience enhancements or decreases of 100%

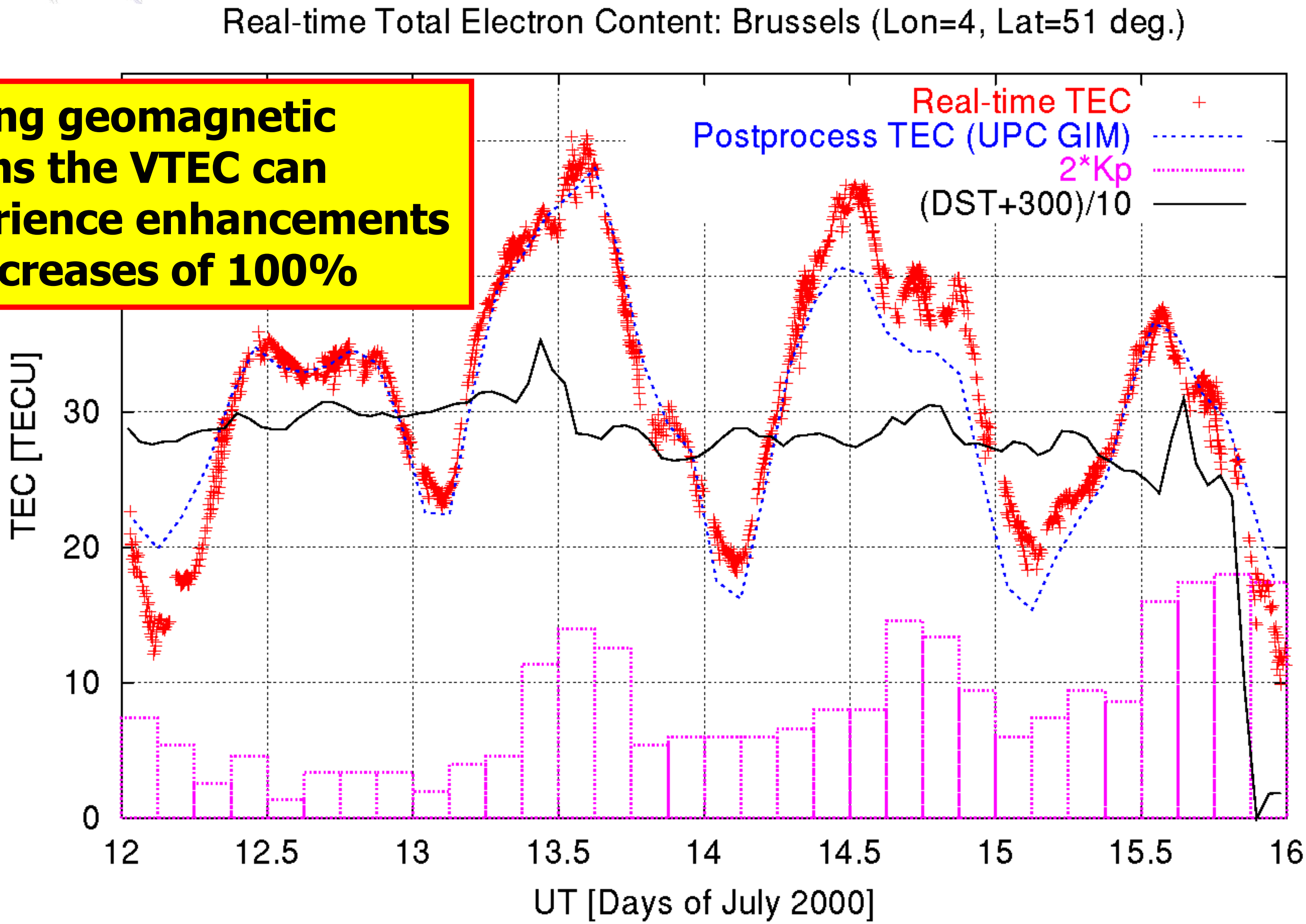

Scintillation: Very rapid VTEC variations

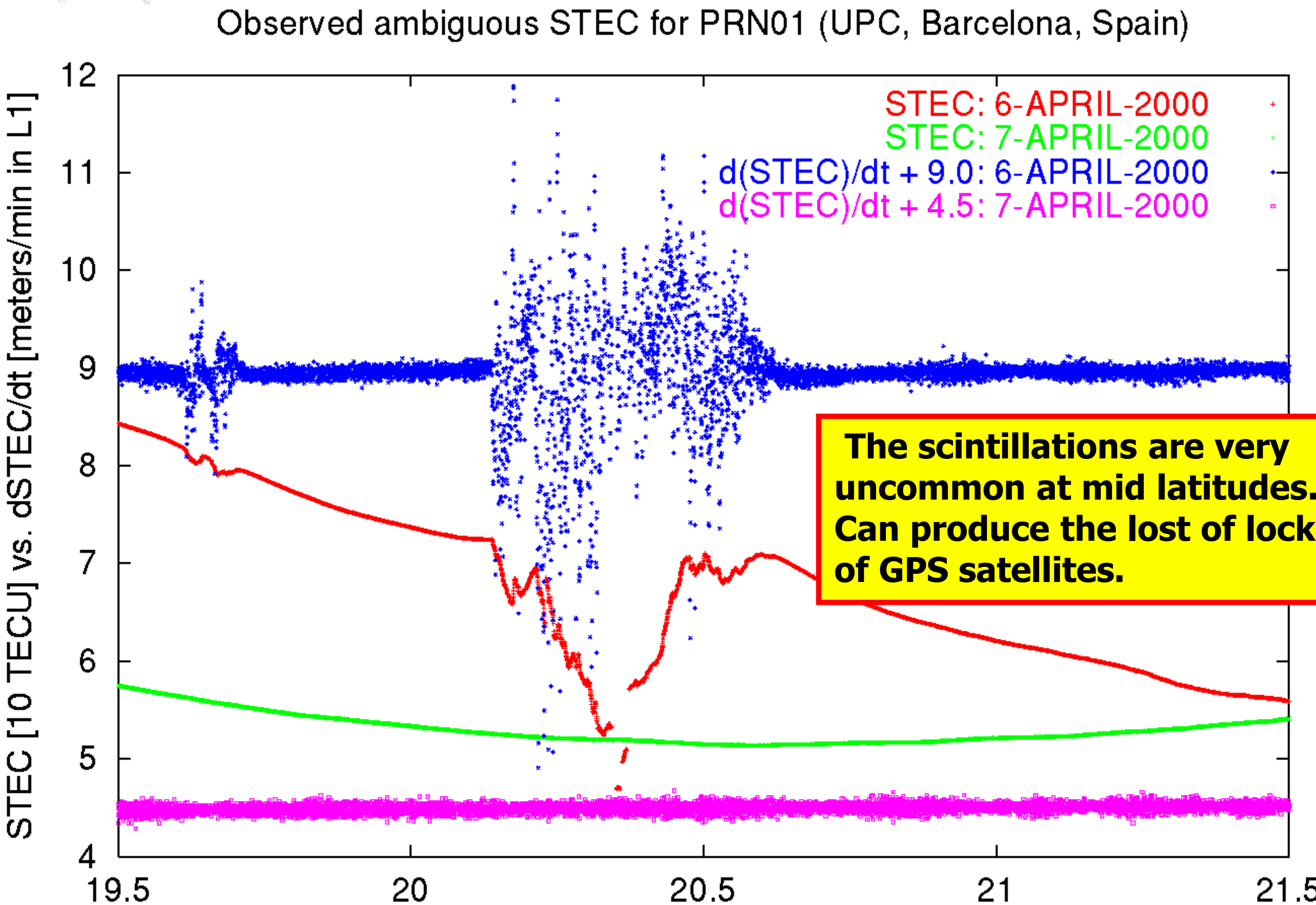

The scintillations are very uncommon at mid latitudes. Can produce the lost of lock of GPS satellites.

UNIVERSITAT POLITÈCNICA DE CATALUNYA BARCELONATECH

STEC can be affected by Travelling Ionospheric Disturbances

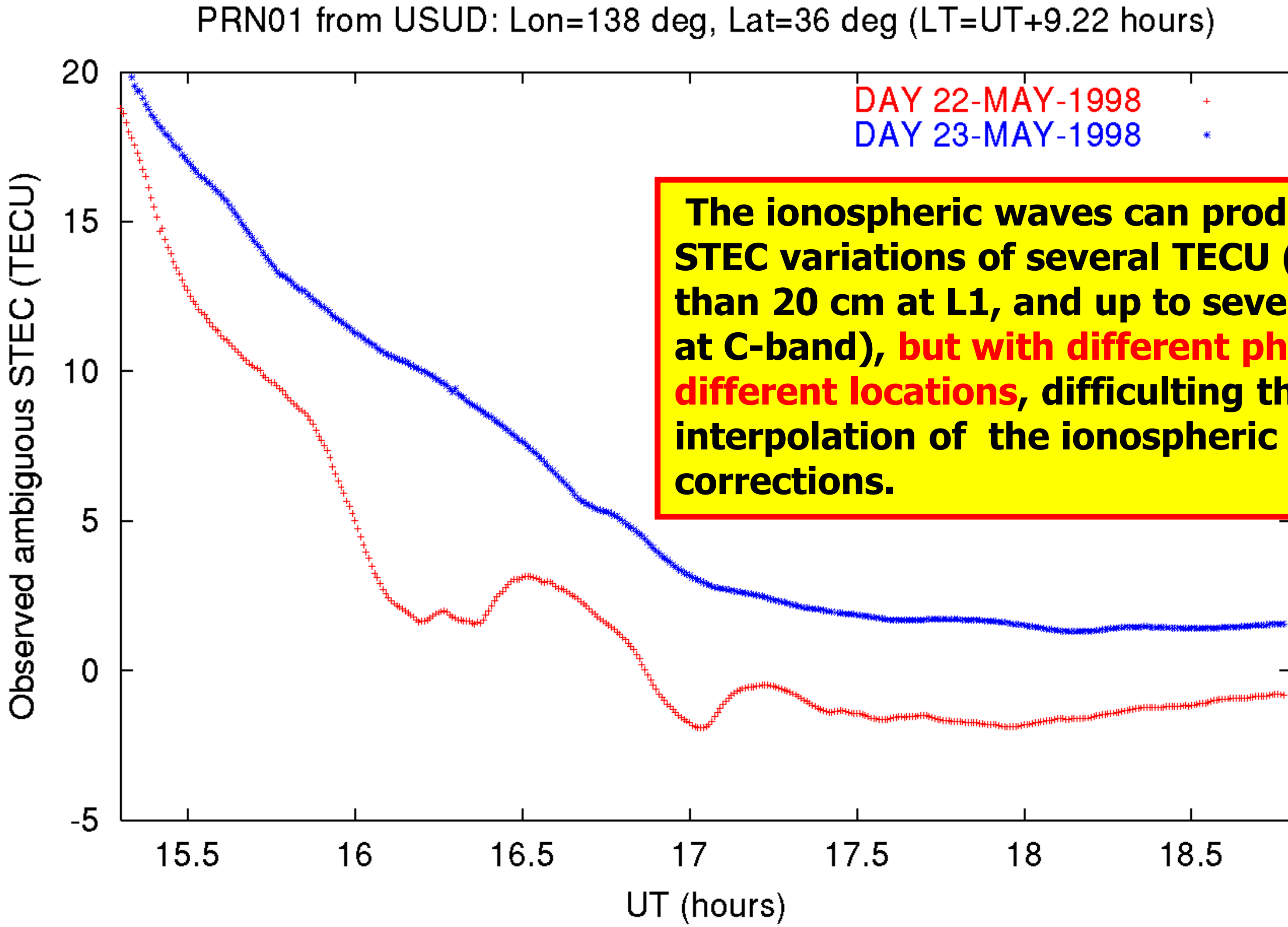

The ionospheric waves can produce STEC variations of several TECU (more than 20 cm at L1, and up to several cm at C-band), but with different phases at different locations, difficulting the interpolation of the ionospheric corrections.

UNIVERSITAT POLITÈCNICA DE CATALUNYA
BARCELONATECH

- From Ionosphere First principles to GPS preprocessing

UNIVERSITAT POLITÈCNICA DE CATALUNYA BARCELONATECH

GPS signal propagation: Appleton Formula

$$m\ddot{\vec{r}} = q\vec{E} + q\vec{v}\times\vec{B} - \gamma m\dot{\vec{r}}$$

$$\begin{cases} m\ddot{x} = qE_x - qB_T\dot{z} - \gamma m\dot{x} \\ m\ddot{y} = qE_y + qB_L\dot{z} - \gamma m\dot{y} \\ m\ddot{z} = qE_z + q\left(B_T\dot{x} - B_L\dot{y}\right) - \gamma m\dot{z} \end{cases}$$

$$m\ddot{\boldsymbol{r}} = e\boldsymbol{E} + (e\dot{\boldsymbol{r}}\times\boldsymbol{B}) - m\nu\dot{\boldsymbol{r}} \qquad (3.1)$$

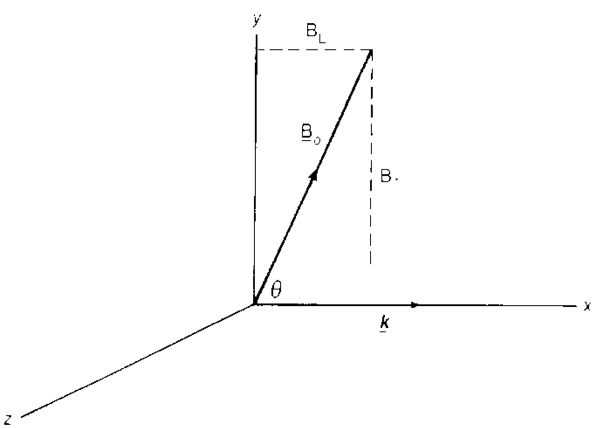

Fig 3.1 *System of orthogonal axes x, y, and z*
The x-direction is the direction of phase propagation, and the external magnetic field lies in the x y plane. The y z plane is the plane of the wavefront

Multiplying throughout by the charge density N_e, replacing first and second x derivative by iωx and $-\omega^2 x$,…, using P_x=Nqx,…, the components of the volume polarization, taking into account the wave polarization relatioships (R=Dz/Dy=-Hy/Hz=Ez/Ey=Pz/Py=z/y), we can get the **Appleton formula**:

$$n^2 = (\mu - i\chi)^2 = 1 + \frac{P_y}{\varepsilon_0 E_y} = 1 - \frac{X}{1 - iZ + iY_L R} =$$

$$1 - \frac{X}{1 - iZ - \frac{Y_T^2}{2(1-X-iZ)} \pm \sqrt{\frac{Y_T^4}{4(1-X-iZ)} + Y_L^2}}$$

$$X = \frac{\omega_p^2}{\omega^2}, Y_L = -\frac{\omega_g}{\omega}\cos\theta, Y_T = -\frac{\omega_g}{\omega}\sin\theta, Z = \frac{\gamma}{\omega}$$

Being the plasma and gyro frequencies:

$$\omega_p^2 = \frac{Nq^2}{m\varepsilon_0}, \omega_g = \frac{Bq}{m}$$

UNIVERSITAT POLITÈCNICA DE CATALUNYA
BARCELONATECH

IonSAT

Plasma and gyro frequencies

$$m\ddot{\vec{r}} = q\vec{v} \times \vec{B}$$

$$m\frac{v^2}{r} = qvB_\perp$$

$$\omega_g = \frac{qB_\perp}{m}$$

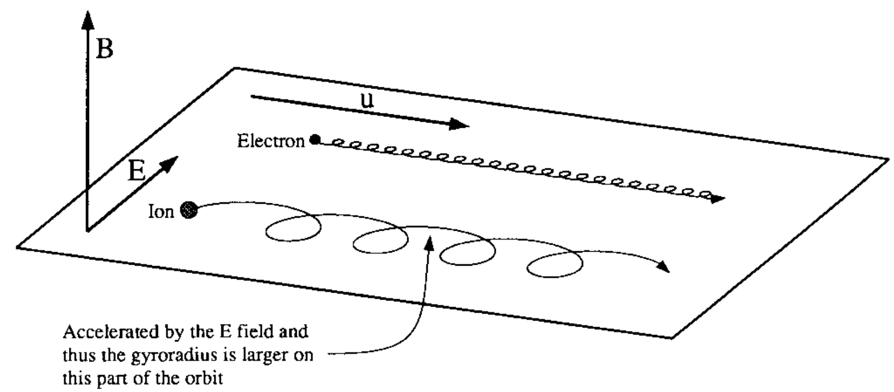

$$\nabla \cdot \vec{E} = \frac{\rho}{\varepsilon_0} \Rightarrow \frac{\partial E}{\partial x} = \frac{\rho}{\varepsilon_0} \Rightarrow E \approx -\frac{N_e |q_e|}{\varepsilon_0}\delta$$

$$\frac{F}{A} = \left(-\frac{N_e |q_e|}{\varepsilon_0}\delta\right)\left(N_e |q_e| L\right) = \left(LN_e m_e\right)\ddot{\delta}$$

$$\ddot{\delta} = -\frac{N_e q_e^2}{m_e \varepsilon_0}\delta \Rightarrow \omega_p^2 = \frac{N_e q_e^2}{m_e \varepsilon_0}$$

From the Appleton formula, with the first order approximation and neglecting collisions, the plasma frequency produces no propagation (n=0, X=1, $\omega=\omega_p$, reflexion in vertical sounding for instance).

GPS signal propagation and ionospheric terms (first and second order)

$$n_p^2 = 1 - \frac{X}{1 - iZ - \frac{Y_T^2}{2(1 - X - iZ)} \pm \sqrt{\frac{Y_T^4}{4(1 - X - iZ)^2} + Y_L^2}} \approx$$

$$\approx \{Z = 0 \ \& \ high.freq.\} \approx 1 - \frac{X}{1 \pm Y_L} \Rightarrow n \approx 1 - \frac{1}{2} X (1 \mp Y_L)$$

$$\delta L_I = \int_{\vec{r}_{rec}}^{\vec{r}_{tra}} \left(\frac{c}{v_p} - 1 \right) ds = \int_{\vec{r}_{rec}}^{\vec{r}_{tra}} (n_p - 1) ds = - \int_{\vec{r}_{rec}}^{\vec{r}_{tra}} \frac{1}{2} \frac{\omega_p^2}{\omega^2} \left(1 \pm \underbrace{\frac{\omega_g}{\omega} \cos \theta}_{(GPS) \approx \frac{10^6}{1.6 \cdot 10^9} \leq 6 \cdot 10^{-4}} \right) ds =$$

$$= \{ordinary - wave\} = \left\{ K_1 = \frac{q^2}{8 \pi^2 m \varepsilon_0} \approx 40.3 (MKS) \right\} =$$

$$- \frac{K_1}{f^2} \left[\underbrace{\int_{\vec{r}_{rec}}^{\vec{r}_{tra}} N_e ds}_{STEC} + \frac{q}{2 \pi m} \frac{1}{f} \int_{\vec{r}_{rec}}^{\vec{r}_{tra}} N_e B \cos \theta .ds \right] = \underbrace{- \frac{K_1}{f^2} STEC}_{FIRST.ORDER} \underbrace{- \frac{K_2}{f^3} \int_{\vec{r}_{rec}}^{\vec{r}_{tra}} N_e B \cos \theta .ds}_{SECOND.ORDER}$$

Being K_1=40.3 and K2=1.13x10^{12} in MKS system units.

GPS ionospheric terms: group delay

$$\psi_1 = Ae^{i(\omega t - kx)}$$

$$\psi_2 = Ae^{i([\omega+\delta\omega]t - [k+\delta k]x)} = Ae^{i(\delta\omega \cdot t - \delta k \cdot x)} e^{i(\omega t - kx)}$$

$$\psi_1 + \psi_2 = \underbrace{A\cos\left(\frac{\delta\omega}{2}t - \frac{\delta k}{2}x\right)e^{i(\delta\omega \cdot t - \delta k \cdot x)/2}}_{Modulated\ .signal} e^{i(\omega t - kx)}$$

$$v_g = \frac{\delta\omega}{\delta k} \approx \frac{d\omega}{dk} = \left\{v_p = \frac{\omega}{k}\right\} = v_p + k\frac{dv_p}{dk}$$

$$n_g - n_p = \frac{c}{v_p v_g}(v_p - v_g) \approx \cdots \approx f\frac{dn_p}{df} = \omega\frac{dn_p}{d\omega}$$

$$n_g - n_p = \left\{n_p = 1 - \frac{1}{2}\frac{\omega_p^2}{\omega^2} - \frac{1}{2}\frac{\omega_p^2\omega_g}{\omega^3}\right\} = \frac{\omega_p^2}{\omega^2} + \frac{3}{2}\frac{\omega_p^2\omega_g}{\omega^3}$$

$$n_g = 1 + \frac{1}{2}\frac{\omega_p^2}{\omega^2} + \frac{\omega_p^2\omega_g}{\omega^3}$$

$$\delta\rho_L = \underbrace{-\frac{K_1}{f^2}STEC}_{FIRST\ .ORDER} \underbrace{-\frac{K_2}{f^3}\overbrace{\int_{\vec{r}_{rec}}^{\vec{r}_{tra}} N_e B\cos\theta\, .ds}^{F}}_{SECOND\ .ORDER}$$

$$\delta\rho_P = \underbrace{+\frac{K_1}{f^2}STEC}_{FIRST\ .ORDER} \underbrace{+2\frac{K_2}{f^3}F}_{SECOND\ .ORDER}$$

Being K_1=40.3 and K2=1.13x10^{12} in MKS system units.

UNIVERSITAT POLITÈCNICA DE CATALUNYA BARCELONATECH

IonSAT

Ionospheric combination of GPS obs.

- **The ionospheric (geometry-free) combination of carrier phases and pseudoranges provides the STEC (in first order, <0.1% error), but affected by biases (ambiguities for LI -can be large- and instrumental delays for PI -typically of few meters-).**
- **The pseudoranges (PI) can be very affected by multipath and noise measurement (1 meter or more).**
- **Thus the ionospheric sounding with GPS should be based on carrier phase measurements, dealing with the carrier phase ambiguity estimation.**

$$\left.\begin{aligned} L &= \rho^{*} + \lambda . b + \lambda . w + pc_{L} - \frac{K_1}{f^2} STEC - \frac{K_2}{f^3} F \\ P &= \rho^{*} + D + pc_{P} + \frac{K_1}{f^2} STEC + \frac{2K_2}{f^3} F \end{aligned}\right\} \quad STEC = \int_{\vec{r}_{rec}}^{\vec{r}_{tra}} N_e \, ds \qquad F = \int_{\vec{r}_{rec}}^{\vec{r}_{tra}} N_e B \cos\theta \cdot ds$$

$$L_I = L_1 - L_2 = \left\{\begin{matrix} 1st - order \\ error < 0.1\% \end{matrix}\right\} = \underbrace{K_1 \frac{(f_1^2 - f_2^2)}{f_1^2 f_2^2}}_{\alpha \approx 1.05 \cdot 10^{-17} \; m / e- / m^2} STEC + \underbrace{\lambda_1 b_1 - \lambda_2 b_2}_{BI} + W_I + pc_I$$

$$P_I = P_2 - P_1 = \cdots = \underbrace{K_1 \frac{(f_1^2 - f_2^2)}{f_1^2 f_2^2}}_{\alpha \approx 1.05 \cdot 10^{-17} \; m / e- / m^2} STEC + D_I + pc_I$$

$$L_I - P_I = B_I + W_I - D_I$$

Being K_1=40.3 and K2=1.13x10[12] in MKS system units, ρ* the non-dispersive terms (geometric distance, clocks errors, tropospheric delay,…), λb the ambiguity and D the instrumental delay.

Ionospheric-free combinations

$$\left.\begin{aligned} L &= \rho^{*} + \lambda . b + \lambda . w + pc_{L} - \frac{K_1}{f^2} STEC - \frac{K_2}{f^3} F \\ P &= \rho^{*} + D + pc_{P} + \frac{K_1}{f^2} STEC + \frac{2K_2}{f^3} F \end{aligned}\right\} \quad \begin{aligned} STEC &= \int_{\vec{r}_{rec}}^{\vec{r}_{tra}} N_e \, ds \\ F &= \int_{\vec{r}_{rec}}^{\vec{r}_{tra}} N_e B \cos\theta \cdot ds \end{aligned}$$

$$L_c = \frac{f_1^2 L_1 - f_2^2 L_2}{f_1^2 - f_2^2} = \rho^{*} + \lambda_n \left(\frac{f_1 b_1 - f_2 b_2}{f_1 - f_2} + \frac{f_1 w_1 - f_2 w_2}{f_1 - f_2} \right) + pc_c + \underbrace{K_2 \frac{STEC \cdot B \cdot \cos\theta}{f_1 f_2 (f_1 + f_2)}}_{I_2}$$

$$P_c = \frac{f_1^2 P_1 - f_2^2 P_2}{f_1^2 - f_2^2} = \rho^{*} - 2K_2 \frac{STEC \cdot B \cdot \cos\theta}{f_1 f_2 (f_1 + f_2)} + pc_c$$

$$L_c - P_c = \lambda_n \left(\frac{f_1 b_1 - f_2 b_2}{f_1 - f_2} + \frac{f_1 w_1 - f_2 w_2}{f_1 - f_2} \right) + 3K_2 \frac{STEC \cdot B \cdot \cos\theta}{f_1 f_2 (f_1 + f_2)}$$

Being K_1=40.3 and K2=1.13x10^{12} in MKS system units, ρ* the non-dispersive terms (geometric distance, clocks errors, tropospheric delay,…), λb the ambiguity and D the instrumental delay.

UNIVERSITAT POLITÈCNICA DE CATALUNYA BARCELONATECH

IonSAT

Extracting the STEC from iono. Li (1)

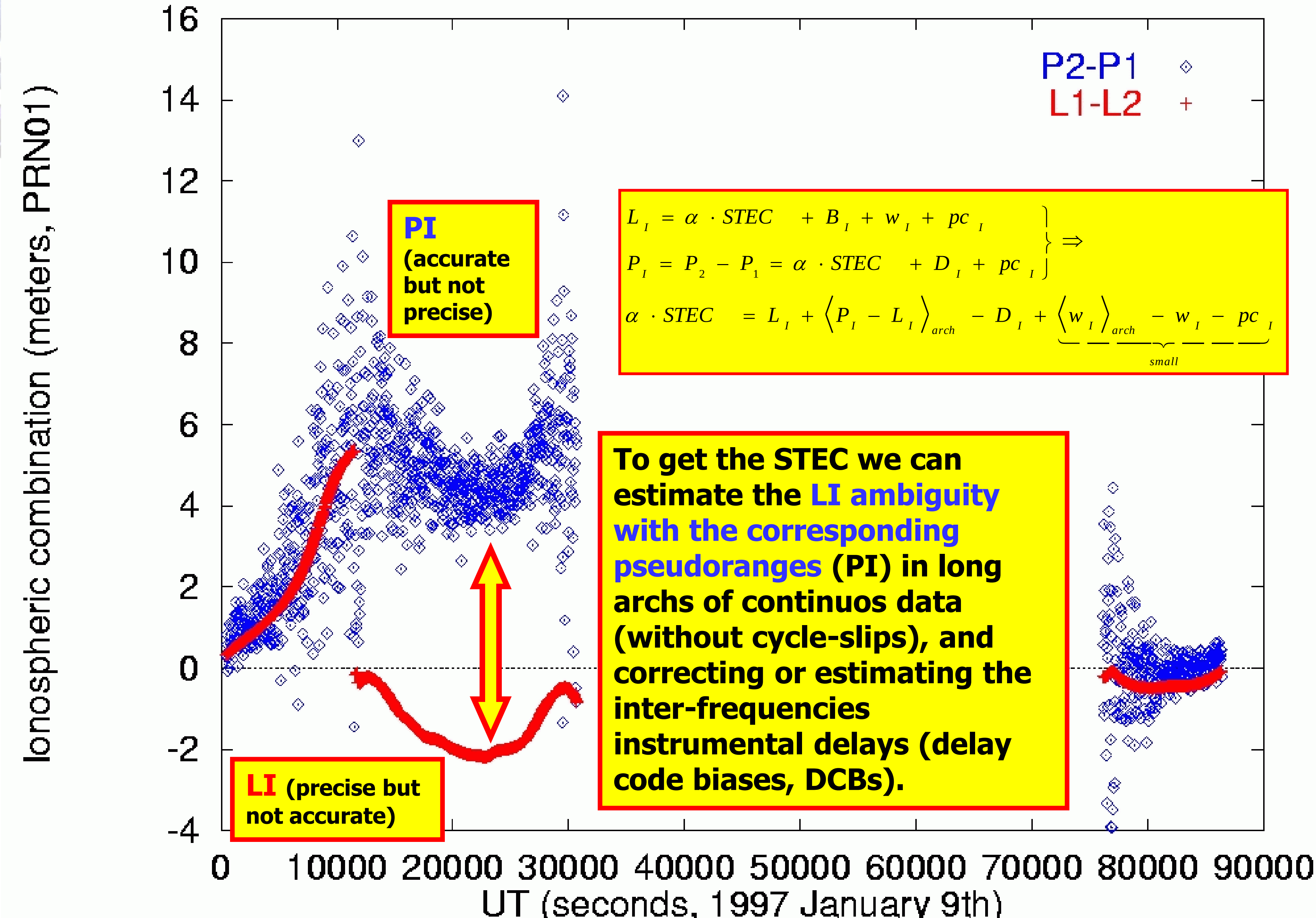

$$L_I = \alpha \cdot STEC + B_I + w_I + pc_I$$
$$P_I = P_2 - P_1 = \alpha \cdot STEC + D_I + pc_I \quad \Rightarrow$$
$$\alpha \cdot STEC = L_I + \langle P_I - L_I \rangle_{arch} - D_I + \underbrace{\langle w_I \rangle_{arch} - w_I - pc_I}_{small}$$

To get the STEC we can estimate the LI ambiguity with the corresponding pseudoranges (PI) in long archs of continuos data (without cycle-slips), and correcting or estimating the inter-frequencies instrumental delays (delay code biases, DCBs).

Extracting the STEC from iono. Li (2)

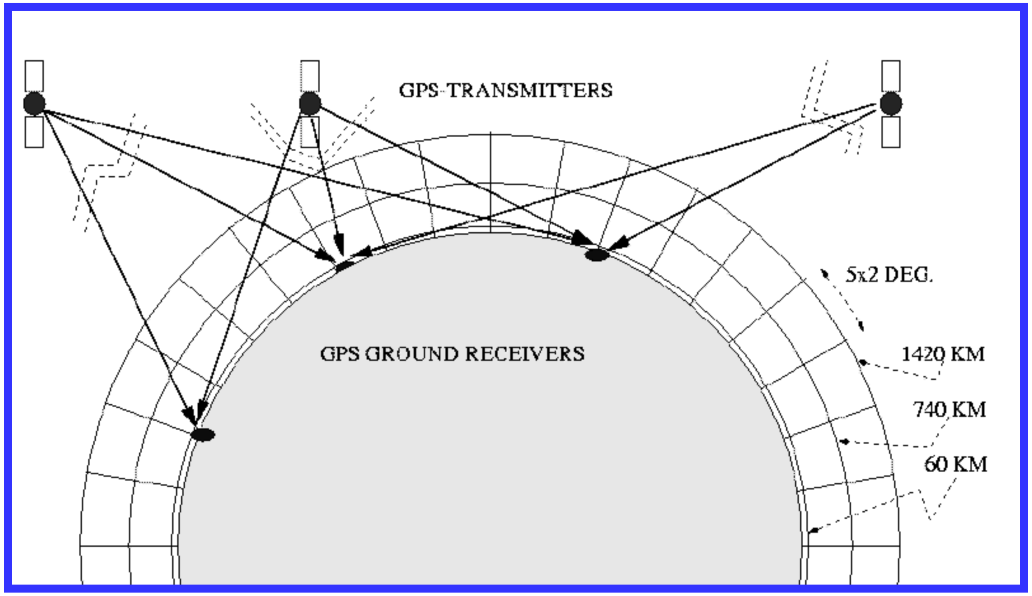

•**Another way to estimate the LI ambiguity is to use just carrier phase data LI, estimating (and decorrelating) it simultaneously to electron content by taking into account the geometry variation (and in the context of a Kalman filter). Not affected by PI multipath & quite convenient for real-time.**

$$L_I = STEC + B_I = \int_{REC}^{SAT} N_e \, dl + B_I = \sum_i \sum_j \sum_k (N_e)_{i,j,k} \Delta s_{i,j,k} + B_I$$

UNIVERSITAT POLITÈCNICA DE CATALUNYA BARCELONATECH

Extracting the STEC from iono. Li (3)

We can get the STEC variation directly (without DCBs and reducing the multipath error) in one sidereal day,(23h56m approx.) in which the geometry transmitter-receiver repeats (the GPS satellite describes 2 orbits and the fixed GPS receiver on the ground describes 1 rotation).

$$\alpha \cdot STEC = L_I + \langle P_I - L_I \rangle_{arch} - D_I + \underbrace{\langle w_I \rangle_{arch} - w_I - pc_I}_{small} \Rightarrow$$

$$\alpha \cdot \delta STEC = \delta L_I + \langle \delta P_I - \delta L_I \rangle_{\delta - arch}$$

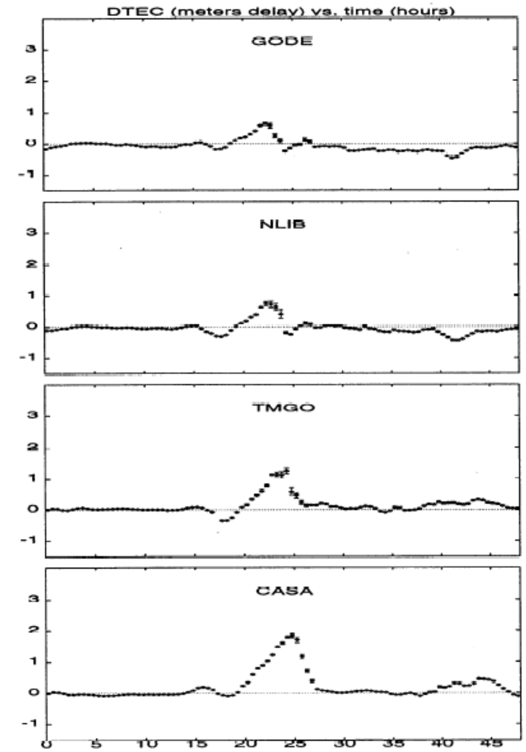

Figure 3. Mean TEC variation at 30-minute intervals are plotted for four permanent GPS stations in North America which are distributed along similar declinations (40 deg. approximately) and with longitudes separated by ≃10-15 deg.: GODE at 283 deg., NLIB at 268 deg., TMGO at 255 deg. and CASA at 241 deg. The data were also collected on 17, 18 and 19 October 1995 and the variation has been calculated referred to 17 October 1995 in meters of delay. The horizontal axis is the time from 18 October 0h UT in hours.

(More details in Hernández-Pajares, M., J.M. Juan, J. Sanz, High resolution TEC monitoring method using permanent GPS receivers, *Geophysical Research Letters, Vol.24, No.13, 1643-1646, July 1, 1997*)

- Obtaining the electron content

Ground-based vs. space-based GPS data

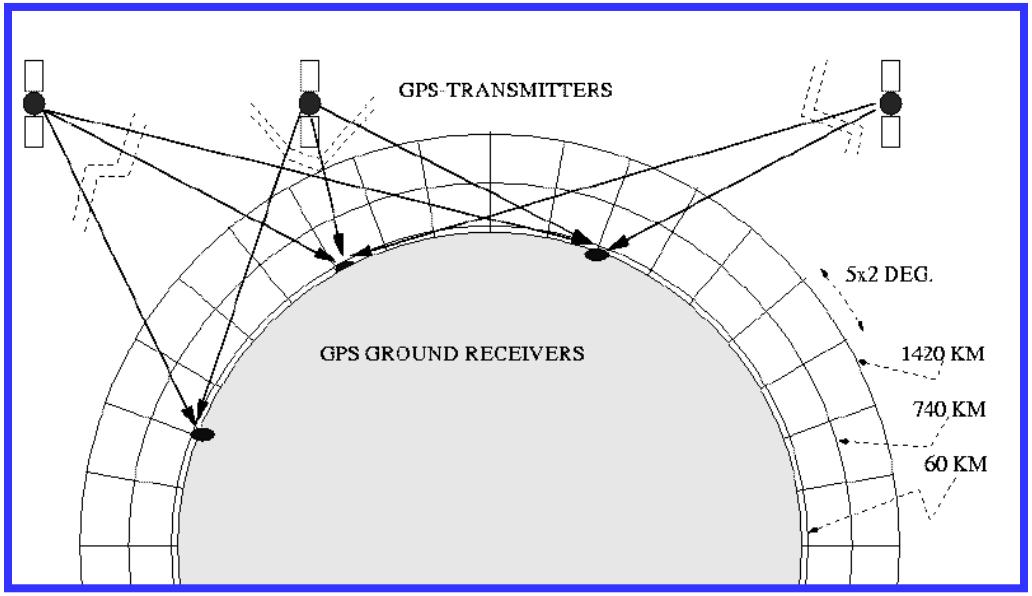

- The **ground based GPS observations are mainly vertical**: so they can provide VTEC estimates with **high horizontal spatial (and temporal) resolution**.
- The **space-based GPS observations (such as those from LEOs) can provide limb observations, which are mainly horizontal**. They can provide **high vertical resolution**.

UNIVERSITAT POLITÈCNICA DE CATALUNYA BARCELONATECH

IonSAT

- Using ground-based GNSS data (VTEC)

From STEC to VTEC: Single layer model

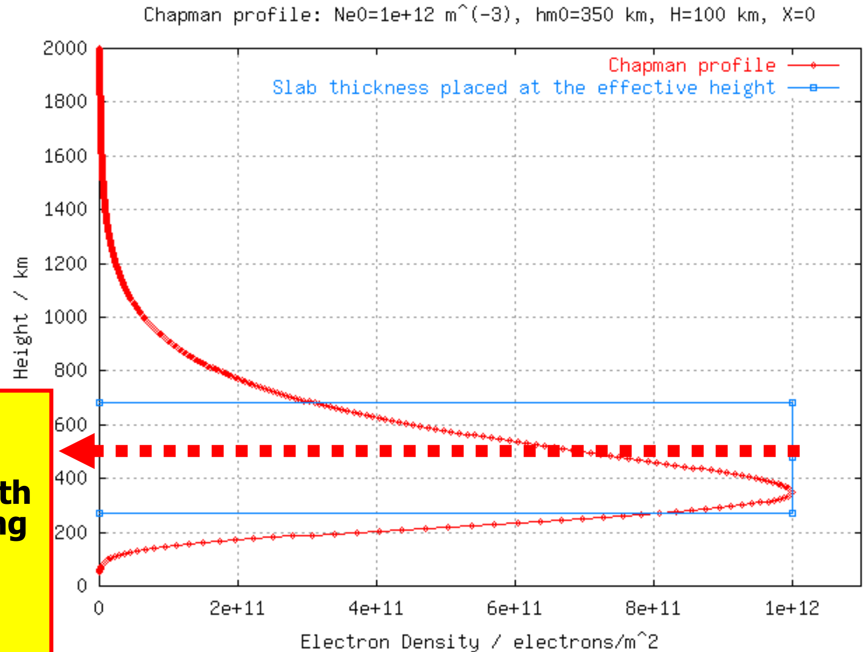

Effective Height
(Sun at zenith and assuming the slab thickness width, VTEC/Ne)

One simple way of obtaining the VTEC from STEC is based on the assumption of electron content concentrated at one shell at fixed *effective height* ("single layer model").

But such effective height can change in terms of Local Time (daylight/night), latitude and geomagnetic activity.

You can see at right the effective height change in terms of the Sun-zenith angle predicted by the Chapman model.

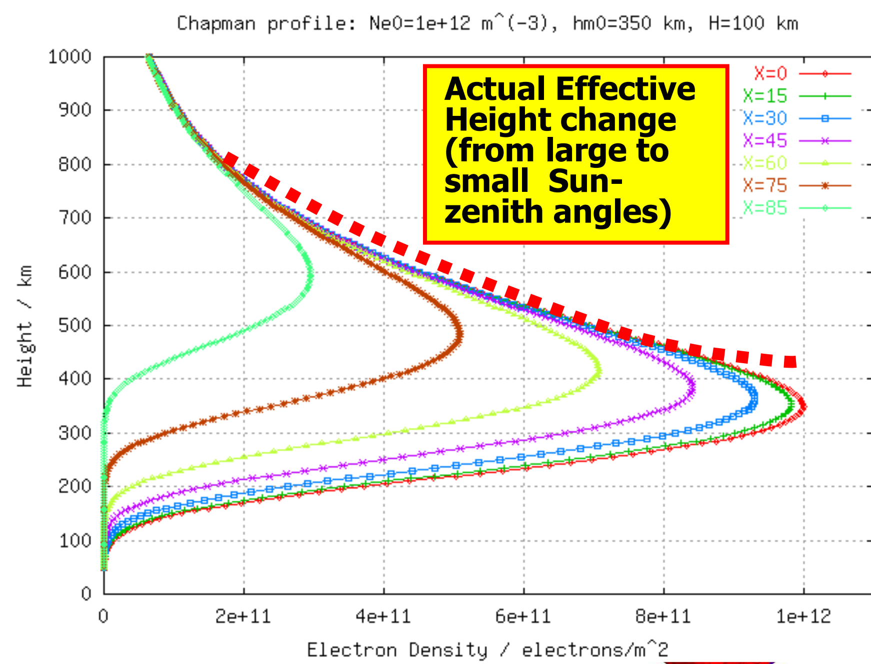

UPC
UNIV
DE C
BARC

Ionosphere & photoionization: Chapman model

$$STEC = M \cdot VTEC$$

$$\left.\begin{array}{l} M = \dfrac{1}{\sin E'} \\ r\cos E = r'\cos E' \end{array}\right\} M = \{r' = r+h\} = \dfrac{1}{\sqrt{1-\dfrac{r^2}{(r+h)^2}\cos^2 E}} \Bigg\} VTEC = STEC \cdot \sqrt{1-\dfrac{r^2}{(r+h)^2}\cos^2 E} \Rightarrow$$

$$\Rightarrow \underbrace{STEC \cdot \sin E}_{h\to 0^+} < VTEC < \underbrace{STEC}_{h\to +\infty}$$

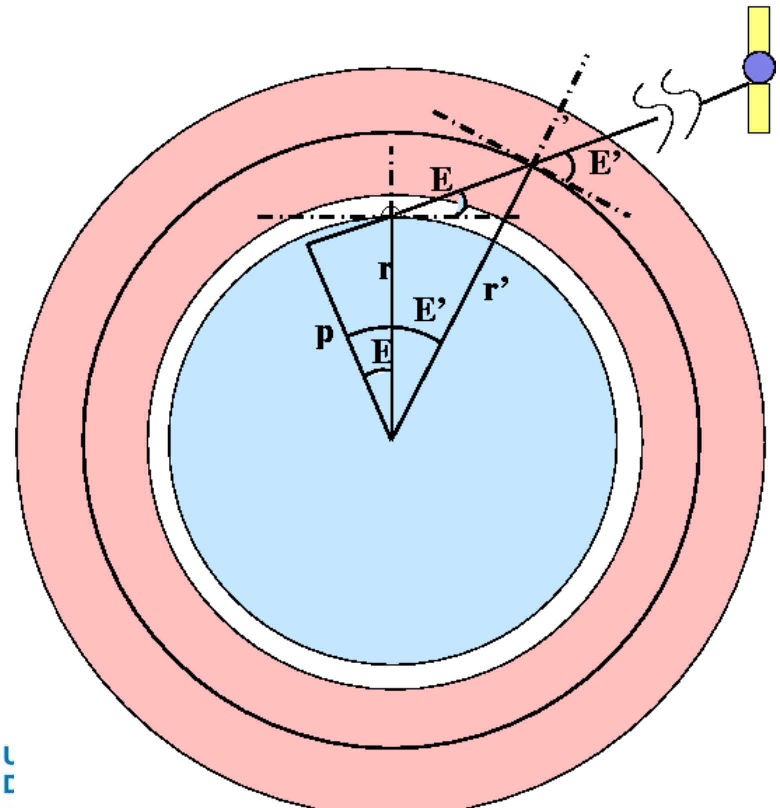

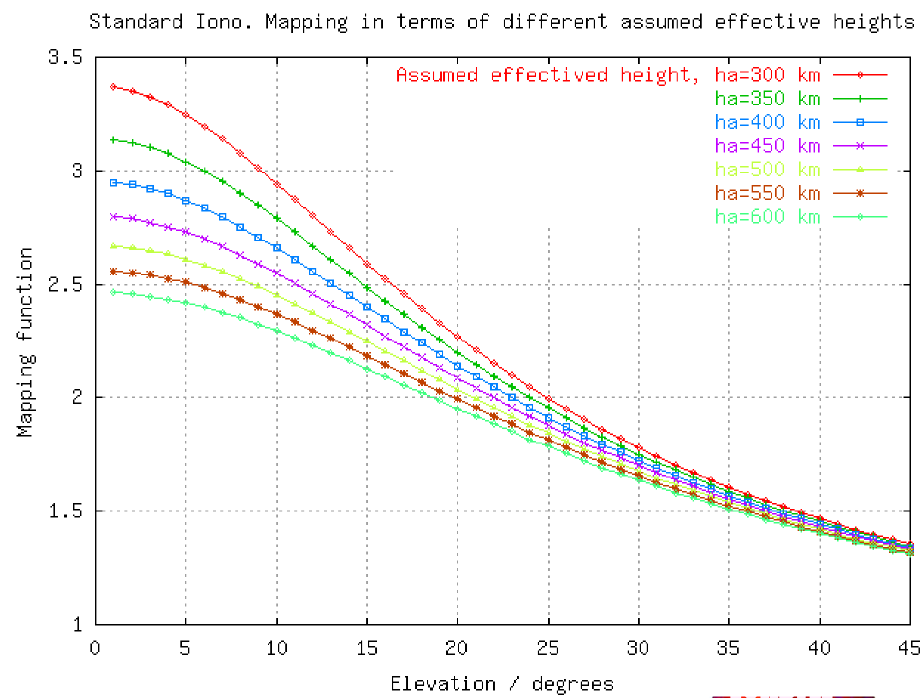

Estimating the ionospheric distribution

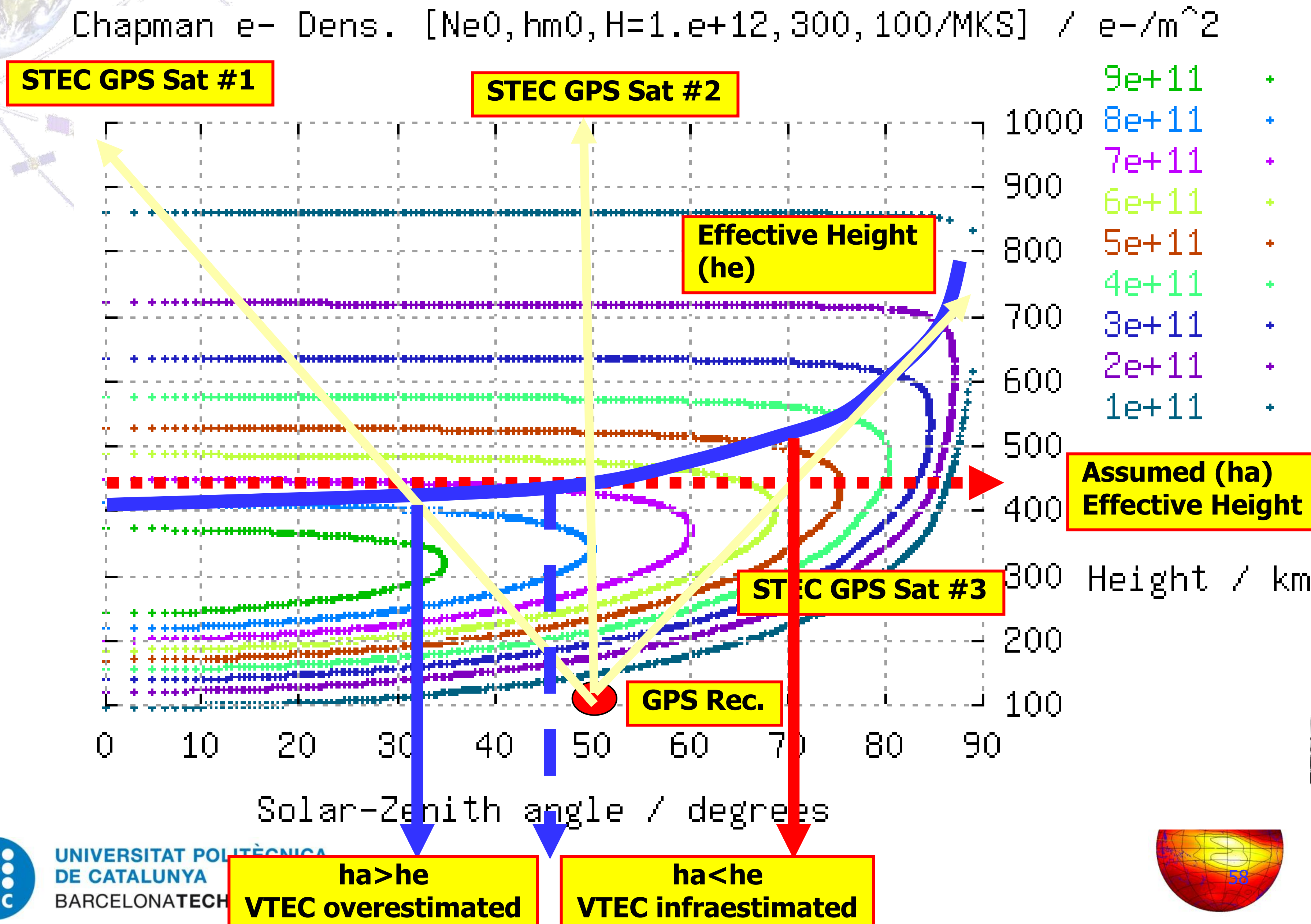

UNIVERSITAT POLITÈCNICA DE CATALUNYA
UPC
BARCELONATECH

Benefits of combining different kind of Iono. Obs. in a 3D Voxel Model

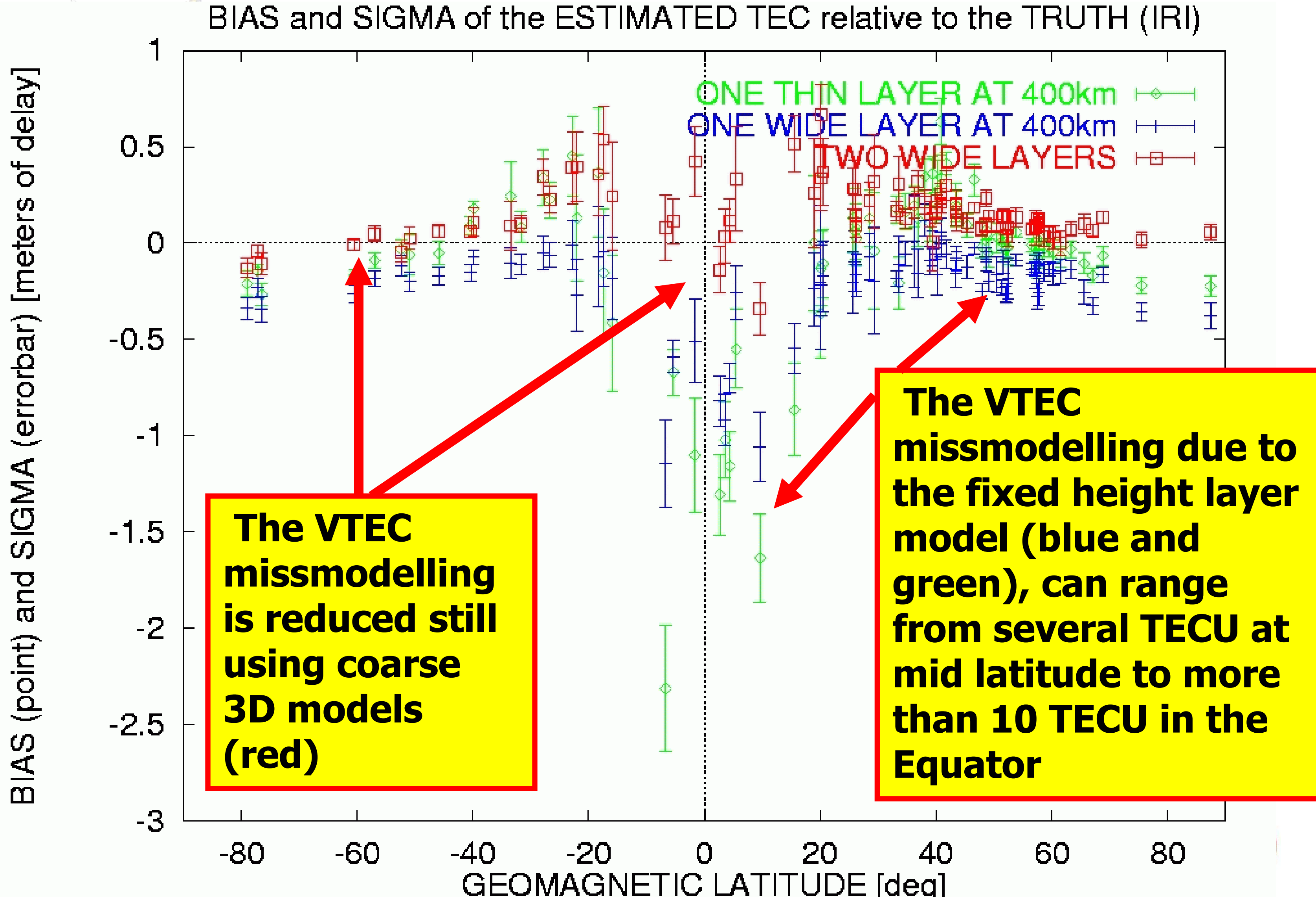

Real-time iono. model

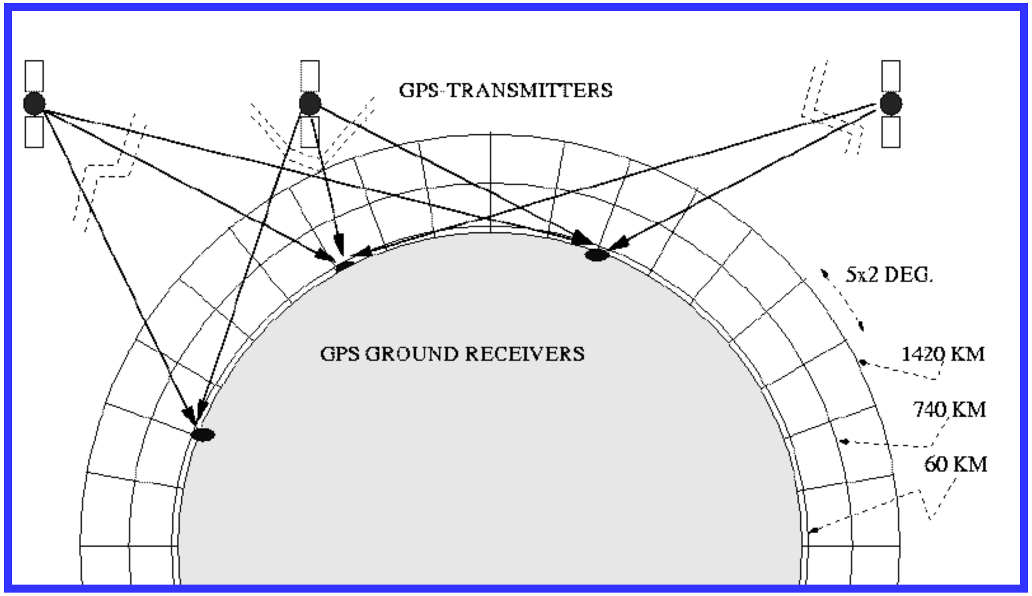

- Only carrier phase data needed
- With tomographic description: more accurate
- DCB's no longer needed
- No affected by pseudorange multipath

$$L_I = STEC + B_I = \int_{REC}^{SAT} N_e \, dl + B_I = \sum_i \sum_j \sum_k (N_e)_{i,j,k} \Delta s_{i,j,k} + B_I$$

UNIVERSITAT POLITÈCNICA DE CATALUNYA
BARCELONATECH

Tomographic implementation

GNSS satellite orbits & clocks, GNSS measurements

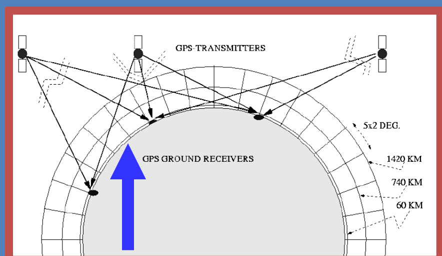

Compute the length of each ray intersection with each illuminated voxel, Δs

$$L_I = STEC + B_I = \int_{REC}^{SAT} N_e \, dl + B_I = \sum_i \sum_j \sum_k (N_e)_{i,j,k} \Delta s_{i,j,k} + B_I$$

Estimating X = (Ne…,Bi,…) in a fordward Kalman filter solving Y = A X, with covariance matrices P:
Ne for each voxel-time (random-walk) and pair receiver-satellite cont. Arch (random variable)

Initialization

$\hat{X}(0)$, $P_{\hat{X}(0)}$

Prediction

$$\hat{X}^-(n) = \Phi \hat{X}(n-1)$$

$$P_{\hat{X}^-(n)} = \Phi P_{\hat{X}(n-1)} \Phi^t + Q$$

$\hat{X}^-(n)$, $P_{\hat{X}^-(n)}$

Measurements

$Y(n)$, $P_{Y(n)}$

Estimation

$$\hat{X}(n) = P_{\hat{X}(n)} \cdot \left[A^t P^{-1}_{Y(n)} Y(n) + P^{-1}_{\hat{X}^-(n)} \hat{X}^-(n) \right]$$

$$P_{\hat{X}(n)} = \left[A^t P^{-1}_{Y(n)} A + P^{-1}_{\hat{X}^-(n)} \right]^{-1}$$

$\hat{X}(n)$, $P_{\hat{X}(n)}$

IonSAT

UNIVERSITAT POLITÈCNICA DE CATALUNYA BARCELONATECH

M.Hernández-Pajares et al.

WARTK: Combining real-time Ionospheric & Geodetic models

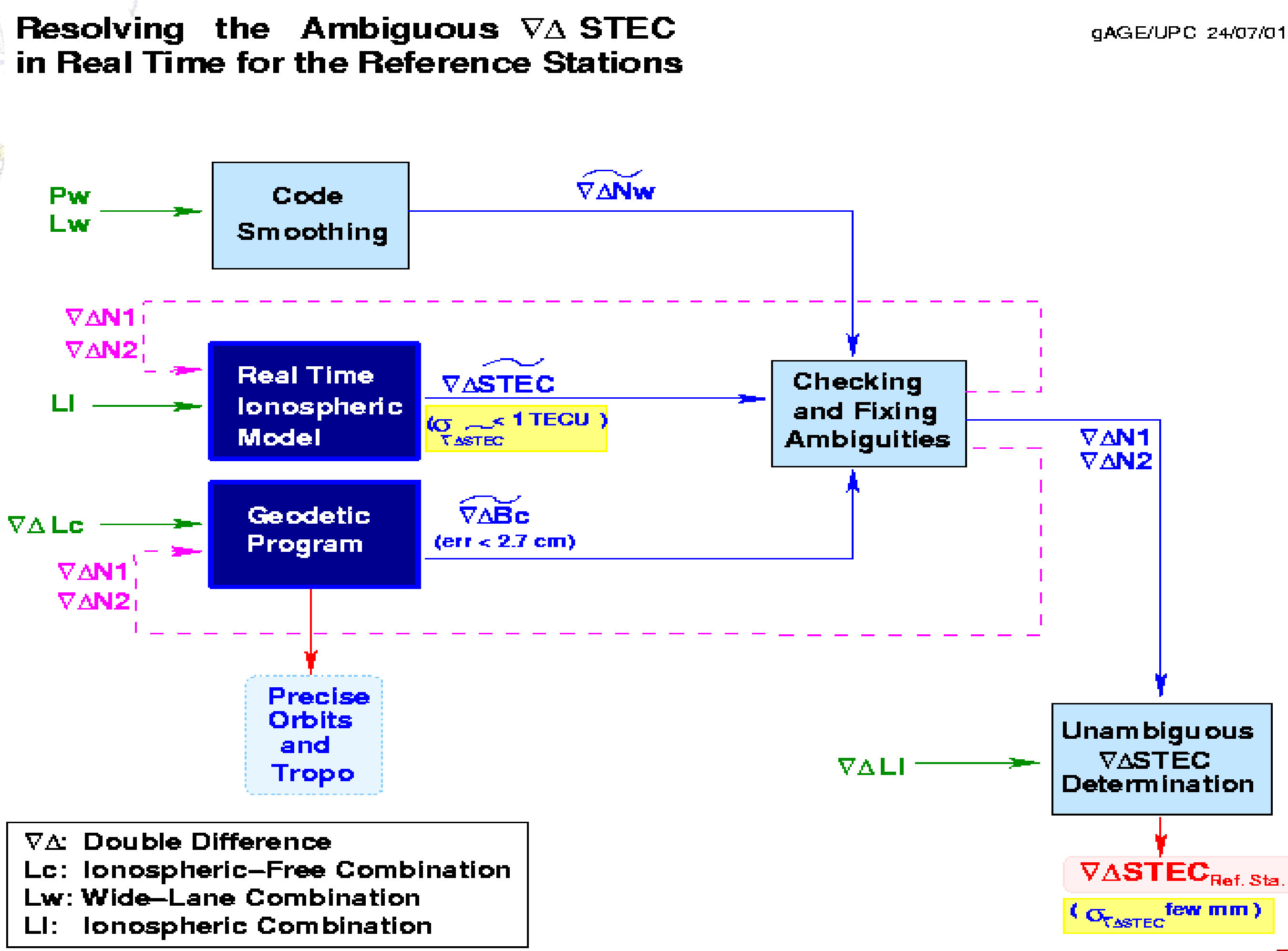

UNIVERSITAT POLITÈCNICA DE CATALUNYA
BARCELONATECH

onSAT

Accurate STEC from fixed GPS sites thousands km far

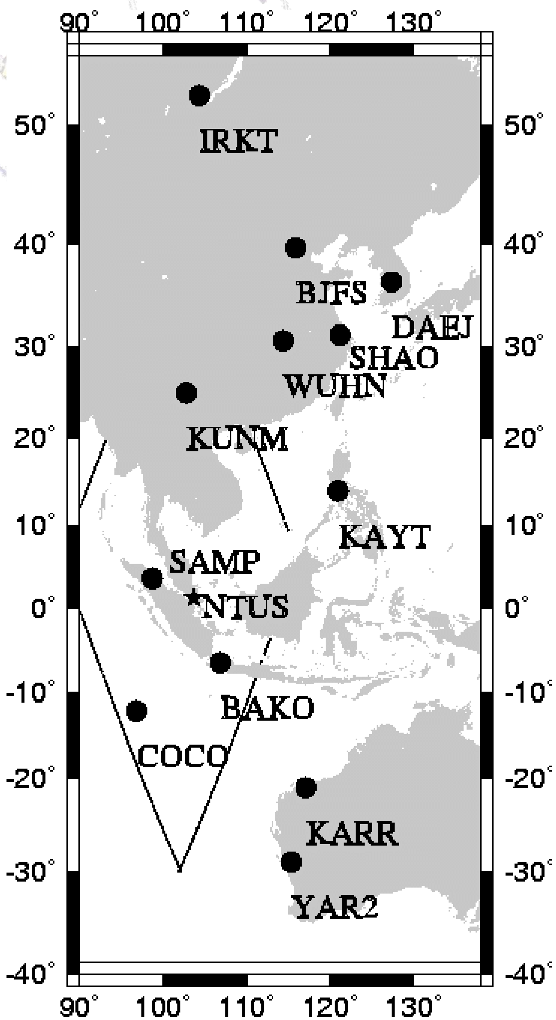

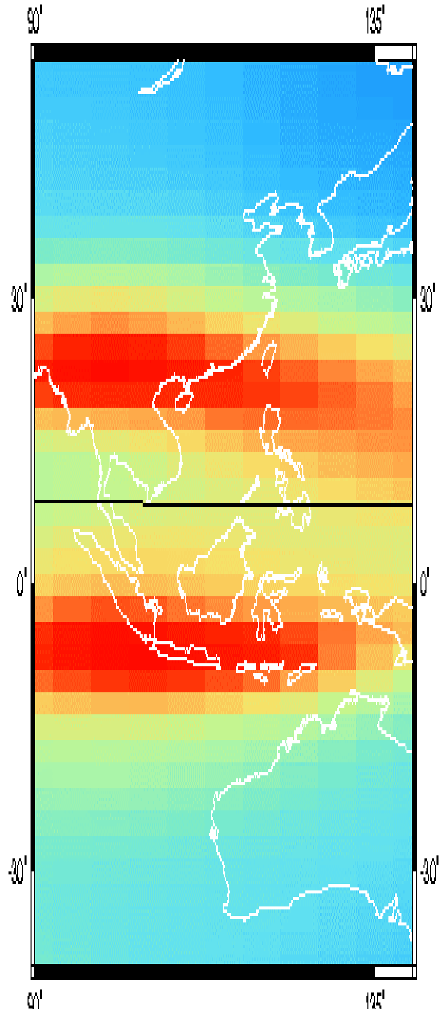

New Experiment:

- 13 IGS stations
- Distances: 1000-3000km
- Including equator, tropics
- 4 weeks 2001 65-92
- Solar Max. conditions
- Seasonal Max.
- With high geom. activity

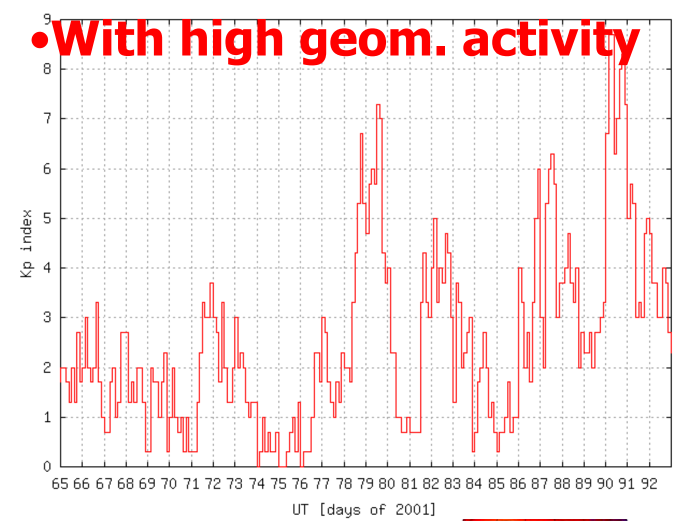

UNIVERSITAT POLITÈCNICA DE CATALUNYA
BARCELONATECH

Tomo Real-Time (green) vs. TOPEX VTEC (red)

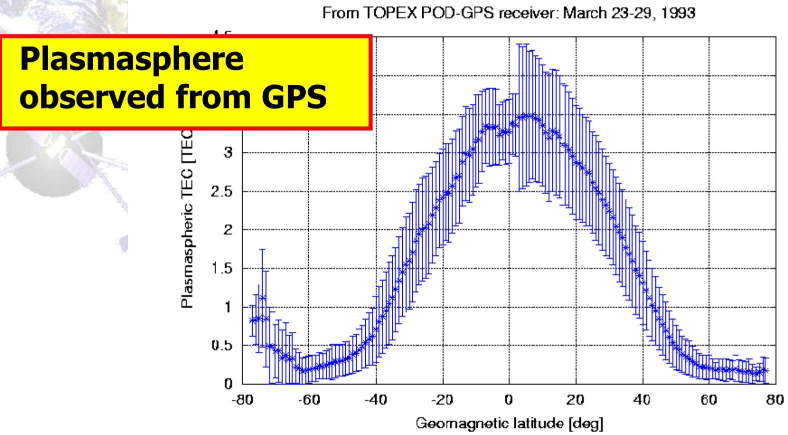

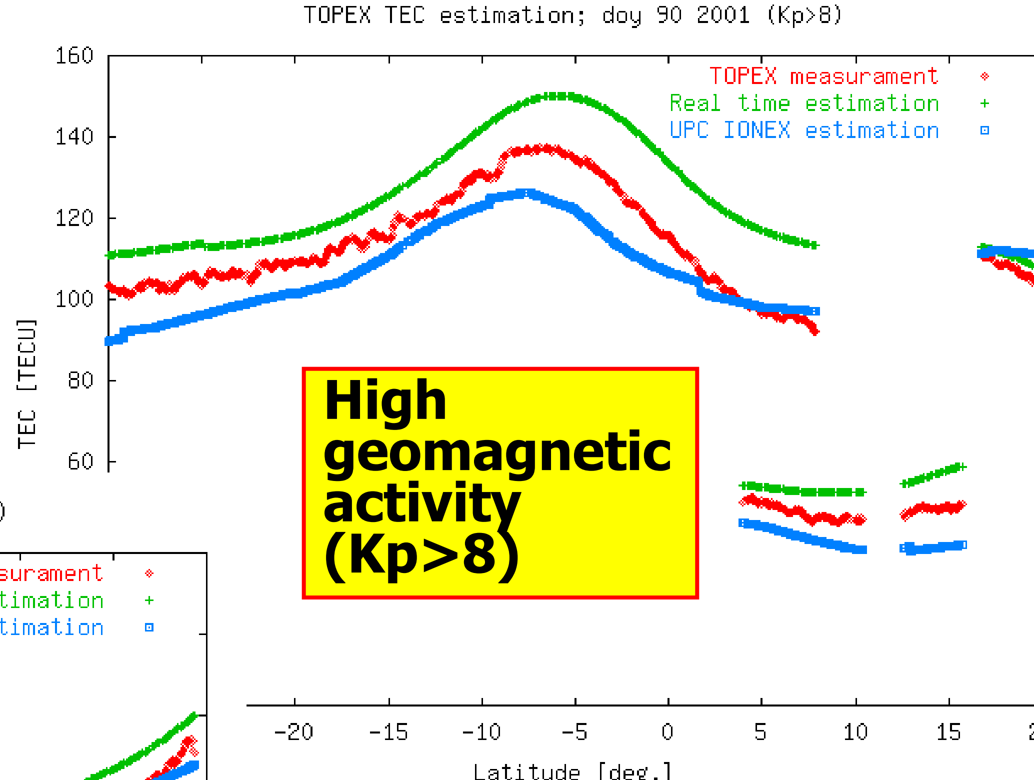

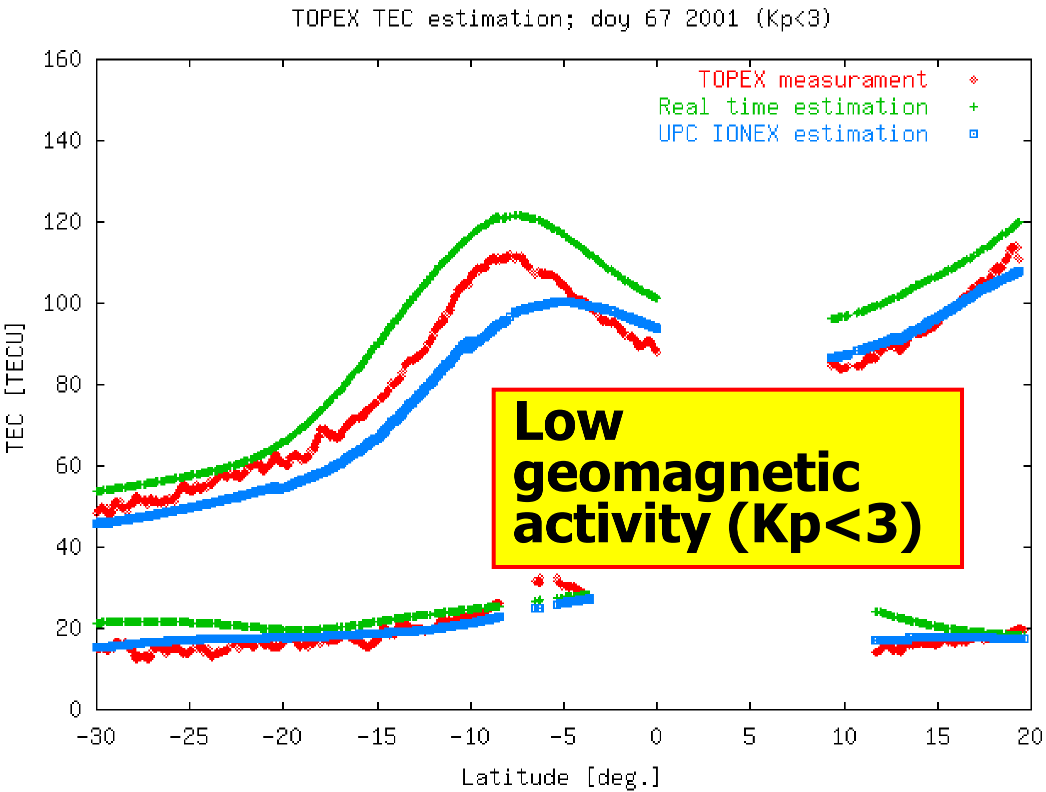

Real-time DDSTEC vs. truth

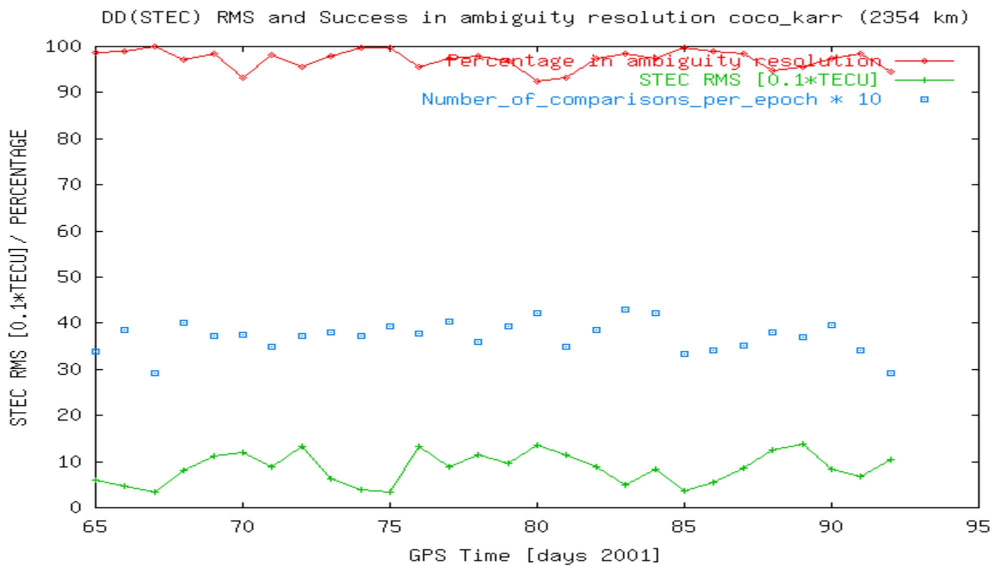

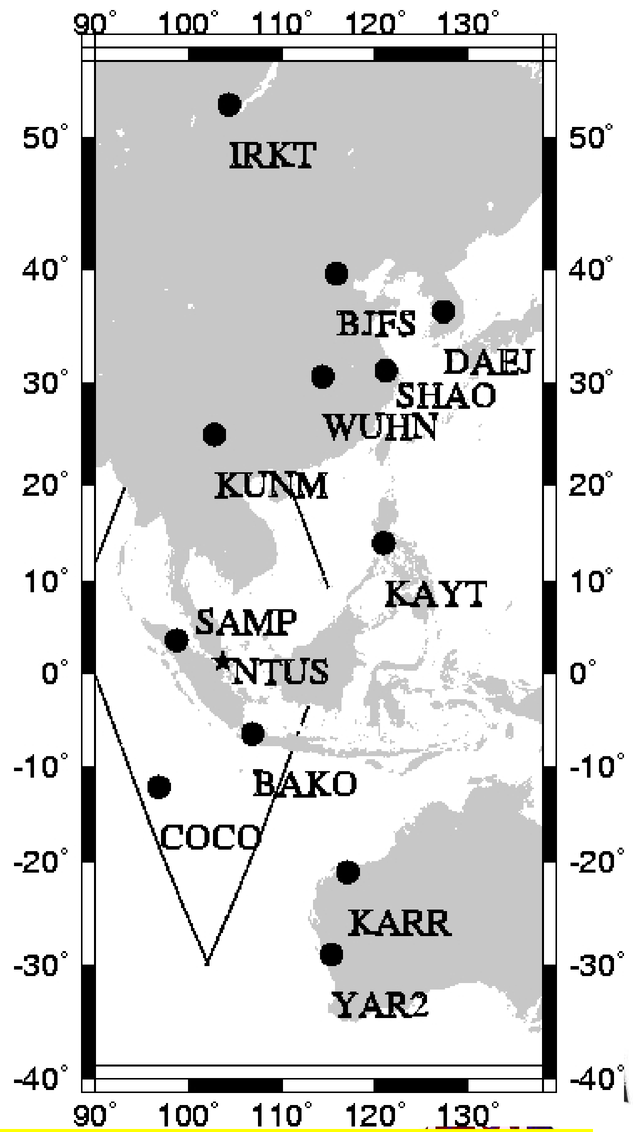

Sta.	Ref.	Dist. (km)	% Succ.	RMS [TECU]	# Obs.
IRKT	DAEJ	2507	93	1.2	8329
BJFS	DAEJ	1067	91	1.4	8131
KUNM	DAEJ	2640	95	1.0	3900
WUHN	DAEJ	1369	92	1.4	6358
SAMP	KARR	3341	95	1.1	6441
COCO	KARR	2354	97	0.9	9963
BAKO	KARR	1939	90	1.5	6121
YAR2	KARR	909	97	0.8	12630

(More details in Hernández-Pajares, M., J.M. Juan, J. Sanz, O.L. Colombo, Improving the real-time ionospheric determination from GPS sites at Very Long Distances over the Equator, *J.Geophys.Res., 107(A10), 1296, October 2002*)

UPC

- Using space-based GNSS data as well (N_e)

UNIVERSITAT POLITÈCNICA DE CATALUNYA BARCELONATECH

IonSAT

- Space-based and ground-based GNSS data

UNIVERSITAT POLITÈCNICA
DE CATALUNYA
BARCELONATECH

IonSAT

Estimating electron density in a 3D Voxel model (regional/global)

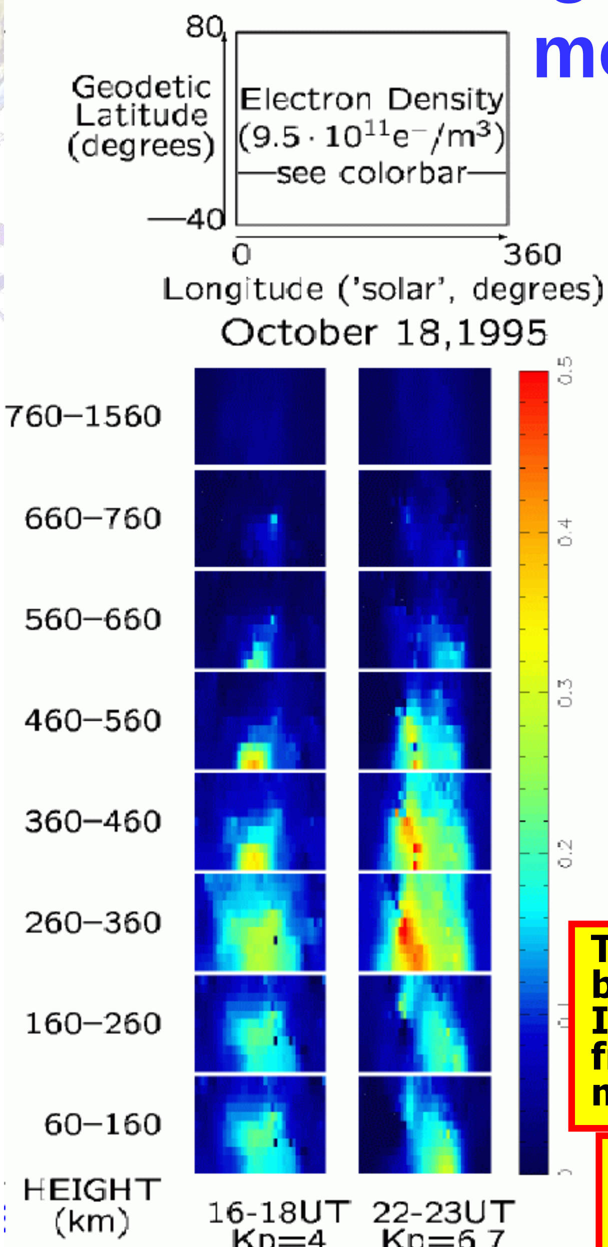

Different kind of data are mixed: occultation and ground GPS data.

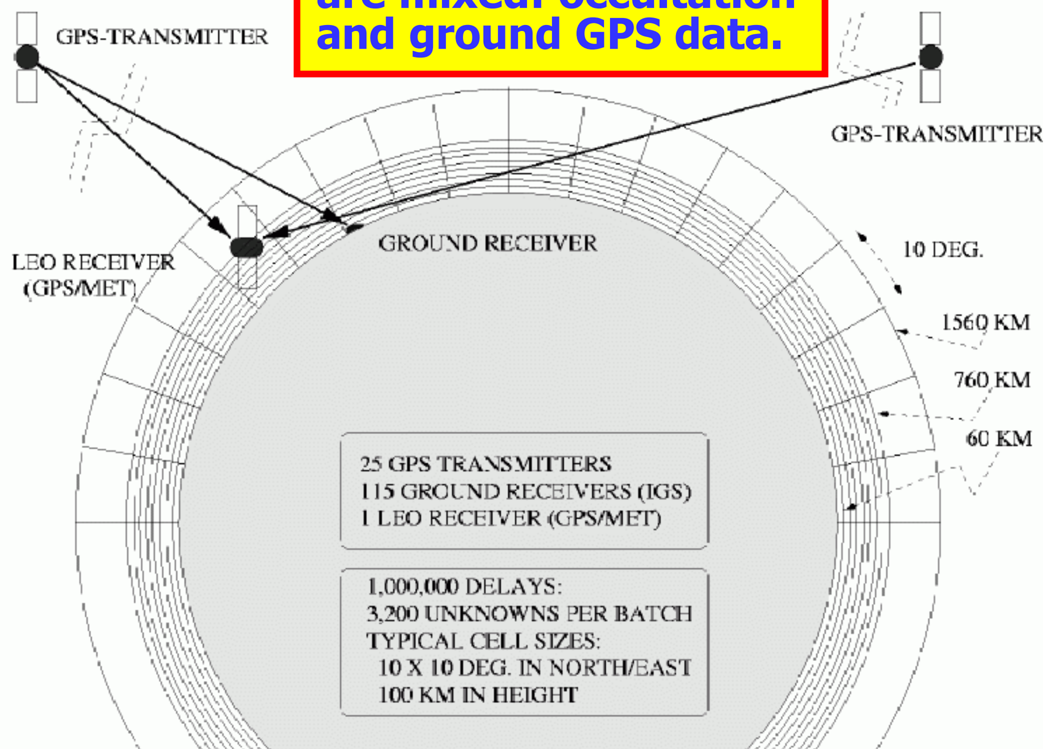

This is an example corresponding to the combination of both complementary type of GPS data (ground-based from IGS network and space-based from GPS/MET LEO) in the framework of a 3D voxel tomographic model solved by means of a Kalman filter (Oct.18, 1995 geomagnetic storm).

More details in: Hernández-Pajares M., J.M. Juan, J. Sanz and J.G. Sole, Global observation of the ionospheric electronic response to solar events using ground and LEO GPS data, *Journal of Geophysical Research-Space Physics*, Vol.61, p.1237-1247, 1998.

DE CATALUNYA
BARCELONATECH

Classical Abel transform (independent estimation for each occultation)

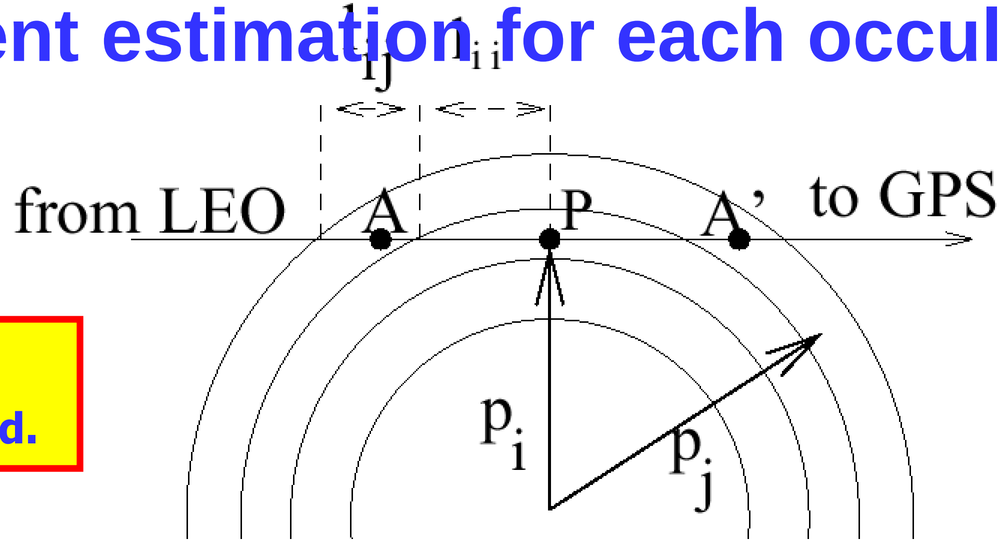

Just the given occultation GPS data are processed.

The classical spherical symmetry hypothesis can be formulatted as:

$$N_e(LT, LAT, H) = \Phi(H)$$

Recursive solution starting from the outer ray. STEC corresponding to the impact parameter p_i:

$$STEC(p_i) = 2 \cdot l_{ii} \cdot N_e(p_i) + \sum_{j=1}^{j=i-1} 2 \cdot l_{ij} \cdot N_e(p_j)$$

UNIVERSITAT POLITÈCNICA DE CATALUNYA BARCELONATECH

Abel Transform vs. 3D-Voxel model

	Abel Transform	3D Voxels
Vertical resolution	$\simeq 1$ km	Tens / hundred km
Computational load	Low ($\simeq 10^2$ unk.)	High ($> 10^3$ unk.)
Sph. Sym. Assump.	Yes	No
Topside mismod.	Yes	No
Assimilation capab.	No	Yes

Our goal: maintaining its other advantages, to avoid these limitations of the classical Abel approach:

- Overcoming the spherical symmetry assumption.
- Overcoming the topside electron content mismodelling.

Separability concept

- $N_e(LT,\quad AT,H) = VTEC(LT,LAT)\cdot F(H)$

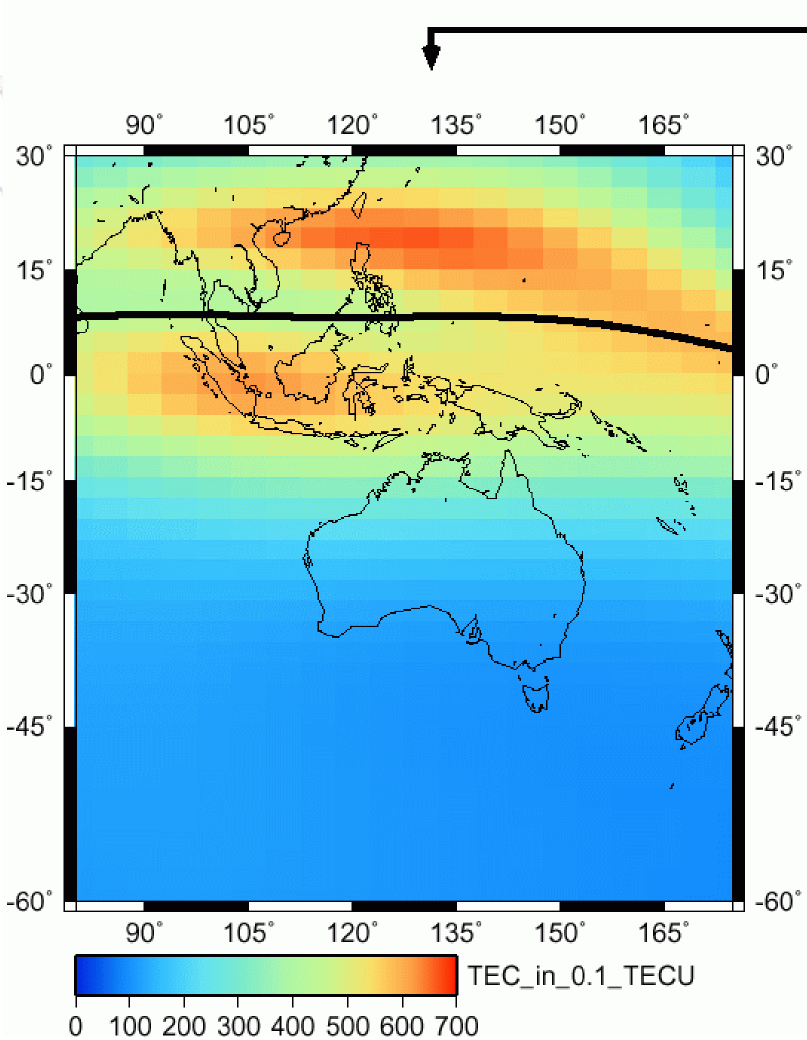

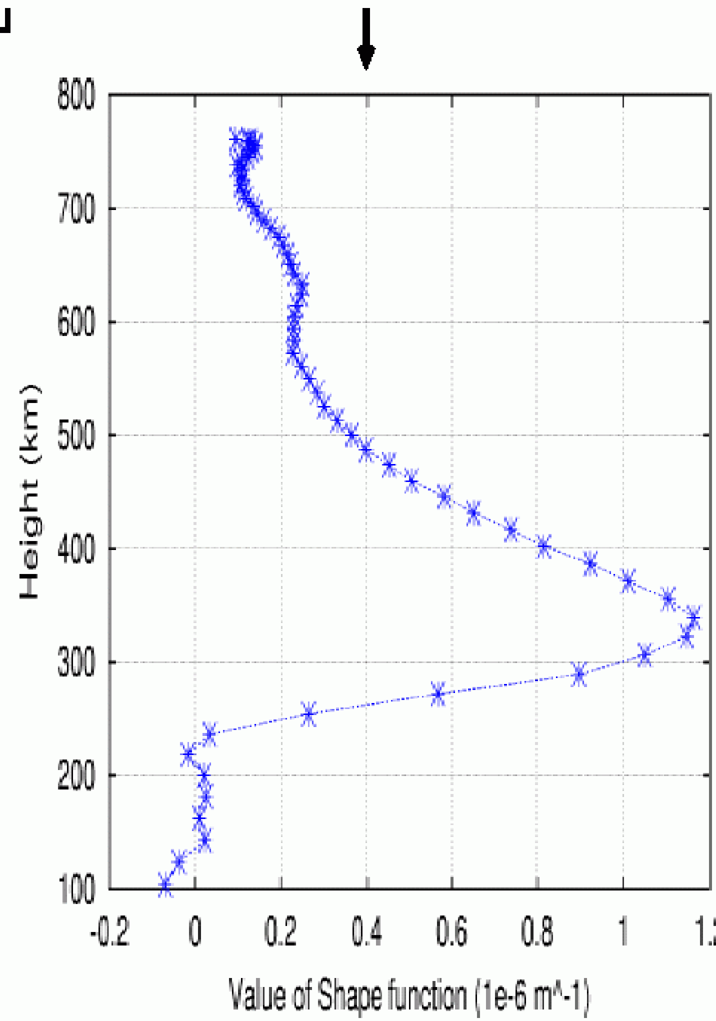

Improved Abel transform

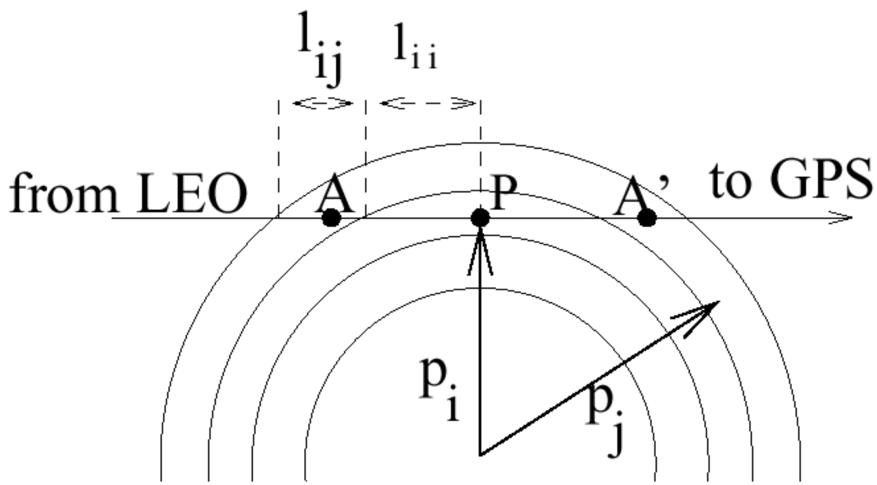

Let's assume a more general hypothesis that just the spherical symmetry:

$$N_e(LT, LAT, H) = VTEC(LT, LAT) \cdot F(H)$$

Starting from the outer ray, the STEC corresponding to the impact parameter p_i can be modeled by:

$$STEC(p_i) = 2 \cdot l_{ii} \cdot VTEC(LT_{ii}, LAT_{ii}) \cdot F(p_i) + \sum_{j=1}^{j=i-1} l_{ij} \cdot \left[VTEC(LT_{ij}, LAT_{ij}) + VTEC(LT'_{ij}, LAT'_{ij})\right] \cdot F(p_j)$$

Benefits of separability hypothesis

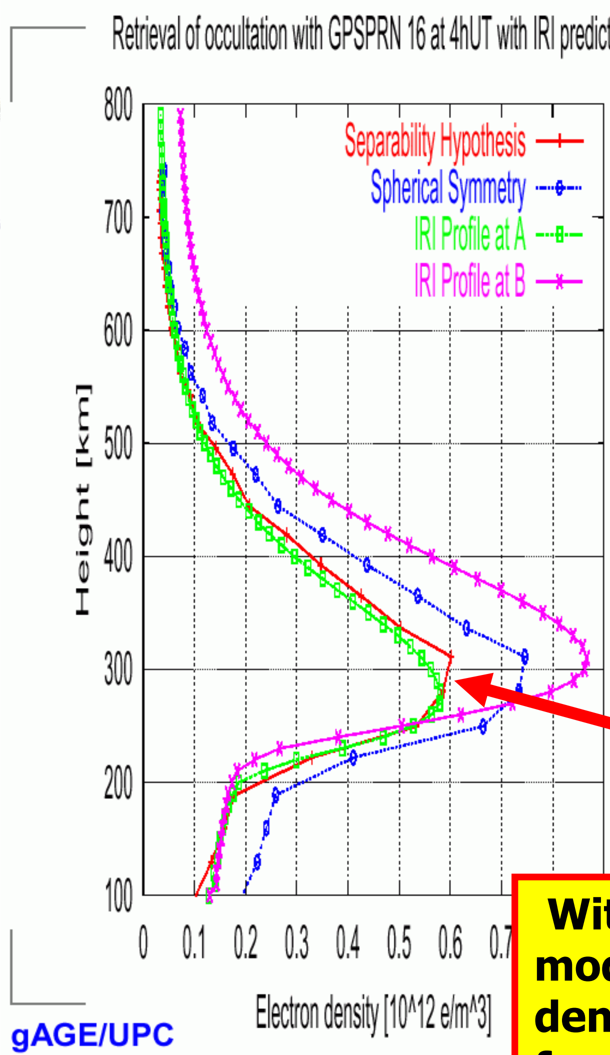

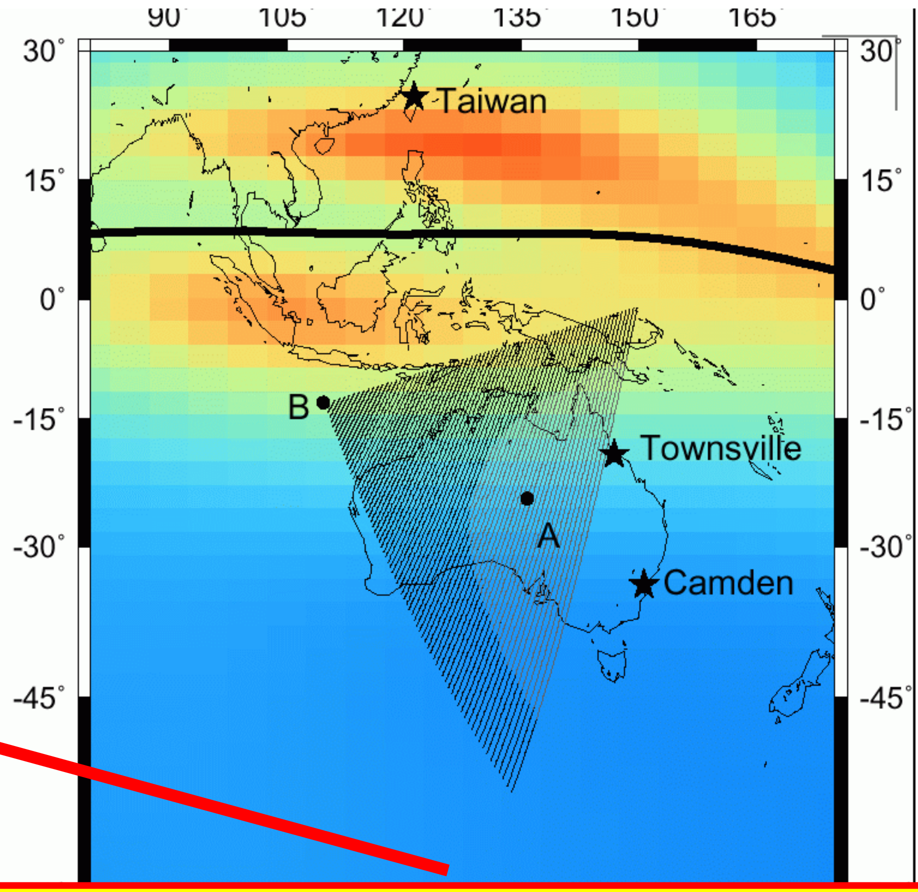

With the TEC (computed from ground GPS data) modelling the horizontal variation, the electron density at tangent point A (green) is estimated from the GPS occultation data better (red) that assuming spherical symmetry (blue).

gAGE/UPC

UNIVERSITAT POLITÈCNICA DE CATALUNYA
BARCELONATECH

Separability: improvement in E layer estimation

The improvement in foE estimates reaches to a reduction of 40% in E layer and near 50% in Es layer

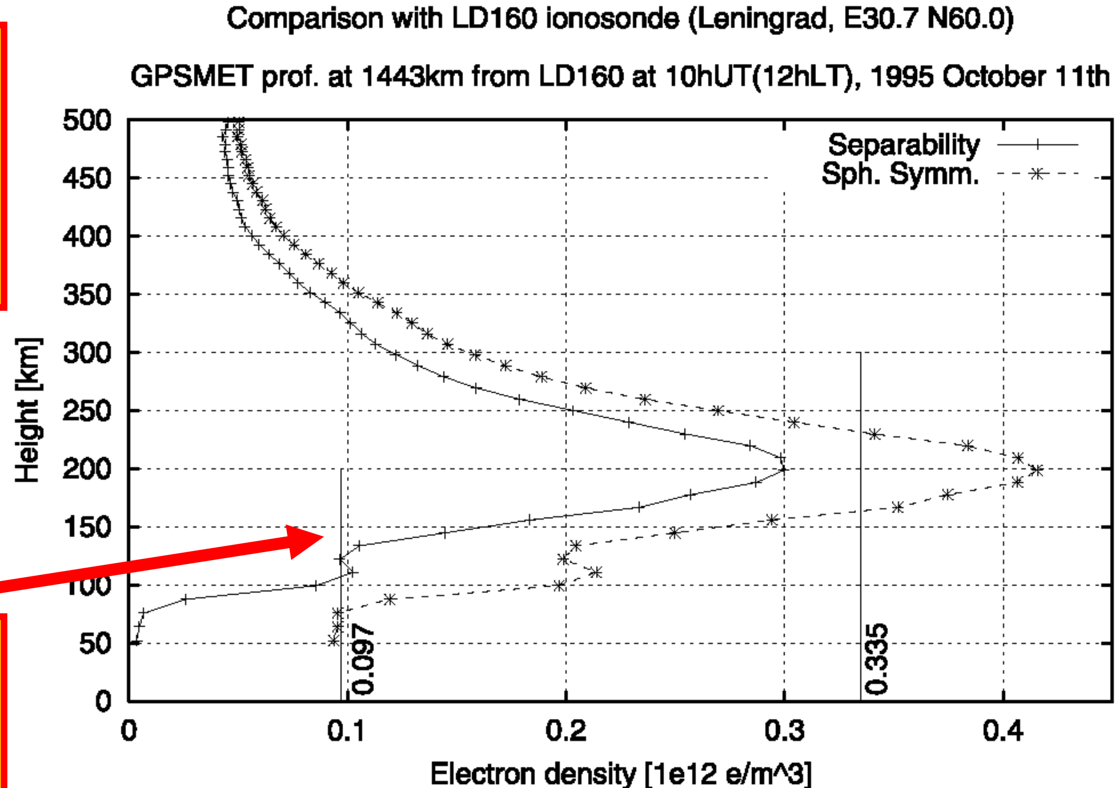

The improved Abel can provide reliable estimates of the NmE value as well (not just NmF2 values).

ble 2. Table of foE Errors With Respect to Ionosonde Value[a]

	N.comp	Sep. Hyp. RMS: MHz [%]	Sph. Symm. RMS: MHz [%]
E layer	135	0.4 [17.1]	0.7 [28.5]
Es layer	35	0.5 [16.2]	1.0 [30.4]

[a]The error is Absolute RMS in MHz and Percentual relative RMS difference in brackets.

UNIVERSITAT POLIT DE CATALUNYA BARCELONATECH

nSAT

3D voxel profile vs Improved Abel+topside 3D voxels

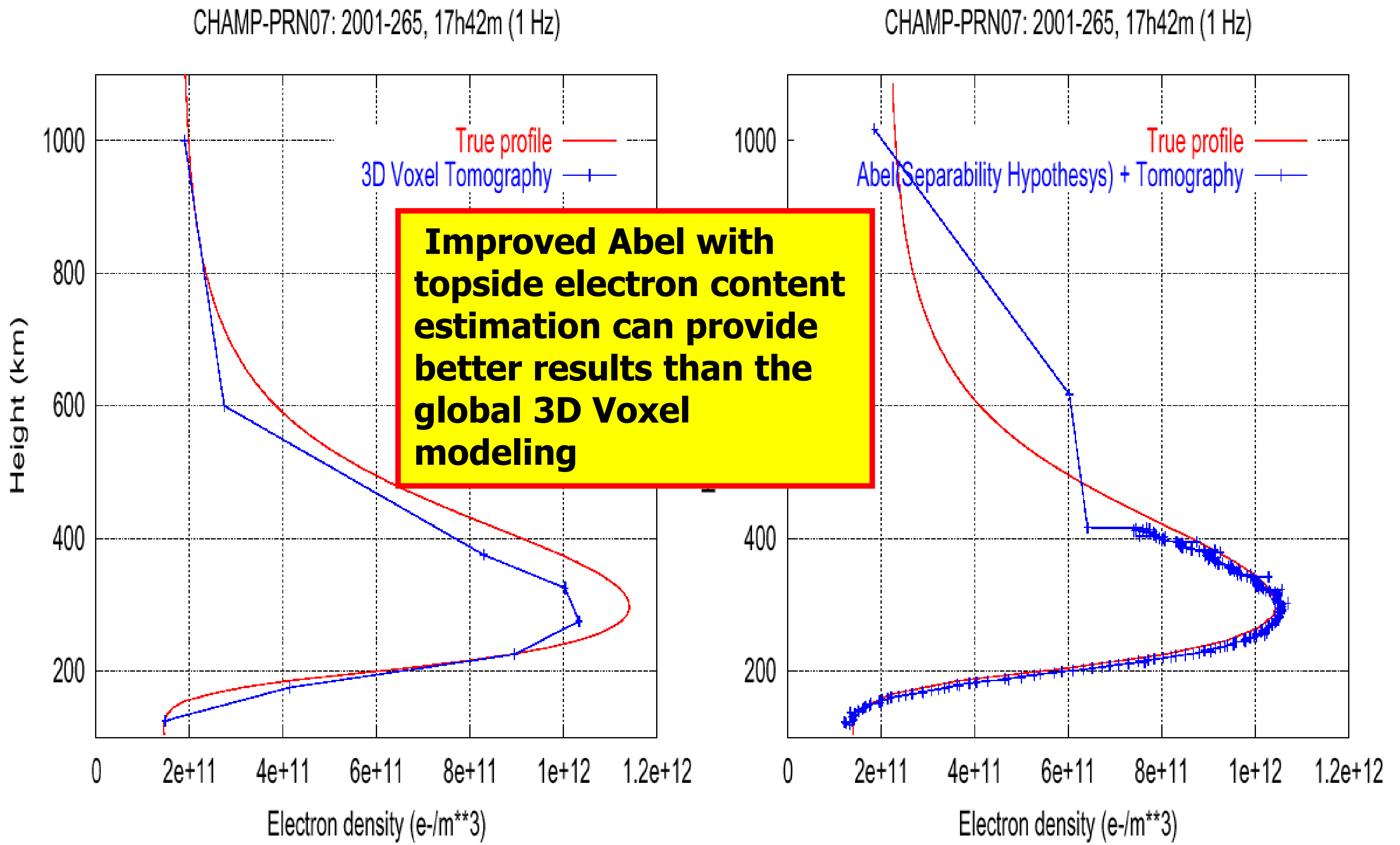

Improved Abel with topside electron content estimation can provide better results than the global 3D Voxel modeling

Results with CHAMP data: Separability vs Spherical Symm. with 3D topside model

The improved Abel transform, including separability hypothesis and upper ionosphere voxel modelling, provides a quite better performance.

This method provides such results without apriori solution, using only carrier phase data for both VTEC and occultation, involving very low computational burden, and can be applied in real-time.

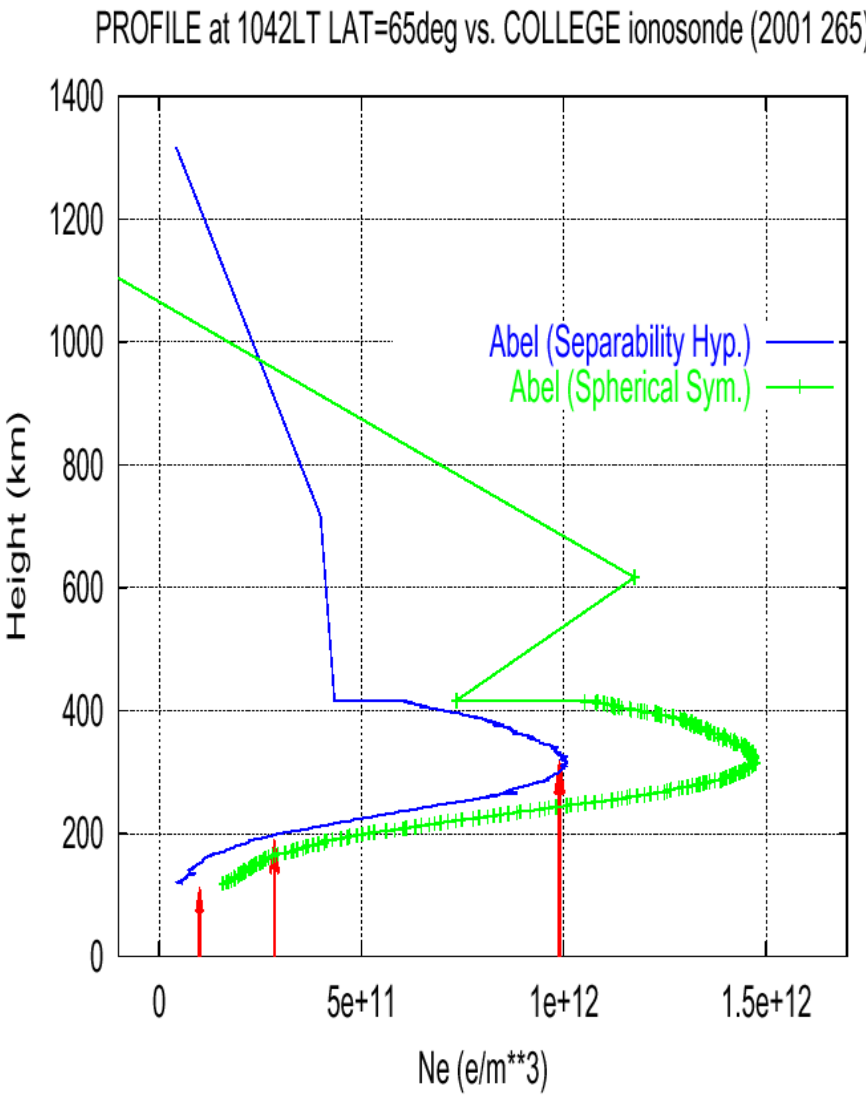

UNIVERSITAT POLITÈCNICA DE CATALUNYA
BARCELONATECH

Example: COSMIC occultations over Korea during day 85, 2011

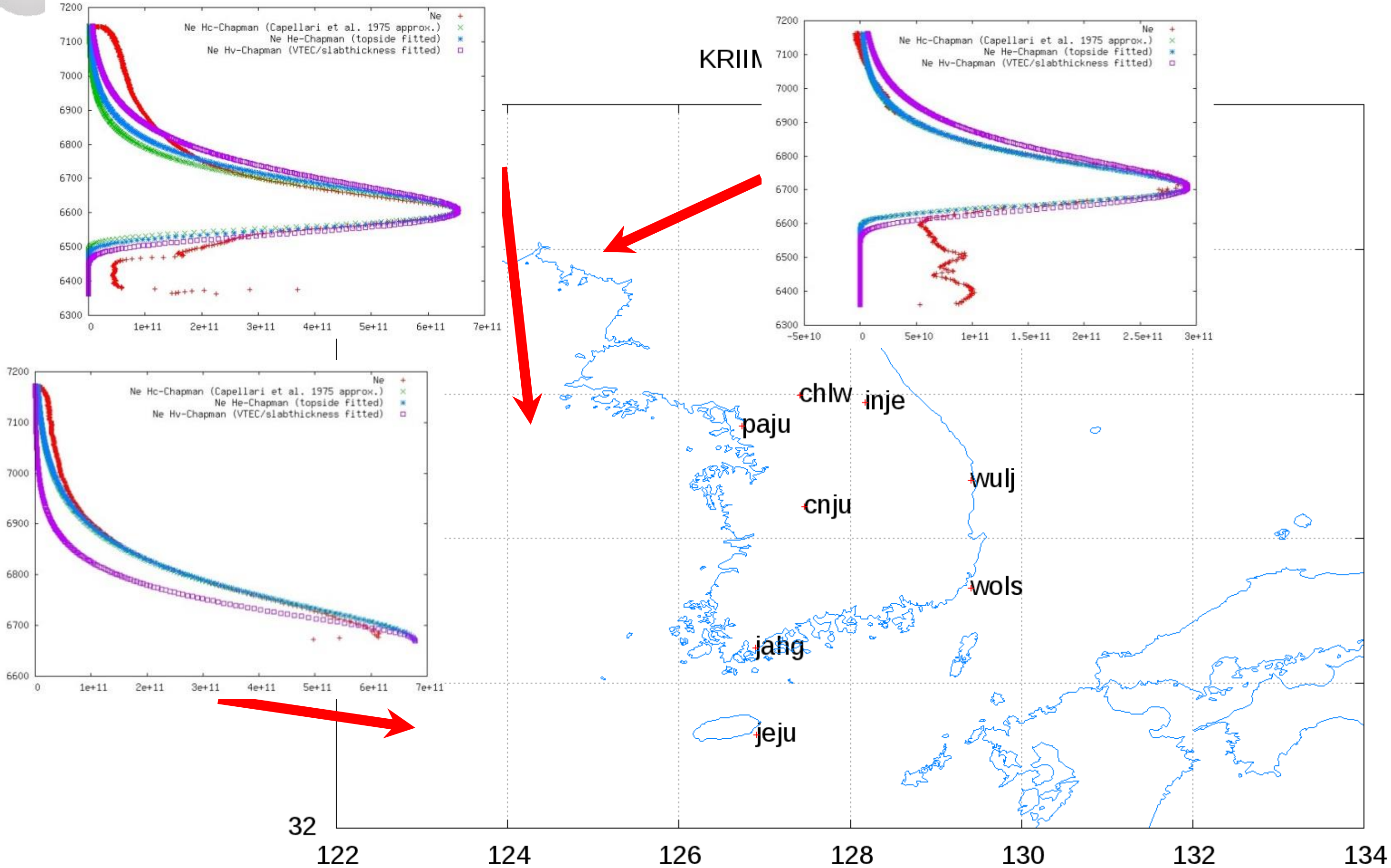

77

- Ground-based GNSS and Ionosonde data

PROS and CONS of different kind of ionospheric data

Type of data	Advantages	Disadvantages
Ionosonde	High resolution data up to the maximum	No information beyond hmF2 Only local vertical profiles
Ground GPS	TEC estimations with errors of few TECUs Extensive GPS networks	Bad vertical resolution
LEO GPS	Vertical information of Ionospheric electron density	Occultations only occur for specific Local Time for different locations

Combination ⇒ Compensation of weak spots with strong points ⇒

1. 3D Ionospheric information possible in either regional or global scale
2. Retrieval of topside information

UNIVERSITAT POLITÈCNICA DE CATALUNYA
BARCELONATECH

IonSAT

Occultation + ground GPS data

Data Assimilation (I): ground and LEO GPS data scheme

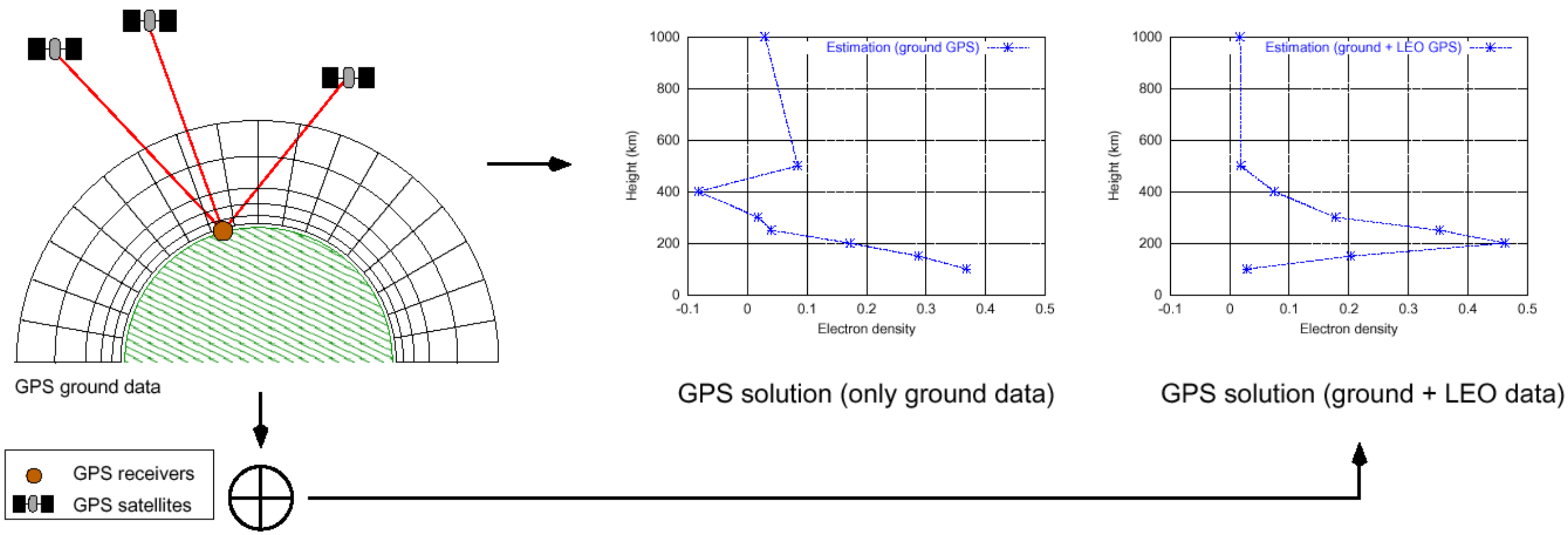

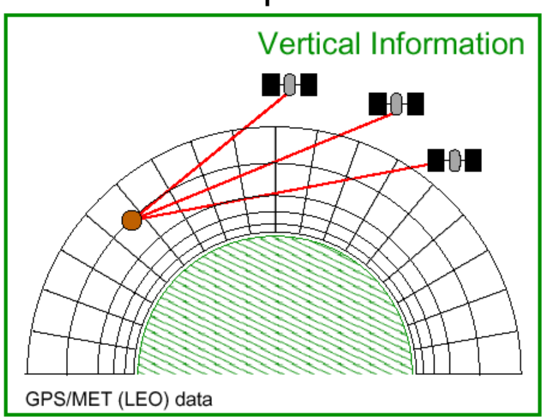

- Steps to compute Electron densities

1. Division of Ionosfere in Local Time × Latitude × Heights (100-150-200-250-300-400-500-1000 km)

2. GPS Solution: Find Ne and biases in equation

$$\mathcal{L}_I \equiv \mathcal{L}_1 - \mathcal{L}_2 = \sum_i \sum_j \sum_k (N_e)_{i,j,k} \cdot l_{i,j,k} + bias$$

UNIVERSITAT POLITÈCNICA DE CATALUNYA
BARCELONATECH

Results with GPS/MET and IGS data

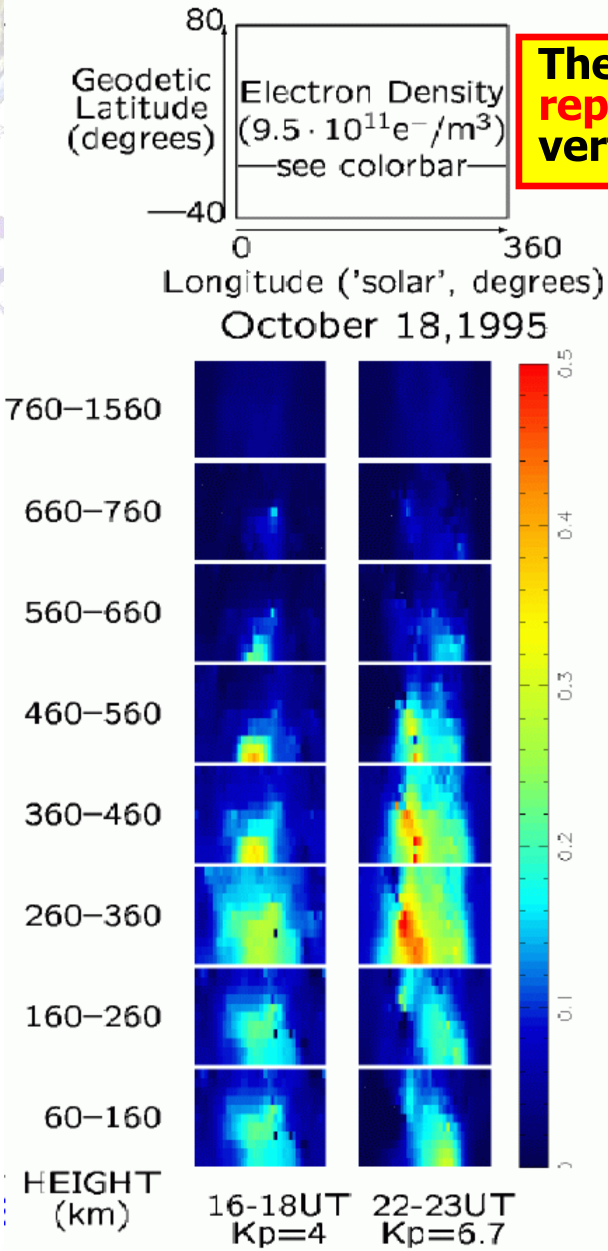

The question is: could the LEO GPS data be efficiently replaced by other kind of ionospheric data with vertical information such as ionosonde data?

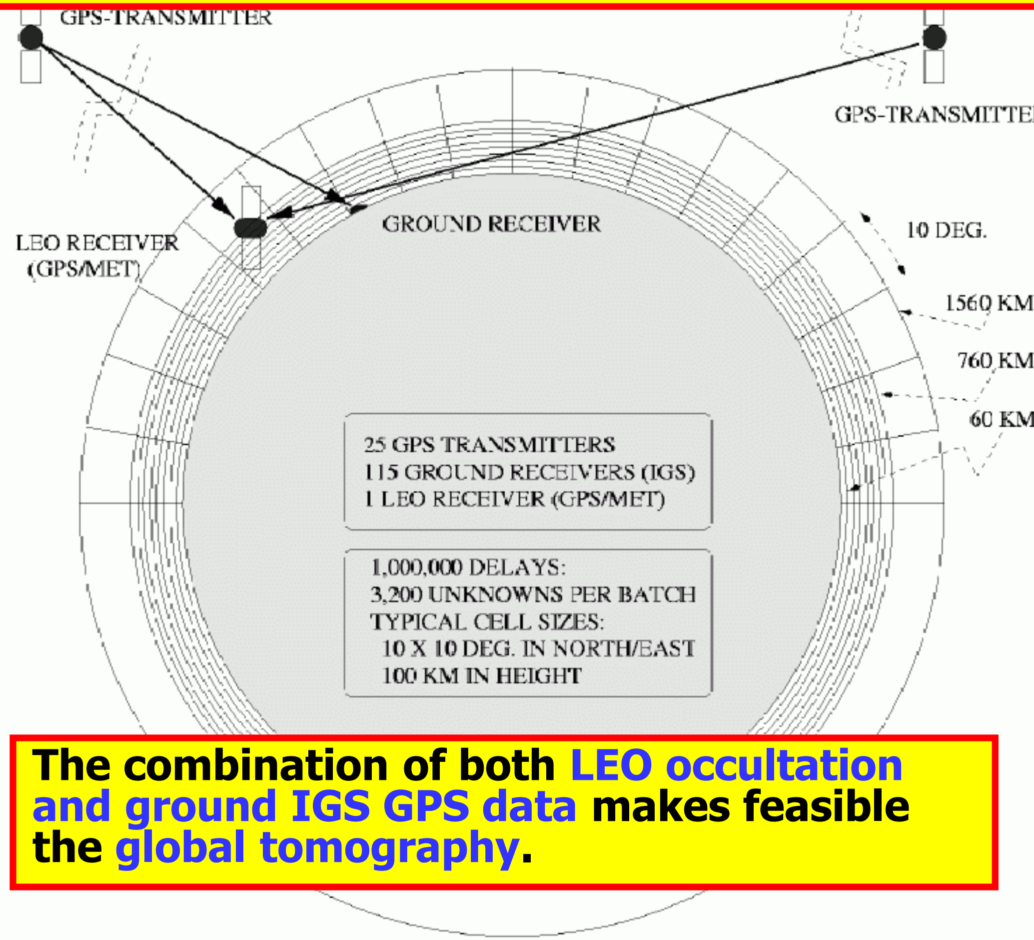

The combination of both LEO occultation and ground IGS GPS data makes feasible the global tomography.

Ionosonde + ground GPS data

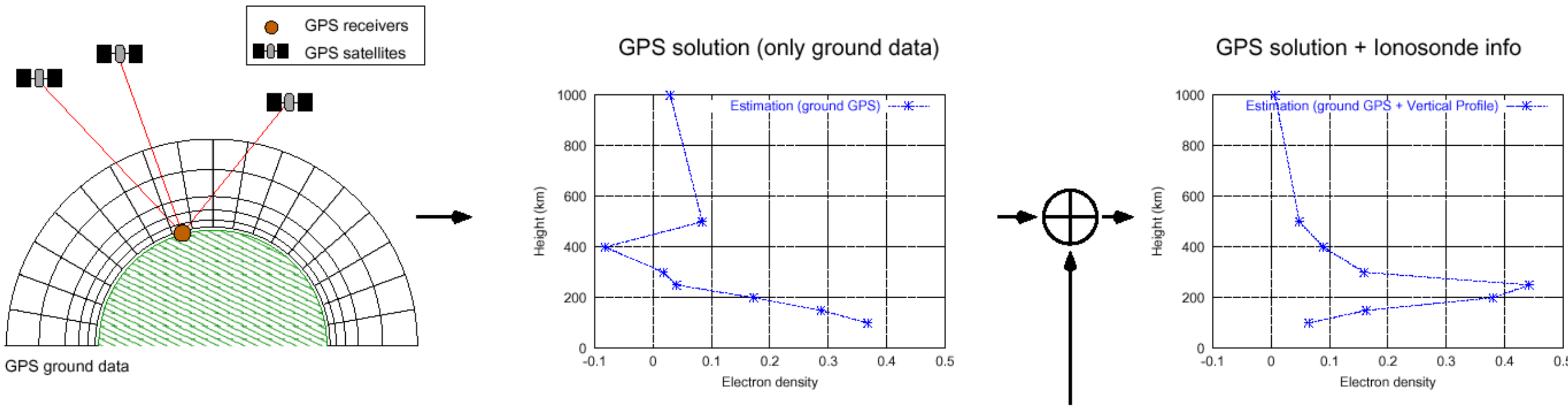

- Steps to compute Electron densities

1. Division of Ionosfere in Local Time × Latitude × Heights (100-150-200-250-300-400-500-1000 km)

2. GPS Solution: Find Ne and biases in equation

$$\mathcal{L}_I \equiv \mathcal{L}_1 - \mathcal{L}_2 = \sum_i \sum_j \sum_k (N_e)_{i,j,k} \cdot l_{i,j,k} + bias$$

3. Apply **Constraining Scheme** with Vertical profile data from models like NeQuick, IRI...

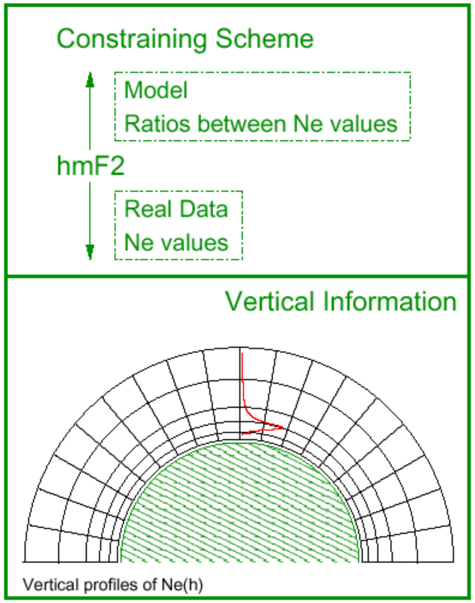

UNIVERSITAT POLITÈCNICA DE CATALUNYA
BARCELONATECH

Ionosondes+ground GPS: Simulation study

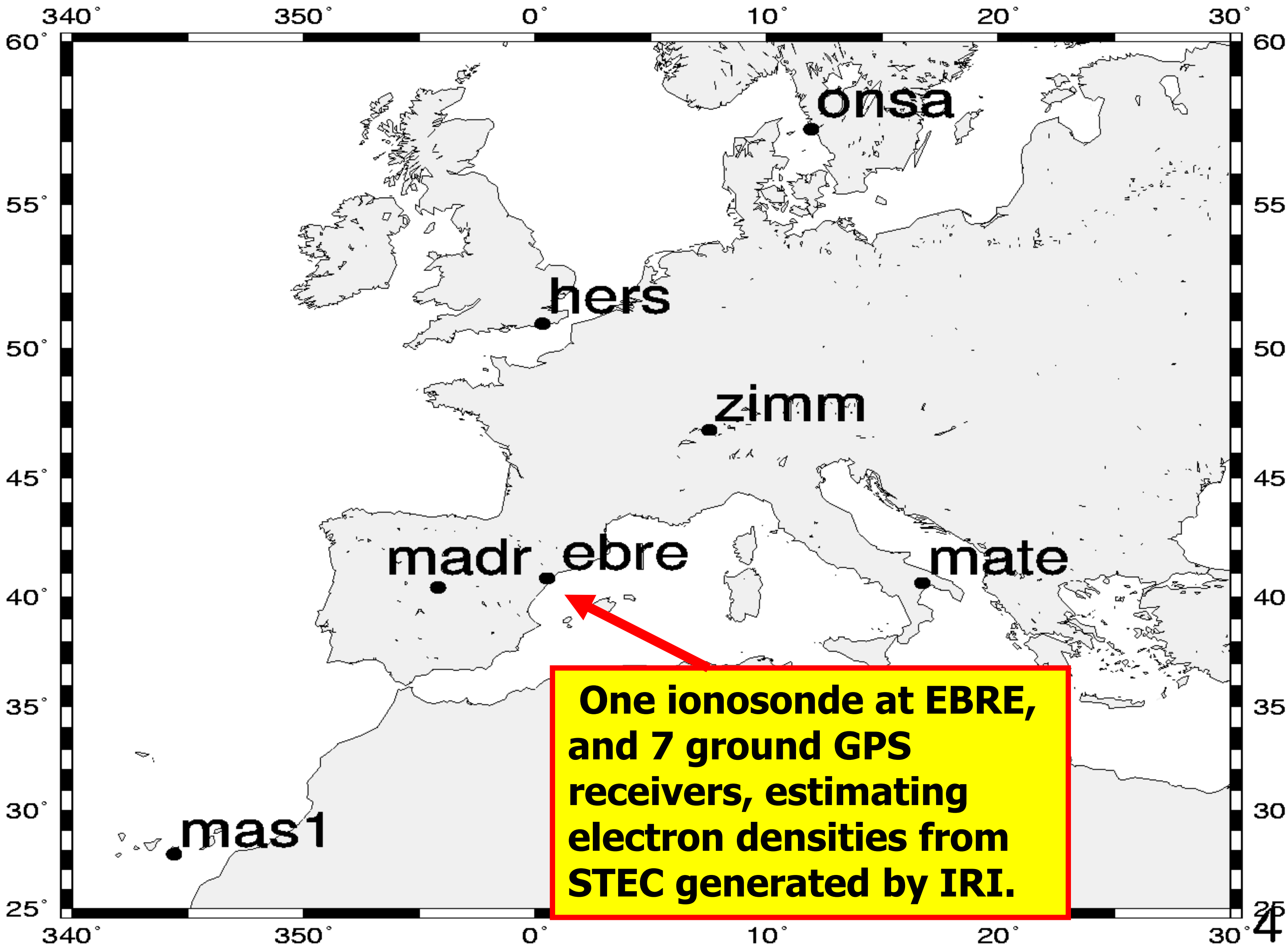

Simulation study: snapshot of results

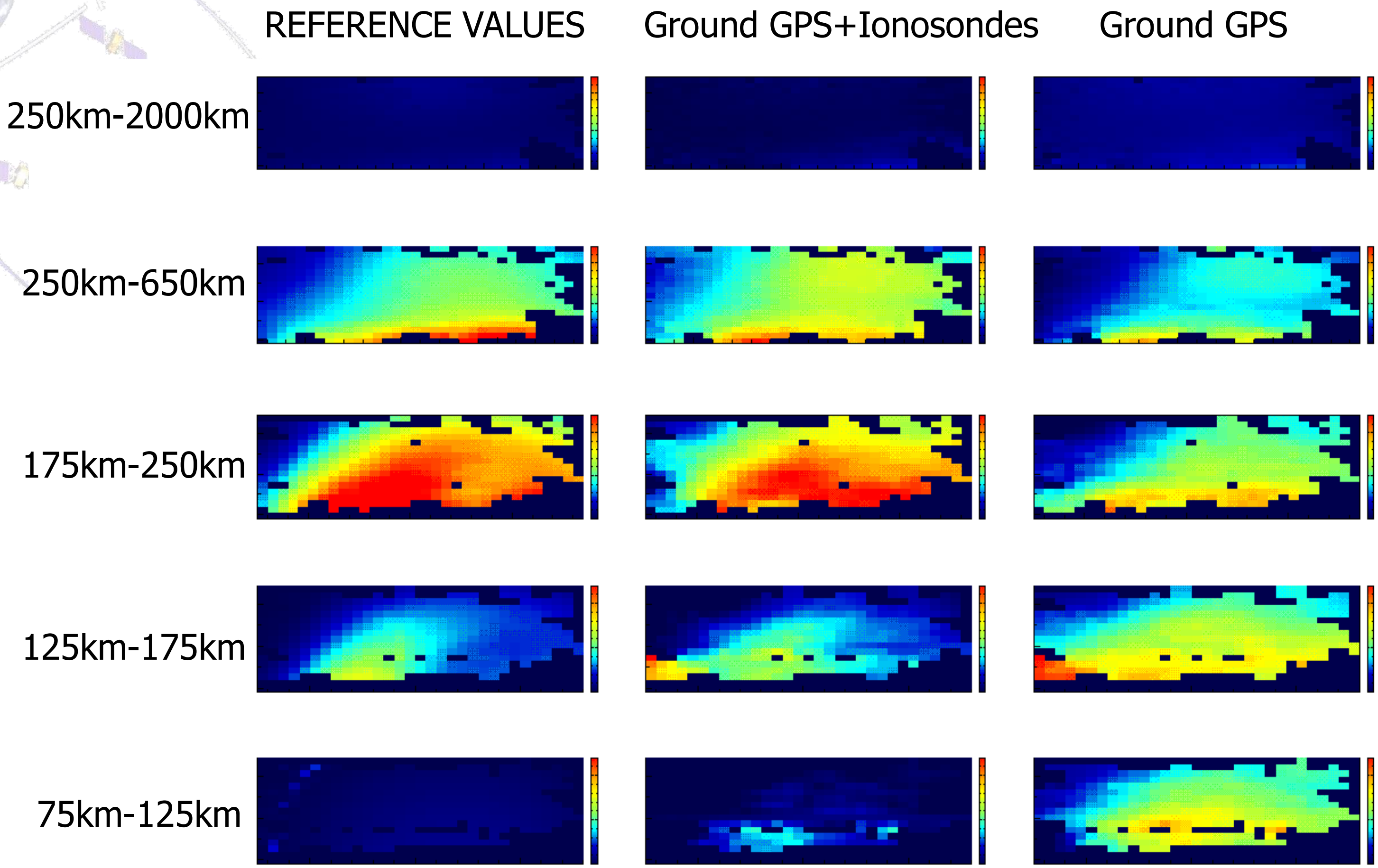

Each plot represent the correspoding mean electron density for layer 1 (bottom) to layer 5
(to ... nd
ion ... 0
(bl ... es
in l ... e).

The mean electron densities obtained with 7 GPS receivers in the ground and with 1 ionosonde are in good agreement. This is not the case using just the ground GPS data (typical correlated solution).

UNIVERSITAT POLITÈCNICA DE CATALUNYA
BARCELONATECH

Results with real data over Europe

- Data set obtained from Ionosonde and ground GPS receiver from Europe, day 1995 October 18th.

- Verification procedure after cell densities have been computed:

  1. GPS to GPS/MET rays divided according to the cells crossed
  2. Modelled STEC reconstructed with the obtained densities
  3. Results compared with actual GPS/MET observations

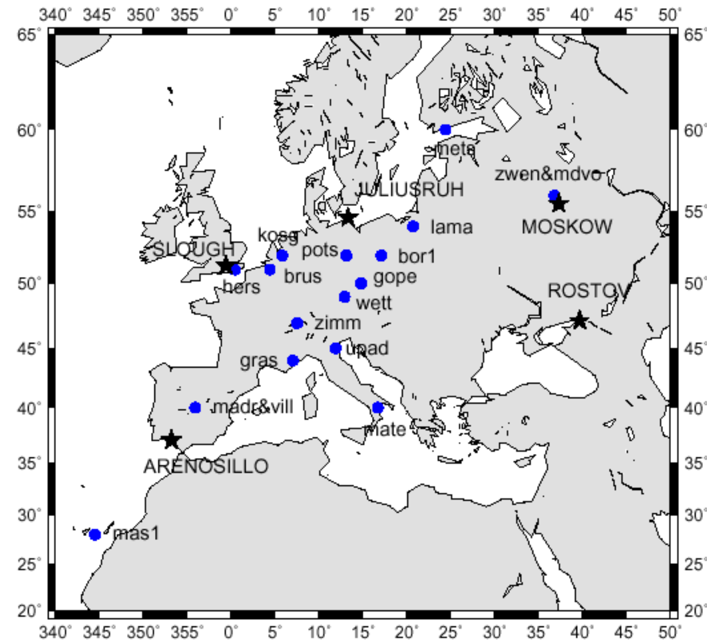

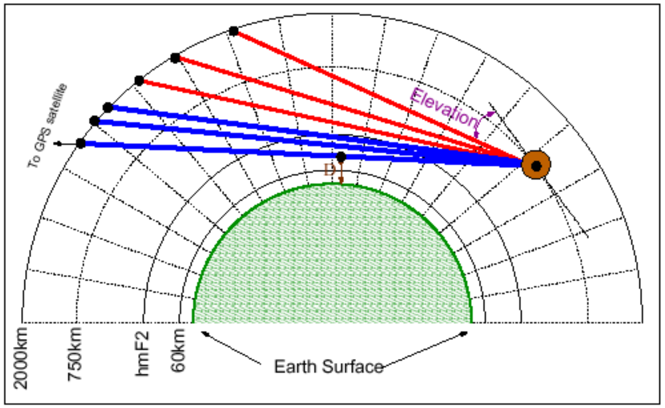

One example of improvement

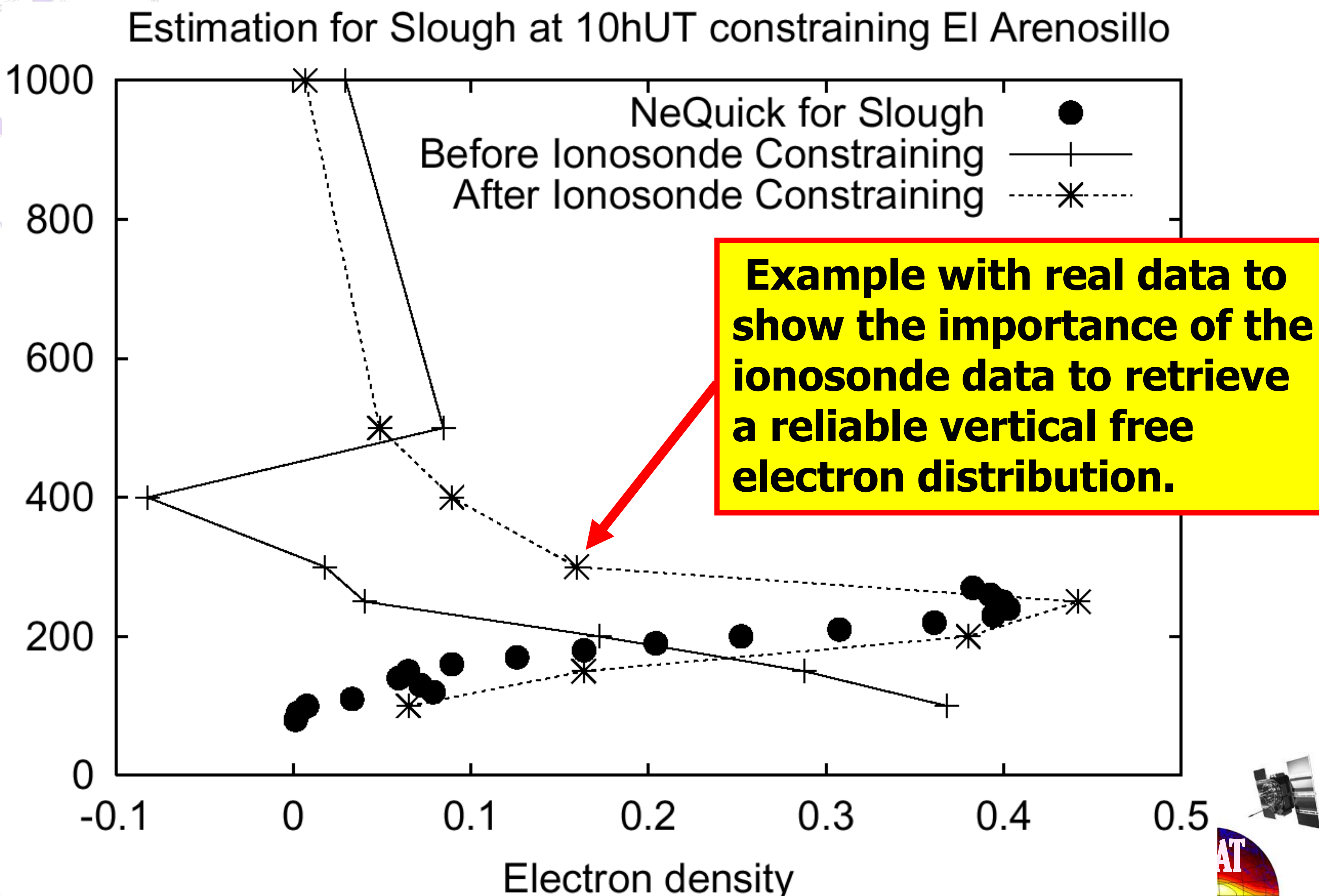

UNIV… DE CATALUNYA BARCELONATECH

Validating with GPS/MET STEC

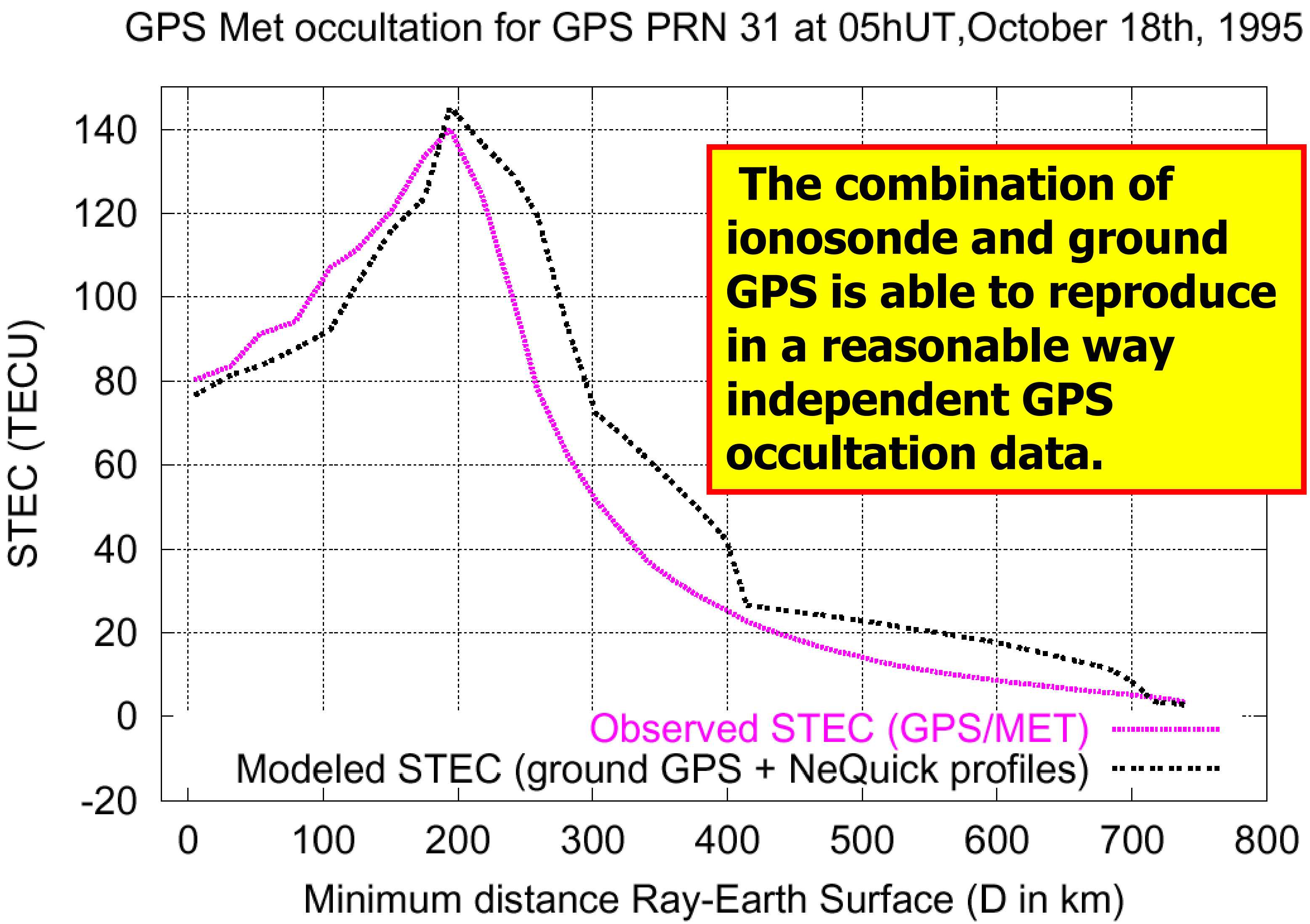

UNIVERSITAT POLITÈCNICA DE CATALUNYA
BARCELONATECH

All the comparisons with GPS/MET STEC

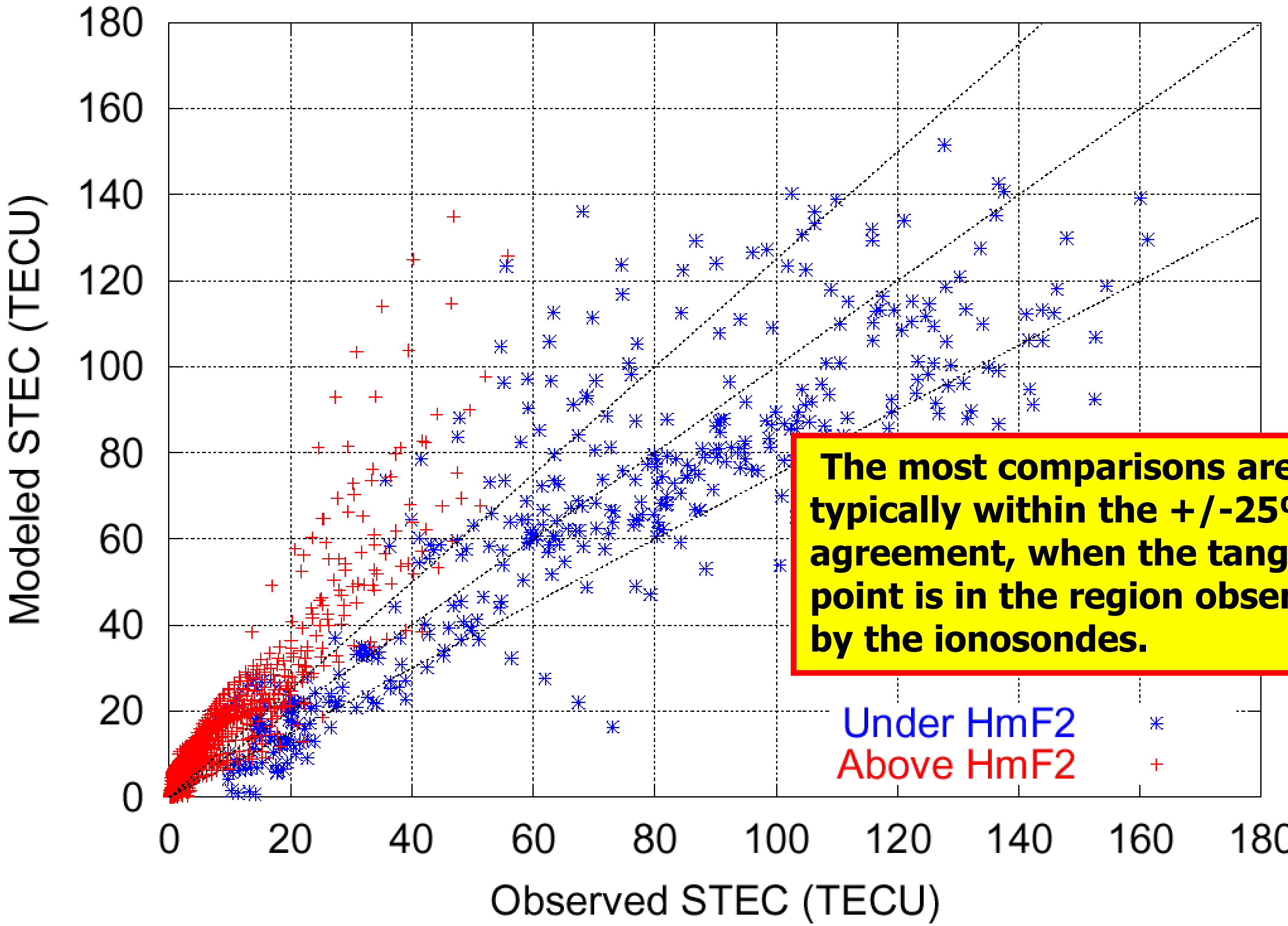

The most comparisons are typically within the +/-25% of agreement, when the tangent point is in the region observed by the ionosondes.

UNIVERSITAT POLITÈCNICA DE CATALUNYA
BARCELONATECH

Example of comparison with occultation GPS profile

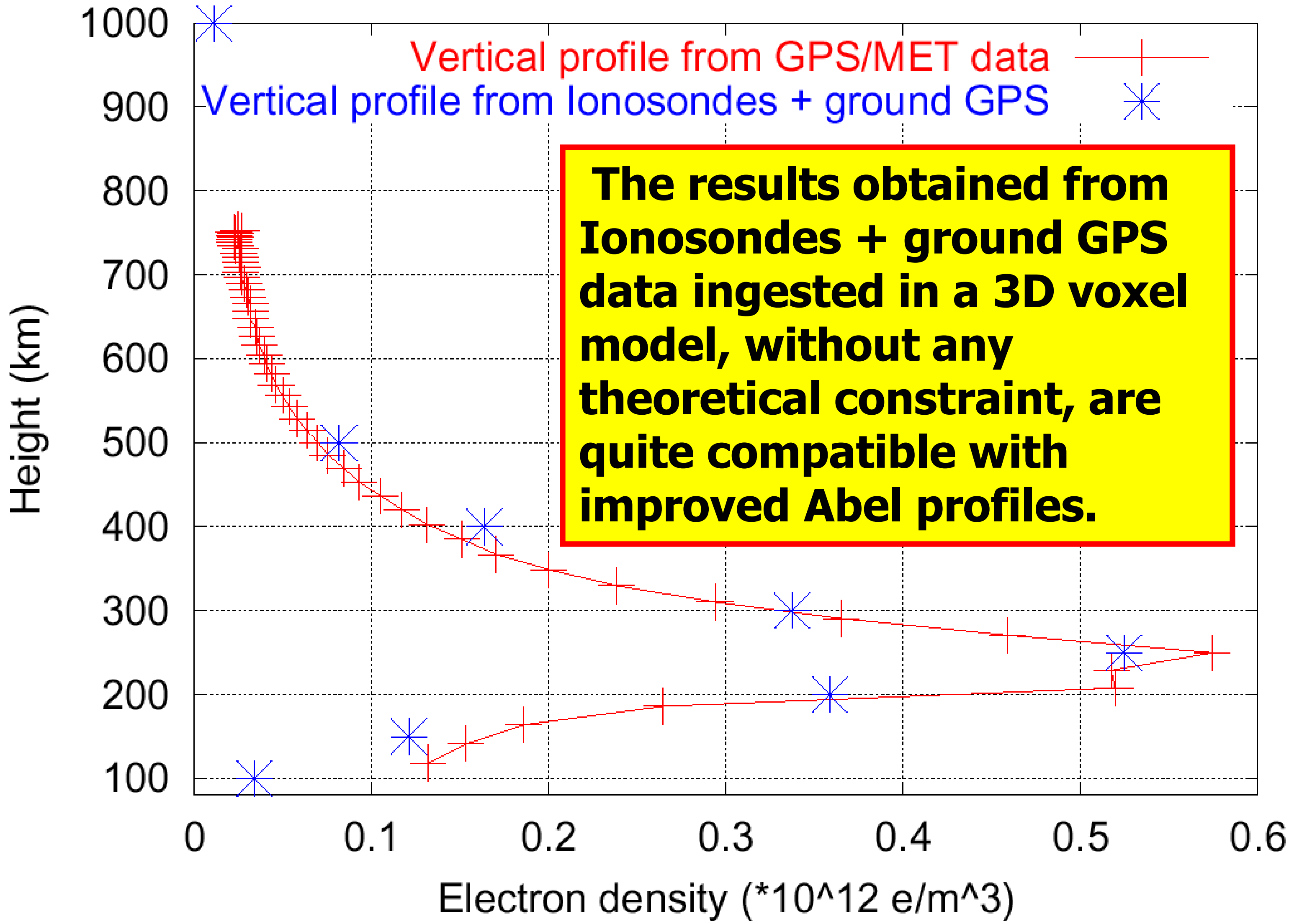

The results obtained from Ionosondes + ground GPS data ingested in a 3D voxel model, without any theoretical constraint, are quite compatible with improved Abel profiles.

- Ionospheric determination at regional/continental scale

UNIVERSITAT POLITÈCNICA DE CATALUNYA
BARCELONATECH

Regional network: Iono. geometry

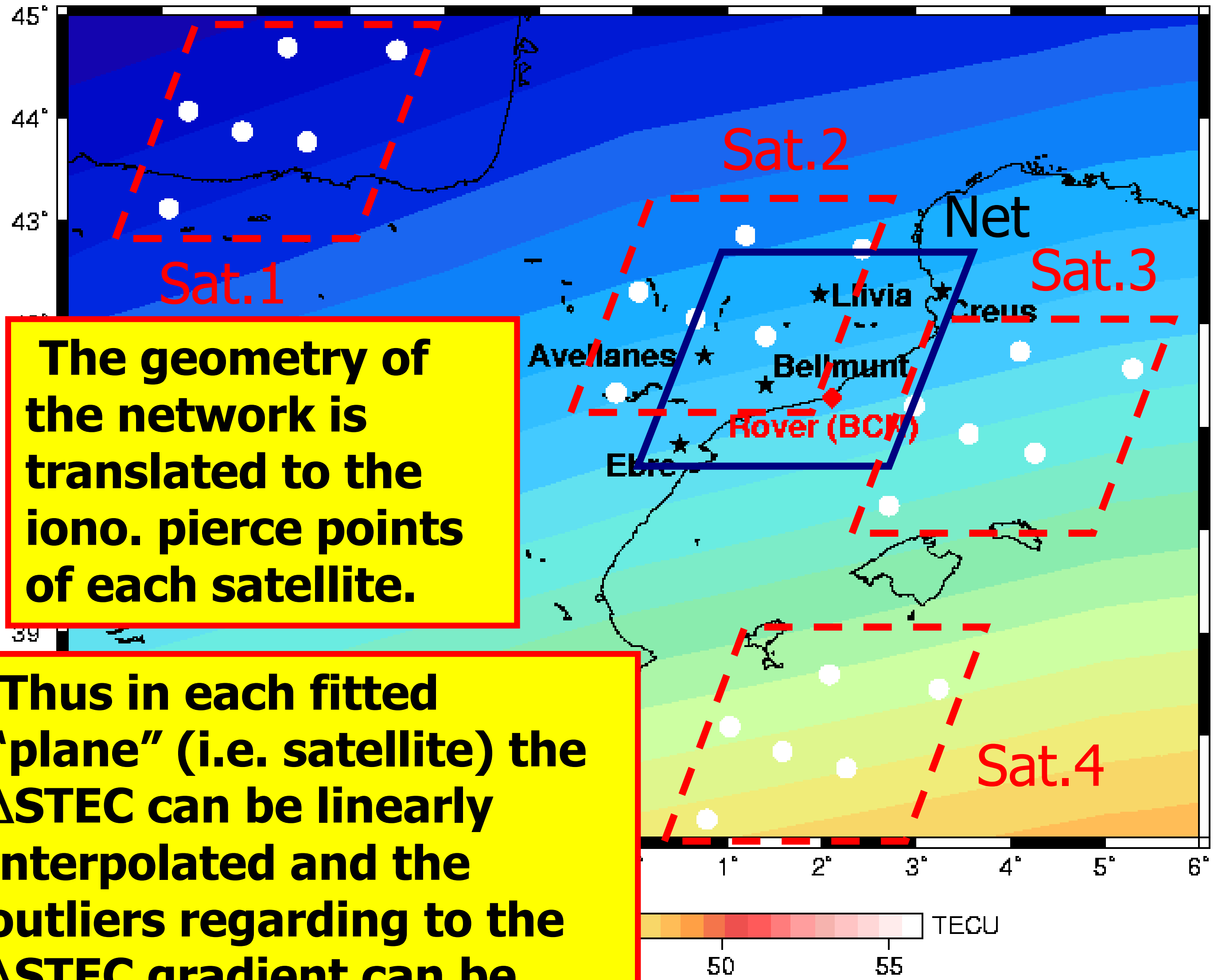

The geometry of the network is translated to the iono. pierce points of each satellite.

Thus in each fitted "plane" (i.e. satellite) the ΔSTEC can be linearly interpolated and the outliers regarding to the ΔSTEC gradient can be detected.

UNI… DE CATALUNYA
BARCELONATECH

Wide Area RTK network layout

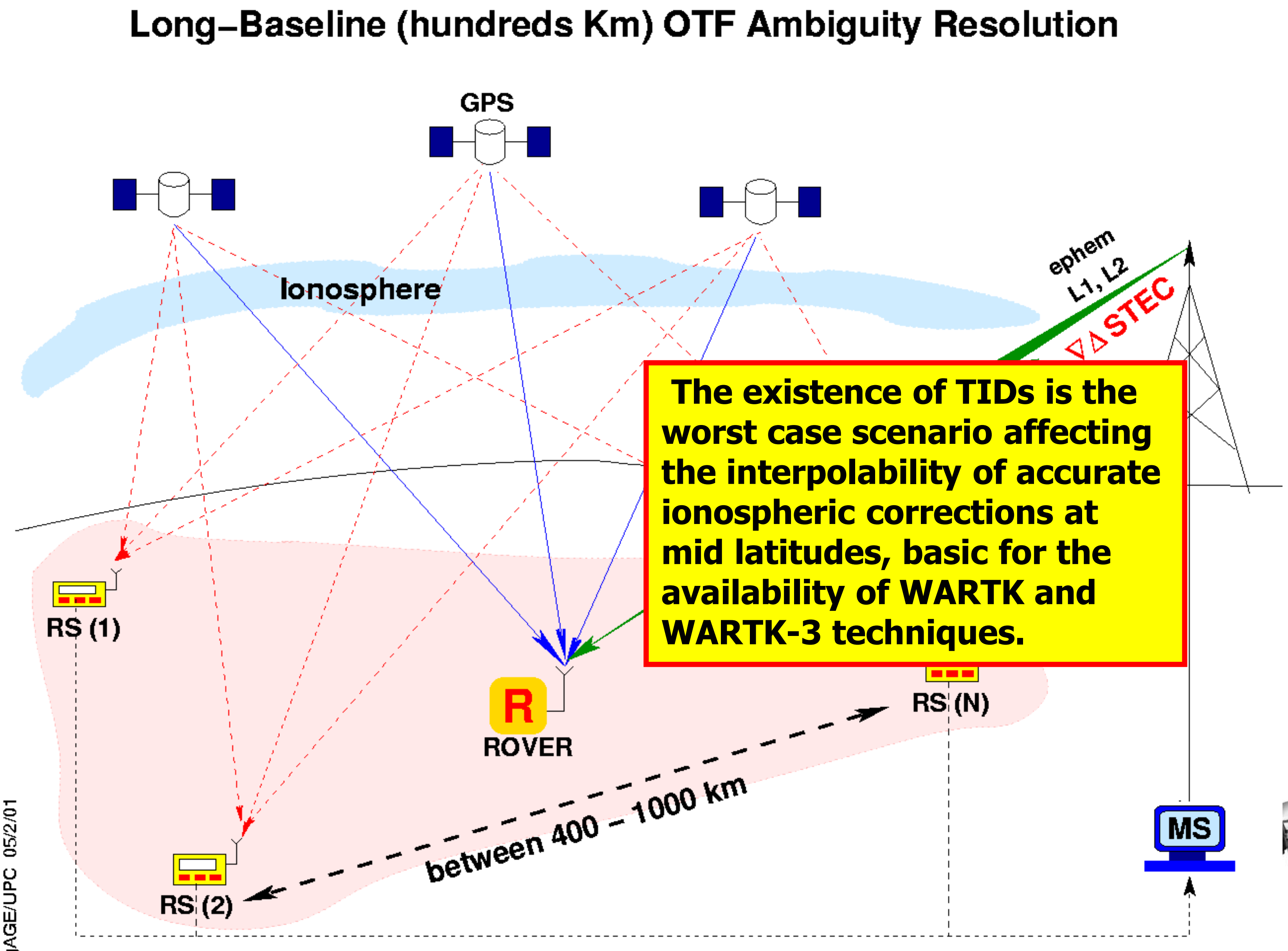

The existence of TIDs is the worst case scenario affecting the interpolability of accurate ionospheric corrections at mid latitudes, basic for the availability of WARTK and WARTK-3 techniques.

UPC
DE CATALUNYA
BARCELONATECH

WARTK fundamentals

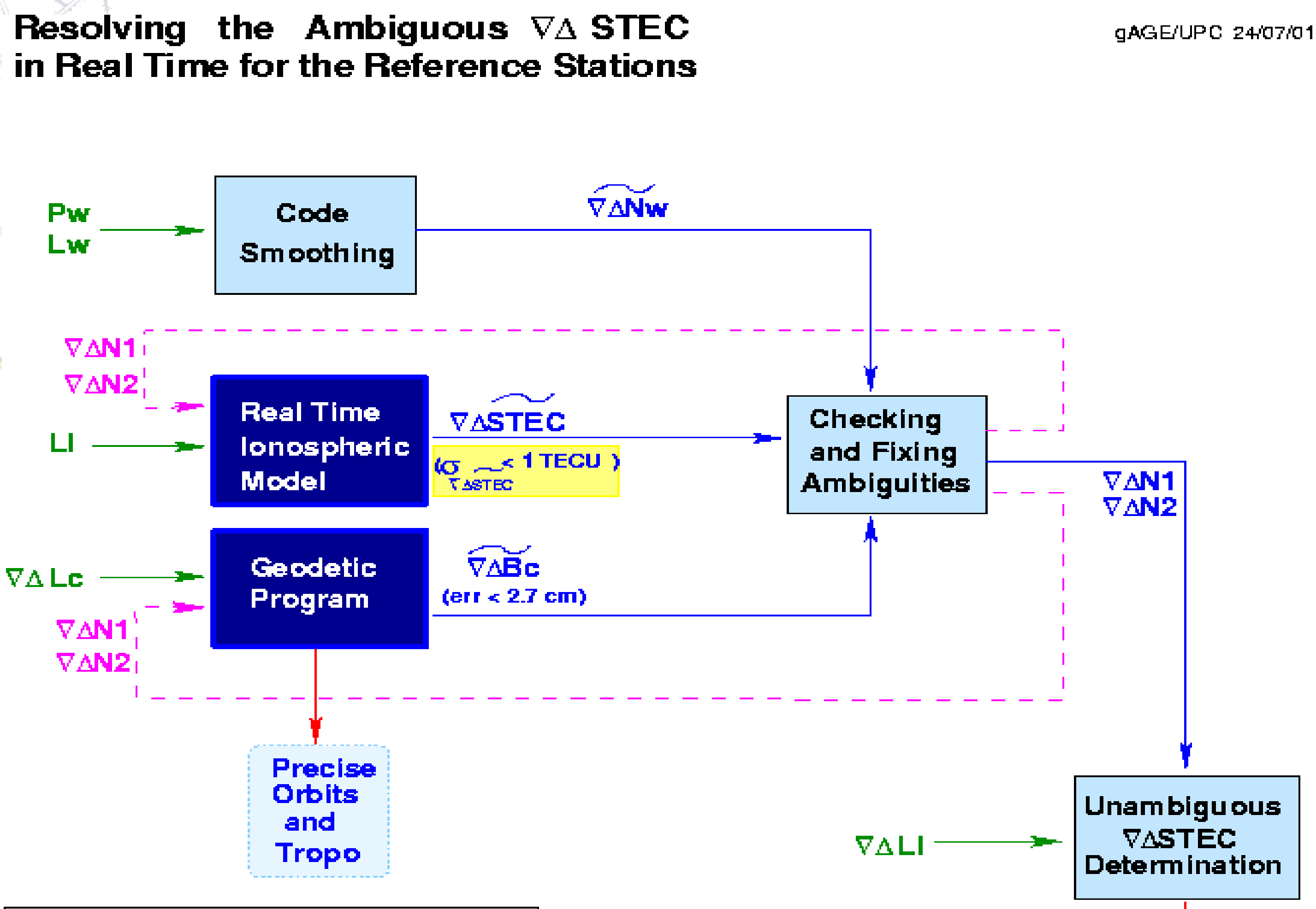

Both filters, ionospheric and navigation ones, are feed with the reference GNSS stations data, sharing the double differenced carrier phase ambiguity unknonws which can be better estimated and fixed, with two benefits: (1) Improving the geodetic and ionospheric outputs, and (2) Providing very accurate differential ionospheric corrections (at the level of 0.1 TECU of error).

GPS receivers involved in the experiment during 2002 to characterize the main problems in the ionospheric interpolations

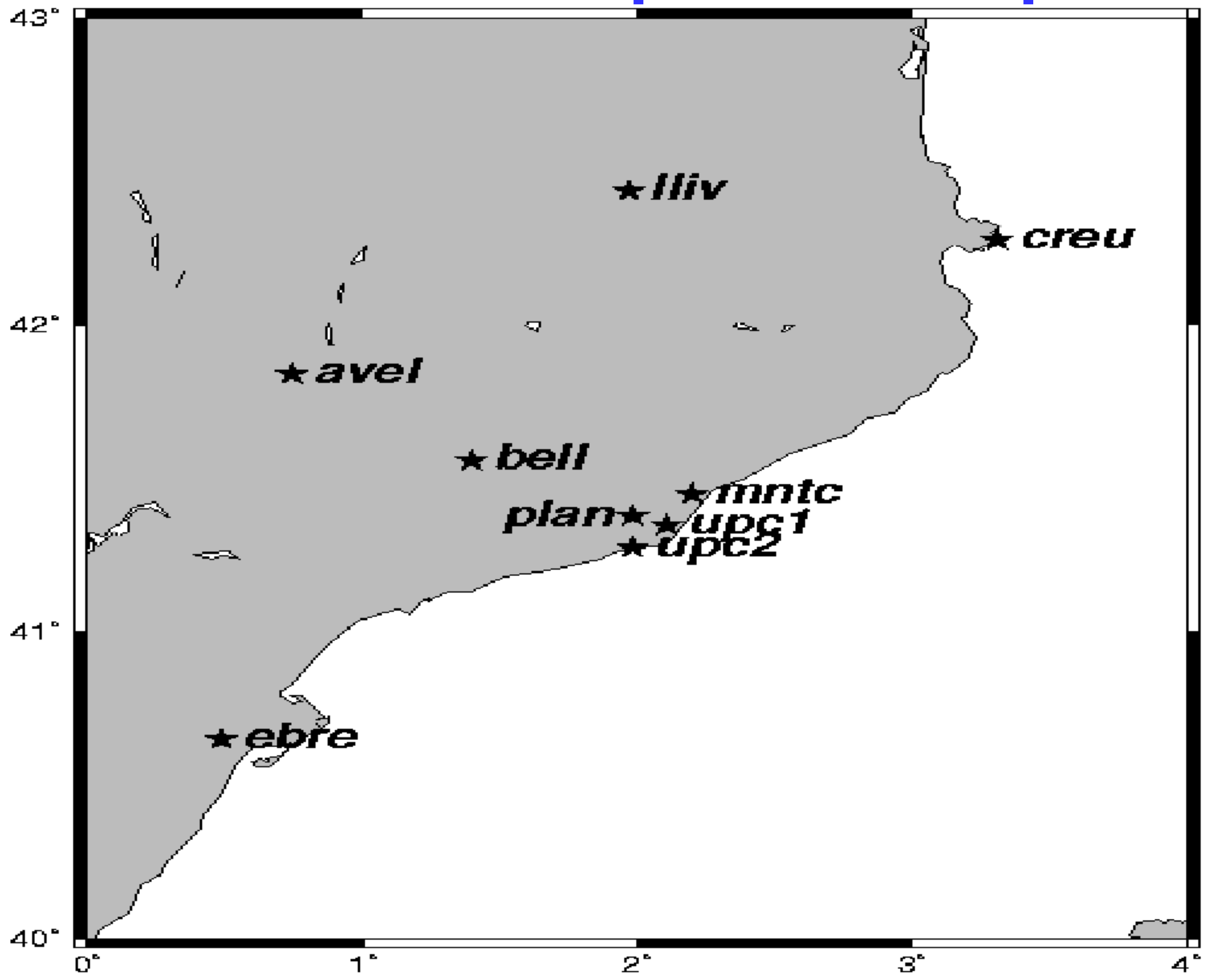

Ionospheric interpolation error vs. TIDs occurence

It can be seen the correlation between poor ionospheric interpolation performance and the occurence of TIDs during 2002

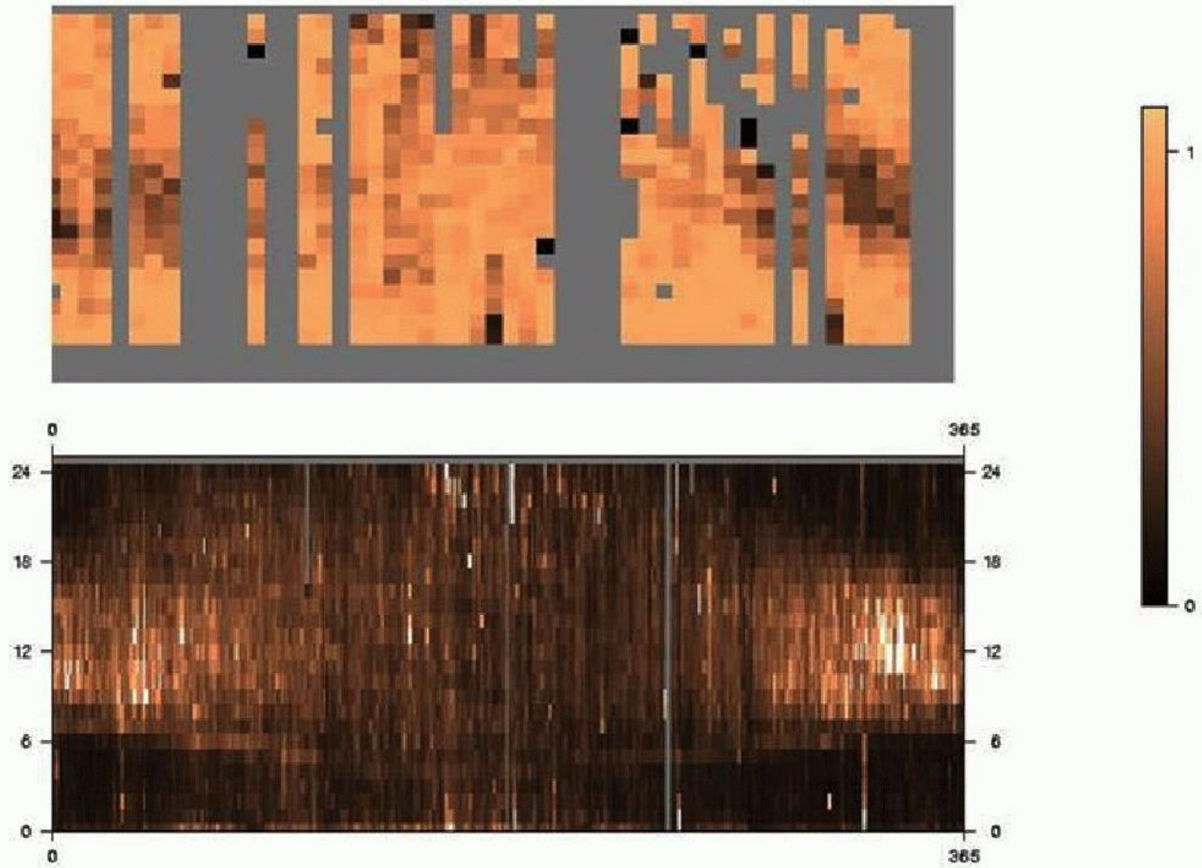

Figure 5: Plot representing the STEC interpolation results at bell (up, extracted from Figure 4), compared with the presence of TIDs (down), computed from **ebre** station VTEC drift rate during 2002 (see details of this computation in Section 3).

Example of TIDs during Winter and Summer

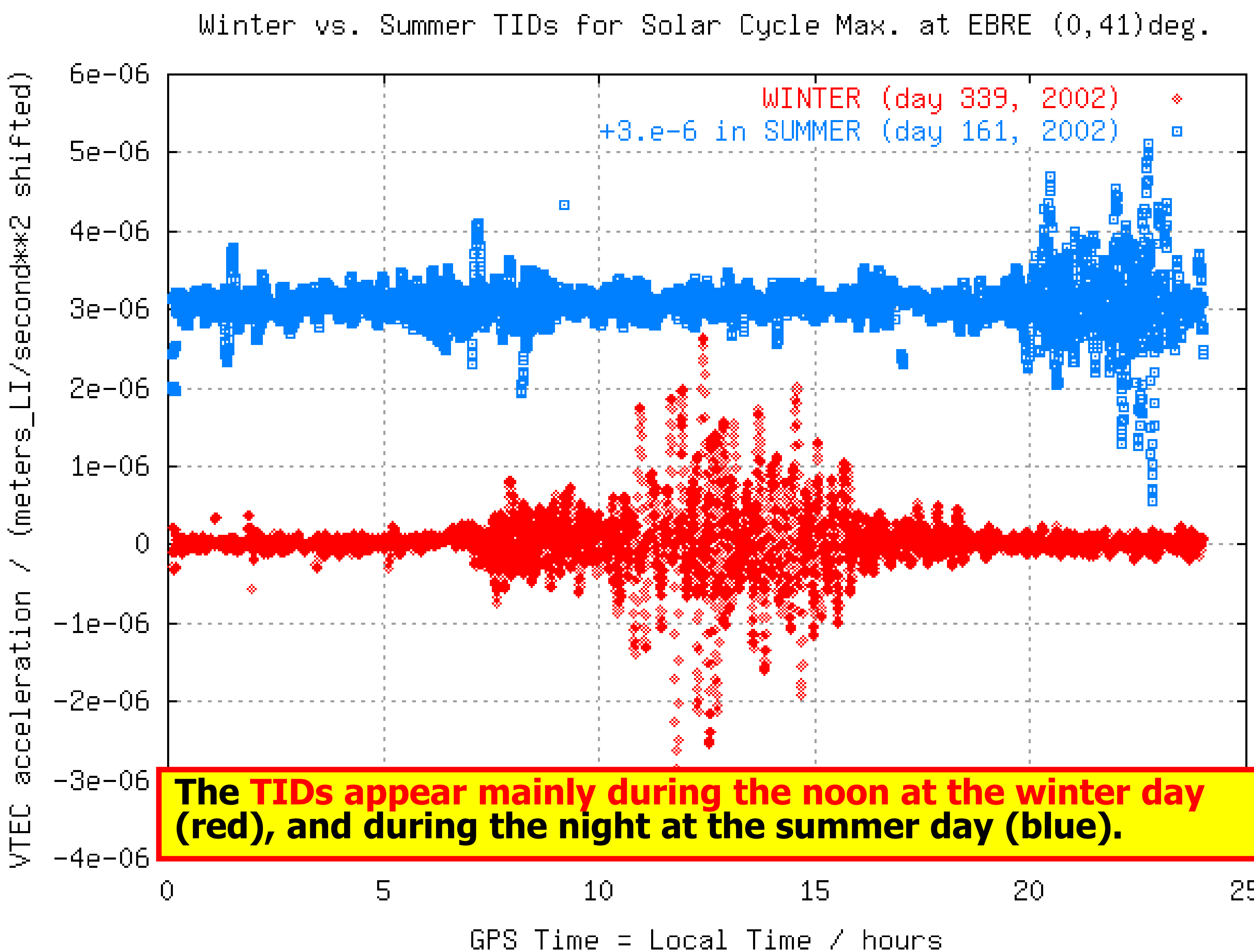

The TIDs appear mainly during the noon at the winter day (red), and during the night at the summer day (blue).

UNIVERSITAT POLITÈCNICA DE CATALUNYA BARCELONATECH

TIDs occurrence since the CATNET setup (end 1996)

The TIDs occurrence since end of 1996 repeats the seasonal dependence observed during 2002, modulated by the Solar Cycle (terminator origin).

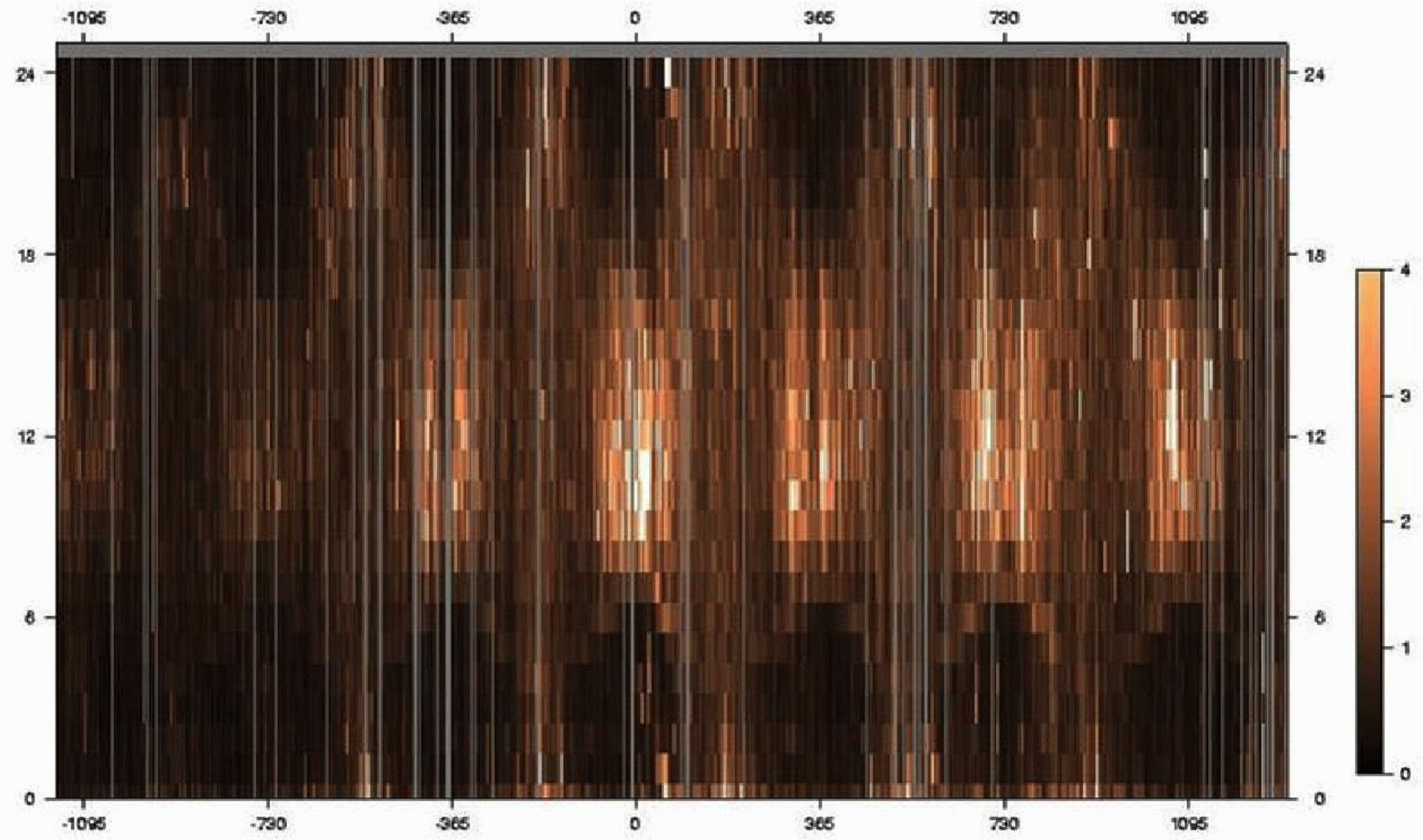

Figure 6: Plot representing the activity's index in TIDs (multiplied by 1e+7). The X axis represents the day of year referred to January 1st, 2000. It starts at the end of the year 1996, (the changes of year coincide with the maximum number of the TIDs, at noon time). Again the Y axis represents the Universal Time at ebre (approximately coinciding with the local time).

Solution: modelling the TIDs from the reference stations network.

- Determining the electron content at global scale

How?: RT-TOMION computing global VTEC maps based on GNSS data

From each obs. we get one STEC value: V=S/M=(Li-Bi)/M.[~1500 val. / 30 sec]

Interpol. [*] by Splines

RT IGS ground GPS data (70 to 195 worldwide receivers)

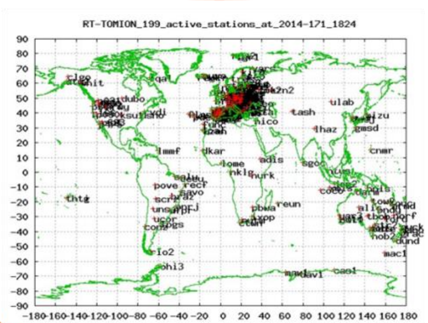

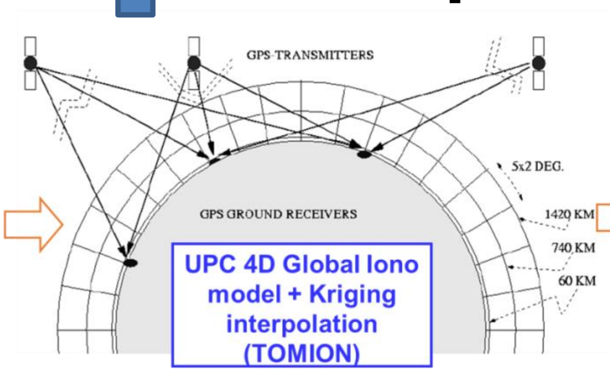

$$L_I = S + B_I \simeq \sum_{i=1}^{n} N_{e,i} \Delta l_i + B_I$$

UPC global VTEC maps

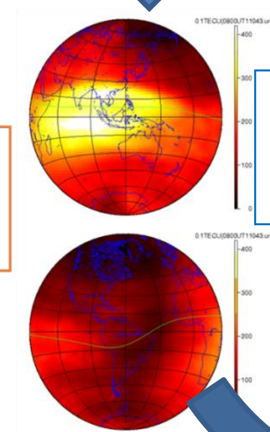

Kriging [*] Interpolation

New RT global VTEC maps

IonSAT

[*] *Performed in Solar-Magnetic Local Time and Latitude coordinates*

Layout summarizing the global VTEC computation from ground GPS data by means of the UPC TOMION software, including the main tomographic equation solved for (data: ionospheric combination of carrier phases LI , and length intersection within each voxel, Δli; unknowns: its ambiguity BI, the STEC, S, which includes the mean electron density within each given voxel, Ne,i).

Coordinates to interpolate

The **ionospheric electron content distribution** is closely tied to:

(1) *The Sun position*, as the main ionizing source in typical geomagnetically quiet conditions.

(2) *The geomagnetic field*, which field lines are the typical ways used by the charged particles, like the electrons, which can move describing circles around them due to the Lorentz force.

In this context **the usage of a reference system to locate the ionospheric pierce points, where the electron content could be considered as much stationary as possible, is an advantage for interpolation**, allowing the combination of VTEC values during a more extended period of time.

The following type of coordinates goes from less, mid up to high stationarity:

Longitude,Latitude => Local Time, Latitude => Solar-Magnetic Local Time, Magnetic Latitude

From Longitude to Local Time

The **transformation from Longitude (LON) to Local Time (LT)** can be aproximated by the following simple expression (assuming a "mean" Sun):

$$LT = UT + LON$$

where UT is the Universal Time.

Solar Geomagnetic coordinates

Z-axis: Boreal Magnetic Pole (from dipolar model), unity vector k = R_B

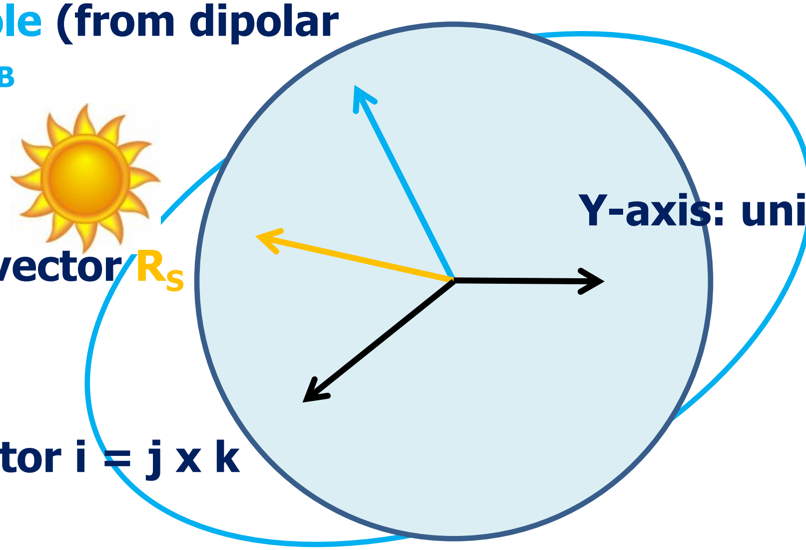

Y-axis: unity vector j = R_B x R_S

Sun pointing vector: unity vector R_S

X-axis: unity vector i = j x k

From the projection of the unity vector pointing to the ionospheric pierce point, **R**, on the new axis, **i**,**j**,**k**, we can retrieve the Solar-Magnetic Local Time (SMLT) and Magnetic Latitude, MLAT:

R·k = sin (MLAT)
R·j = cos (MLAT) * sin (SMLT)
R·i = cos (MLAT) * cos (SMLT)

UNIVERSITAT POLITÈCNICA DE CATALUNYA
BARCELONATECH

Kriging motivation in global VTEC modelling (1)

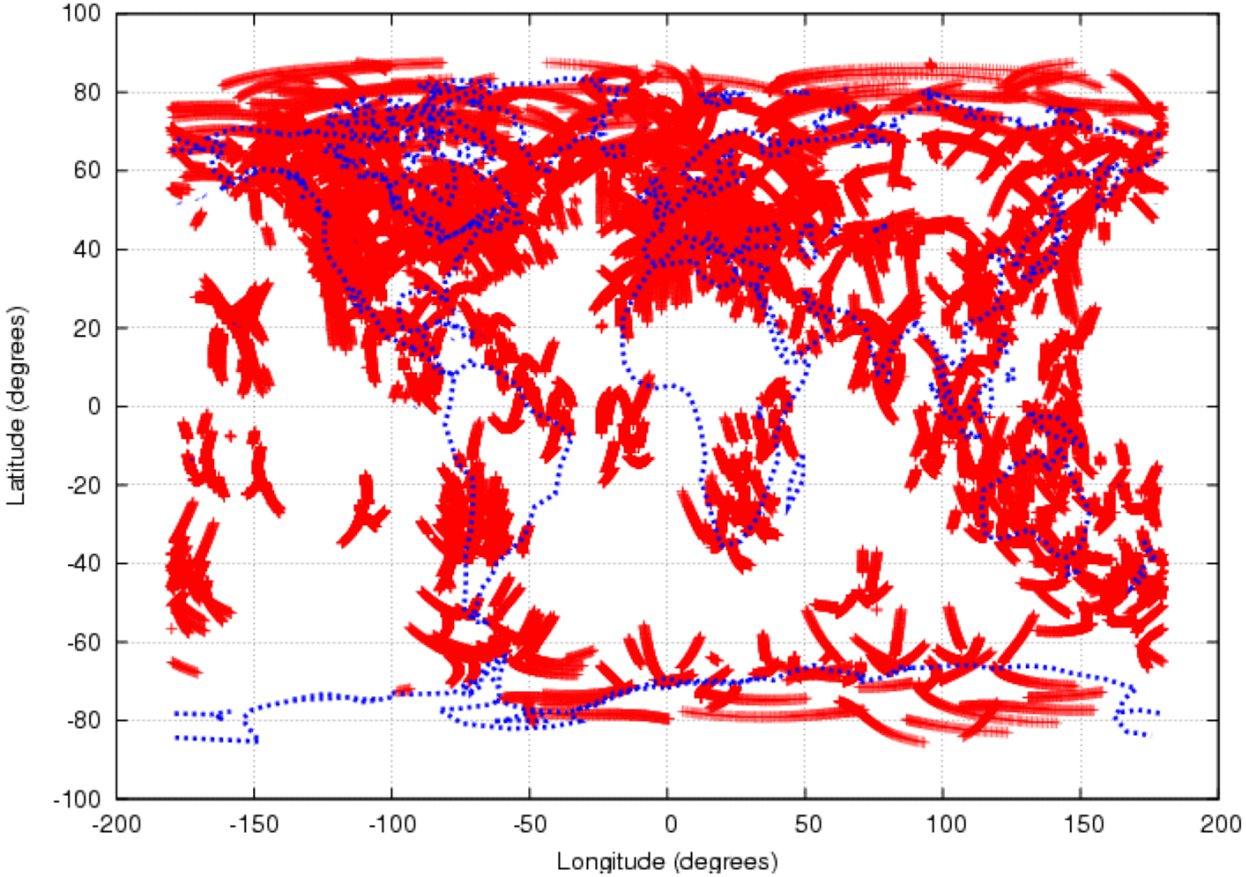

Distribution of the IPPs over a thin shell of 450 km height for an example day of January 3rd 2003 from 3 to 5 UT.

Kriging motivation in global VTEC modelling (2)

- The large areas without observations makes the method used to interpolate/extrapolate crutial.
- Kriging[*] is a Gaussian Process regression: weights (that combine the observed values for the process of interpolation / extrapolation) are computed by consistency with the expected error decorrelation vs. distance. This improves the results...

[*] We apply "Ordinary Kriging" on the residuals (it can be considered a sort of extended "Universal Kriging").

Kriging motivation in global VTEC modelling (3)

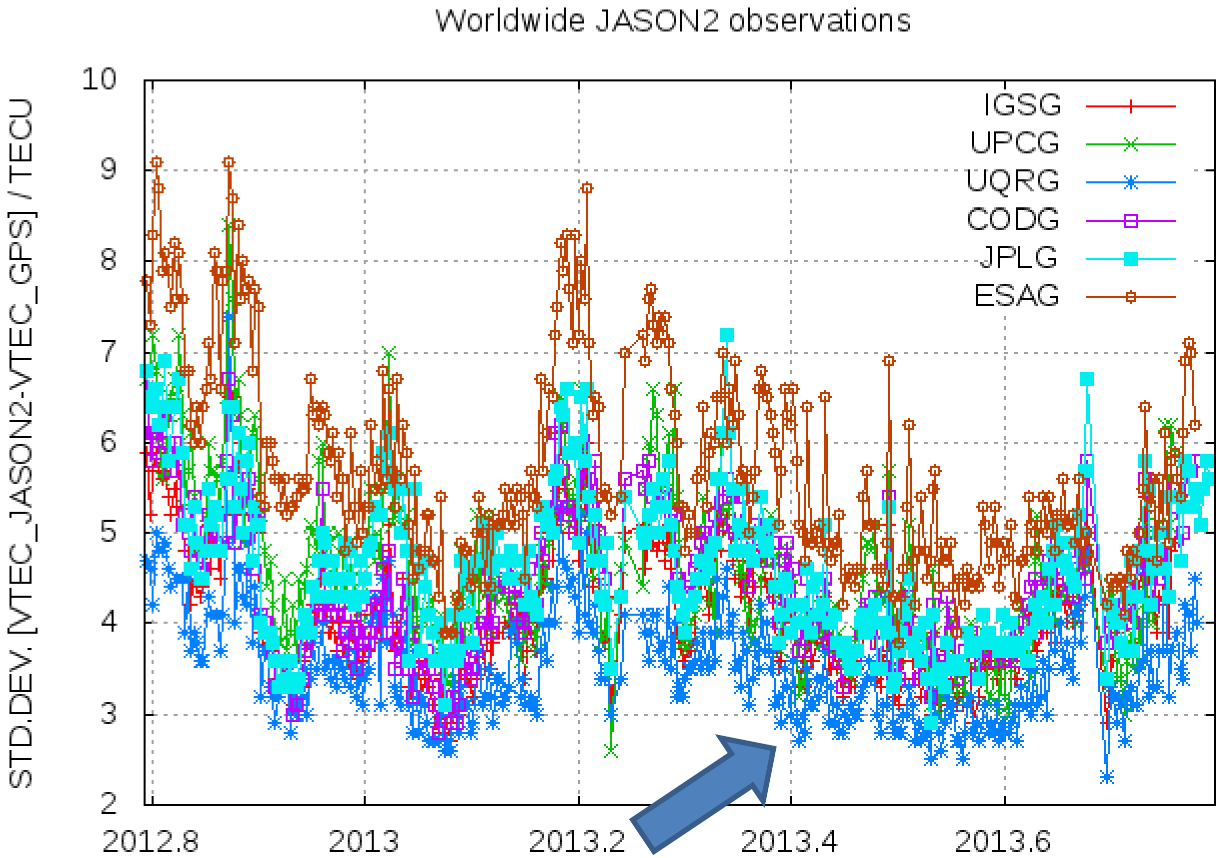

Std.Dev. [JASON2 VTEC – GNSS VTEC] during one year (worldwide). New rapid UPC global VTEC with Kriging (UQRG) works systematically better than all final IGS VTEC maps, including "classic" UPC product for 1 year-

Kriging motivation in global VTEC modelling (4)

- The better behaviour of new UPC global VTEC maps also during the last year confirms the previous comparisons with other models, beyond those of IGS ionospheric analysis centers:
  - Feltens, J., M. Angling, N. Jackson-Booth, N. Jakowski, M. Hoque, M. Hernández-Pajares, A. Aragón-Àngel, R. Orús, and R. Zandbergen (2011), Comparative testing of four ionospheric models driven with GPS measurements, Radio Sci., 46, RS0D12, doi:10.1029/2010RS004584.
  - Gulyaeva T.L., F. Arikan, M. Hernandez-Pajares, I. Stanislawska (2013), GIM-TEC adaptive ionospheric weather assessment and forecast system, Journal of Atmospheric and Solar-Terrestrial Physics, 102 (2013) 329–340.

Assessment with Jason-2 (2013.0-2014.4: ~70 rec. in RT)

Bias (left) and standard deviation (right) boxplots of the differences between the test data and the JASON reference data for the periods 001/2013 to 365/2013 and 001/2014 to 150/2014.

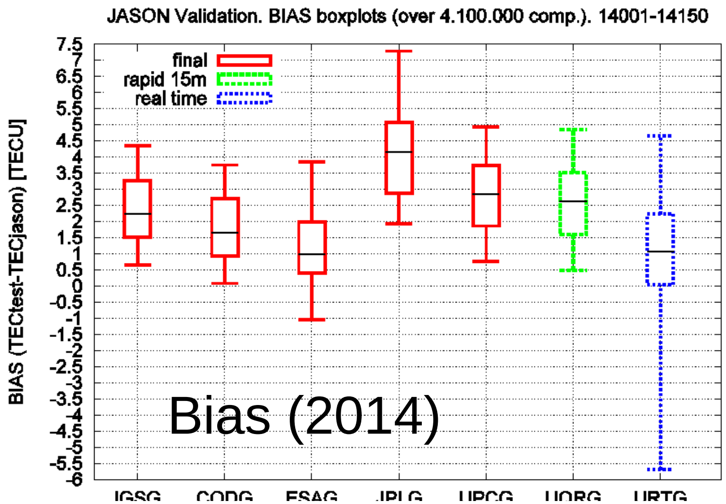

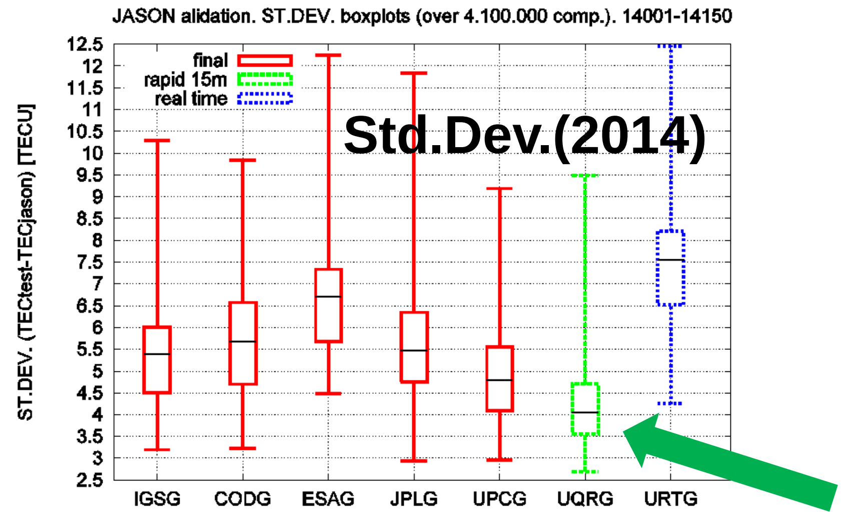

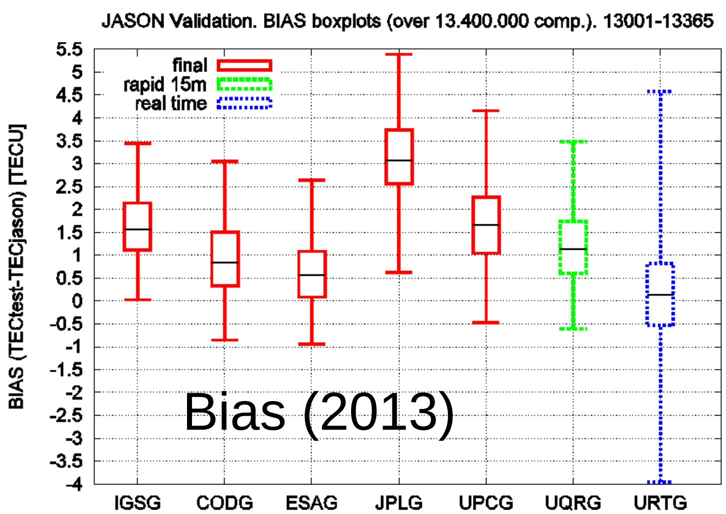

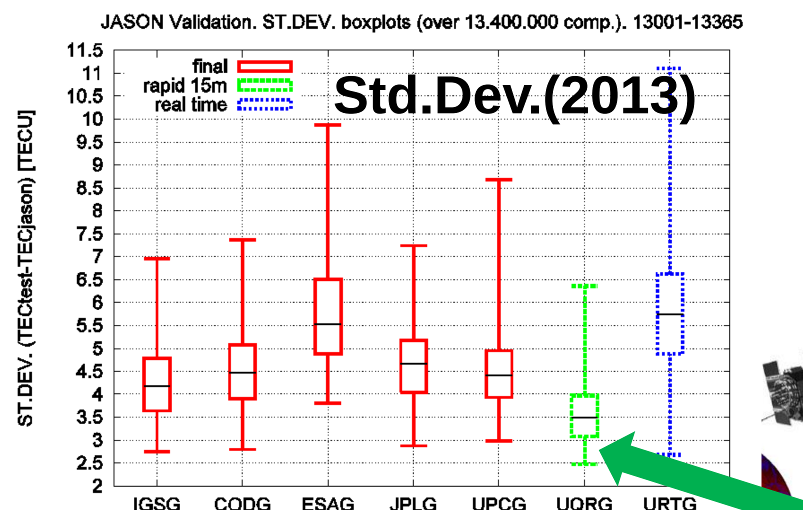

IGS finals | UPC rapid Kriging | UPC RT Kriging

UNIVERSITAT POLITÈCNICA DE CATALUNYA BARCELONATECH
M.Hernández-Pajares et al.

IGS Final Ionosphere Layout

The IGS Ionosphere Working group started its activities in June 1998 with the main goal of a routinely producing IGS Global TEC maps (IGTEC). This is being done now with a latency of 11 days (final product –official-) and with a latency of less than 24 hours (rapid product –still unofficial-).

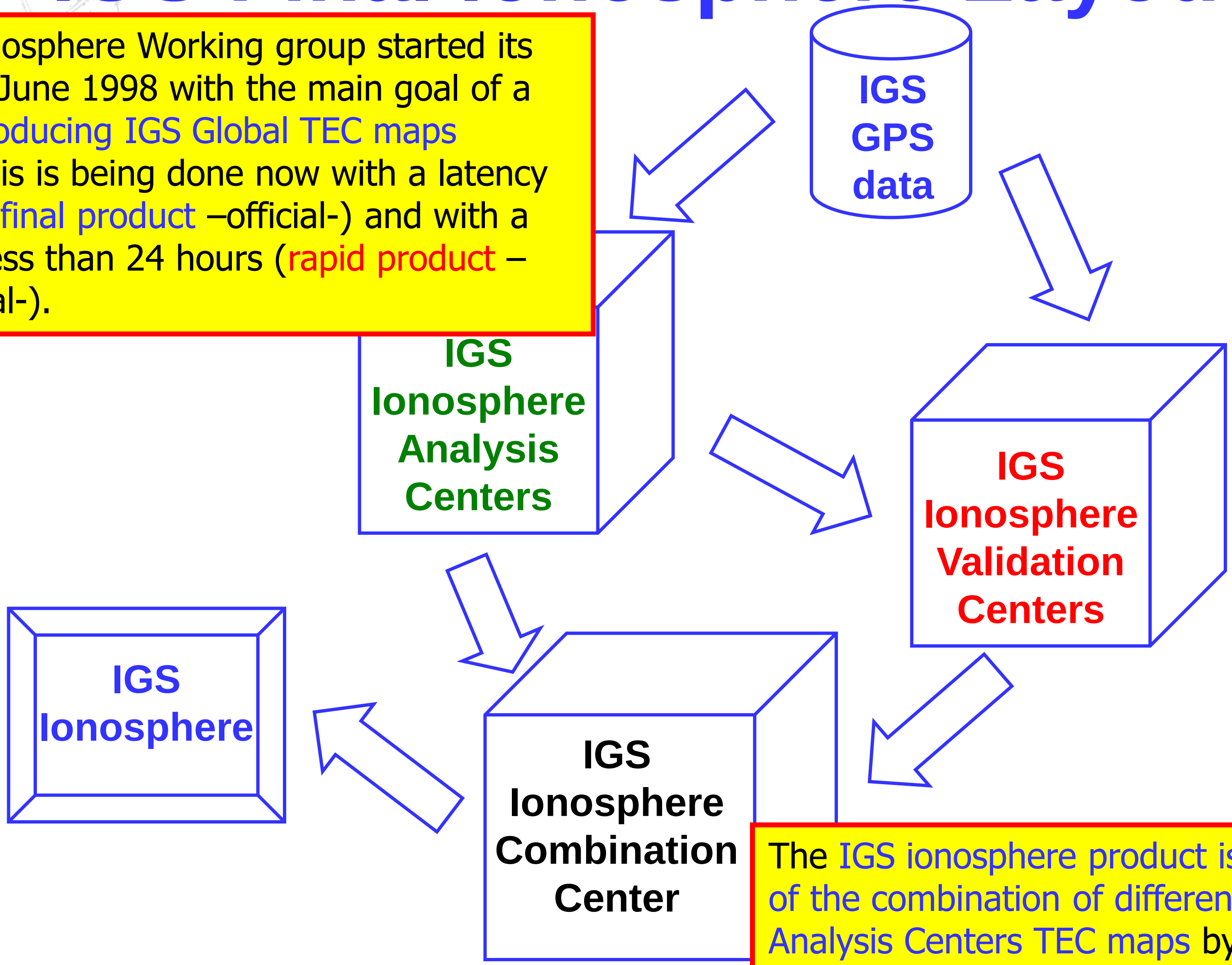

The IGS ionosphere product is a result of the combination of different Analysis Centers TEC maps by using weights computed from GPS data by Validation Centers, in order to get a more accurate product.

Example of IGS Final TEC map: 2003-347-00UT

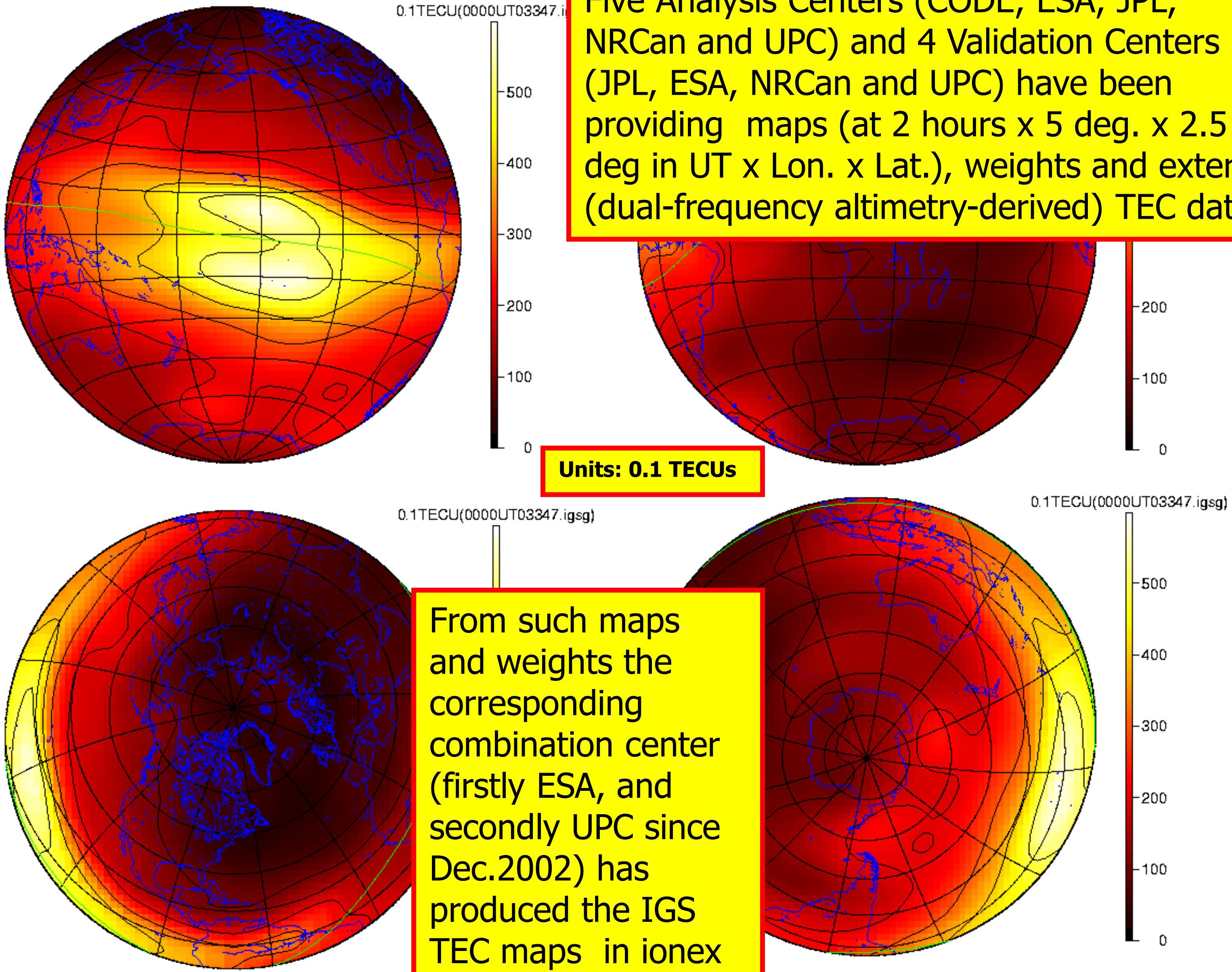

Five Analysis Centers (CODE, ESA, JPL, NRCan and UPC) and 4 Validation Centers (JPL, ESA, NRCan and UPC) have been providing maps (at 2 hours x 5 deg. x 2.5 deg in UT x Lon. x Lat.), weights and external (dual-frequency altimetry-derived) TEC data.

Units: 0.1 TECUs

From such maps and weights the corresponding combination center (firstly ESA, and secondly UPC since Dec.2002) has produced the IGS TEC maps in ionex format.

UNI
DE CATALUNYA
BARCELONATECH

IGS Final Ionosphere Flow-Chart

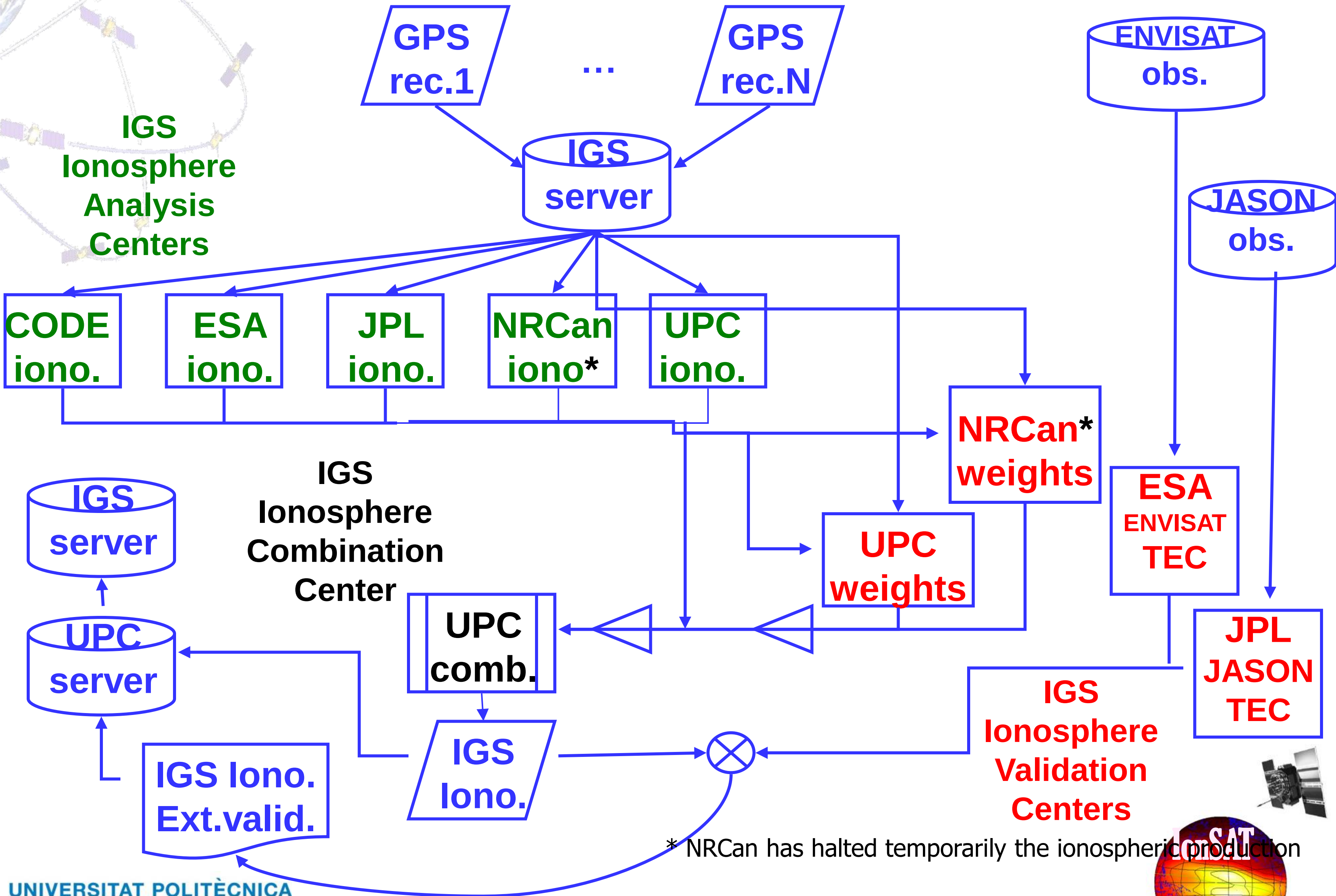

* NRCan has halted temporarily the ionospheric production

Example of comparison of IGS vs JASON: 2003-347 each 6 hours

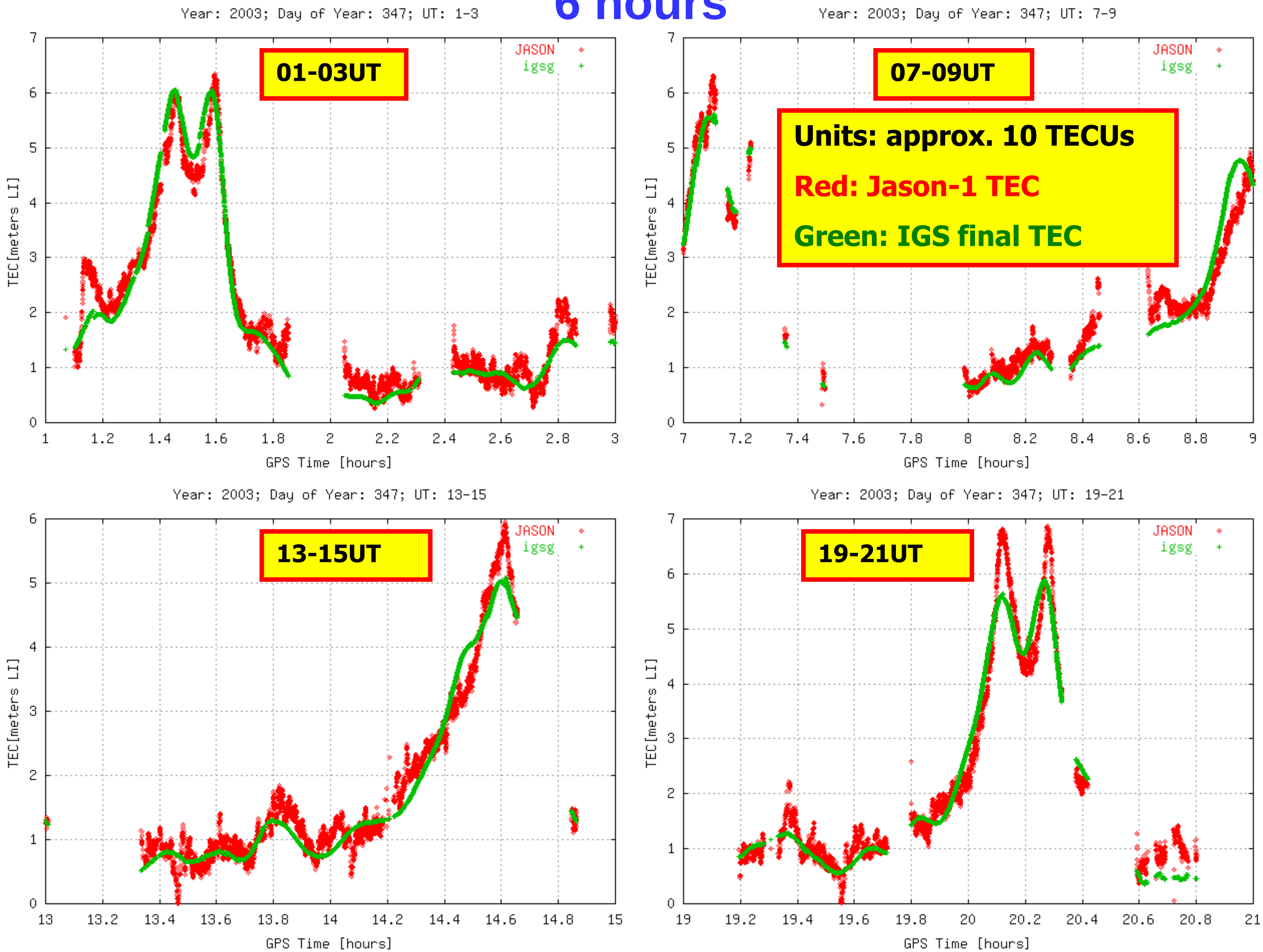

Final IGS TEC vs. JASON TEC

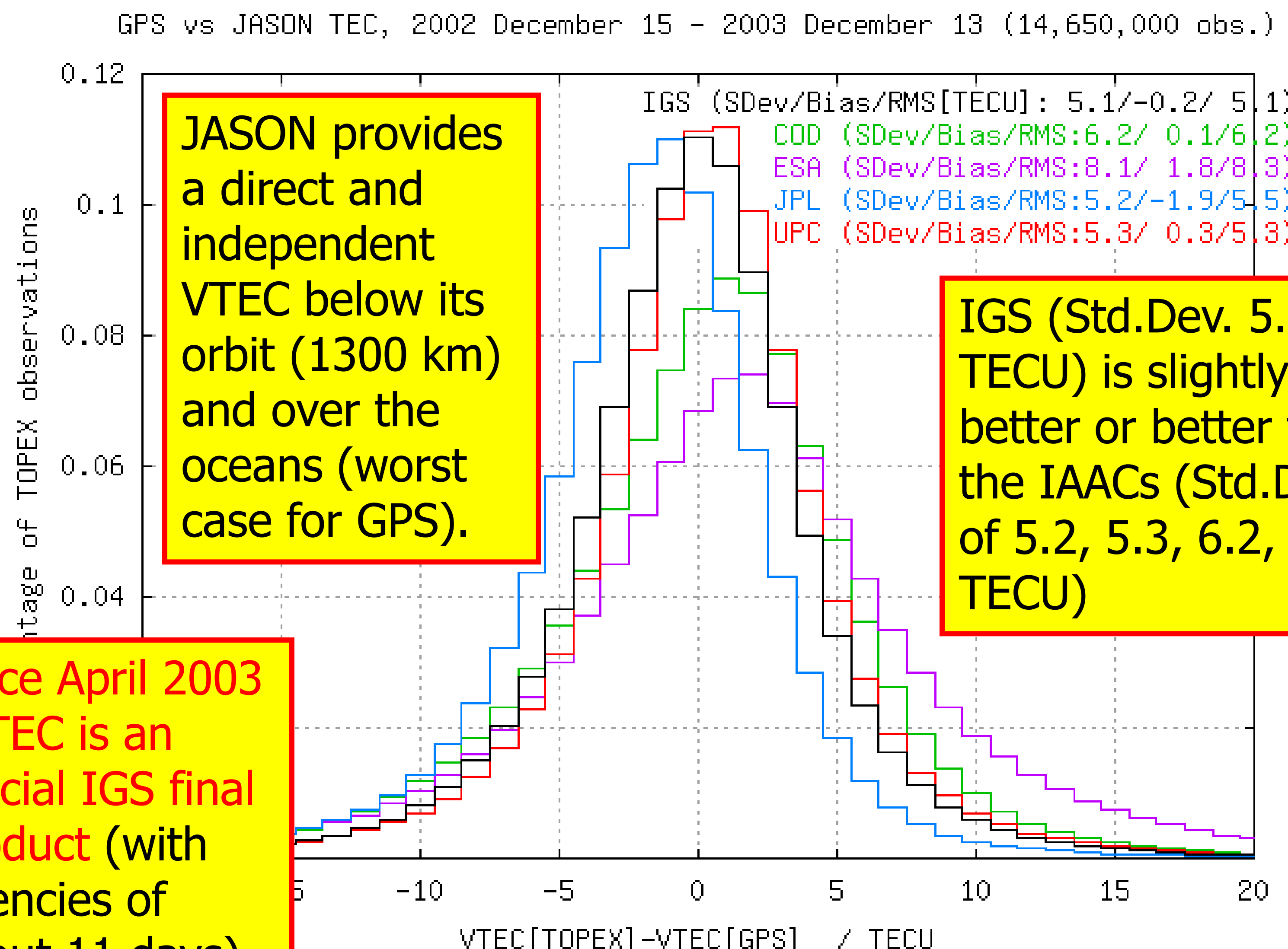

JASON provides a direct and independent VTEC below its orbit (1300 km) and over the oceans (worst case for GPS).

IGS (Std.Dev. 5.1 TECU) is slightly better or better than the IAACs (Std.Dev. of 5.2, 5.3, 6.2, 8.1 TECU)

Since April 2003 IGTEC is an official IGS final product (with latencies of about 11 days).

"Relative Error" vs. JASON (daily)

Typical daily relative error over the oceans of about 20% (15-25%). Sometimes large peaks appear coinciding with large geomagnetic storms (related to the present temporal resolution of 2 hours).

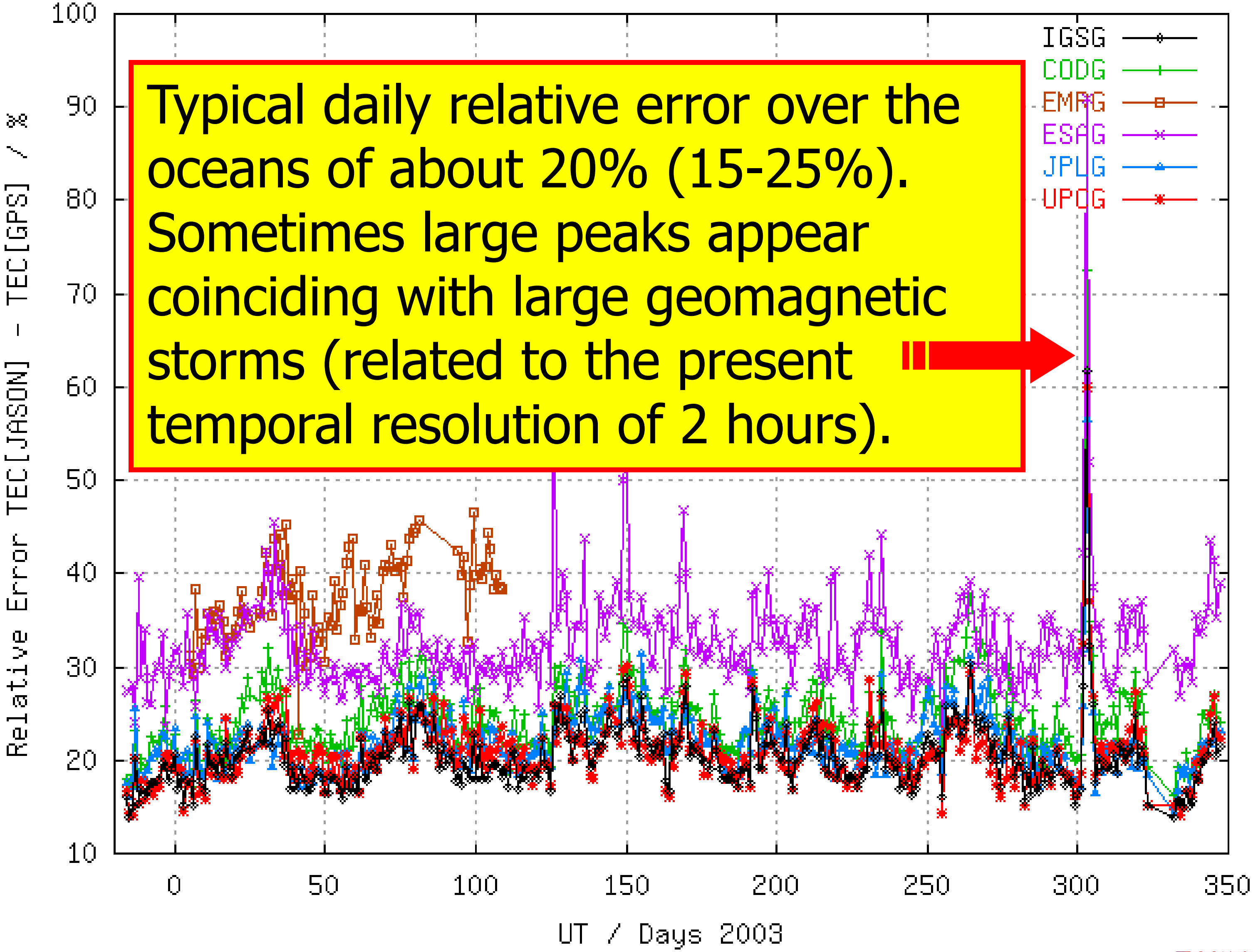

UNIVERSITAT POLITÈCNICA DE CATALUNYA
BARCELONATECH

Ap index vs. "Relative Error"

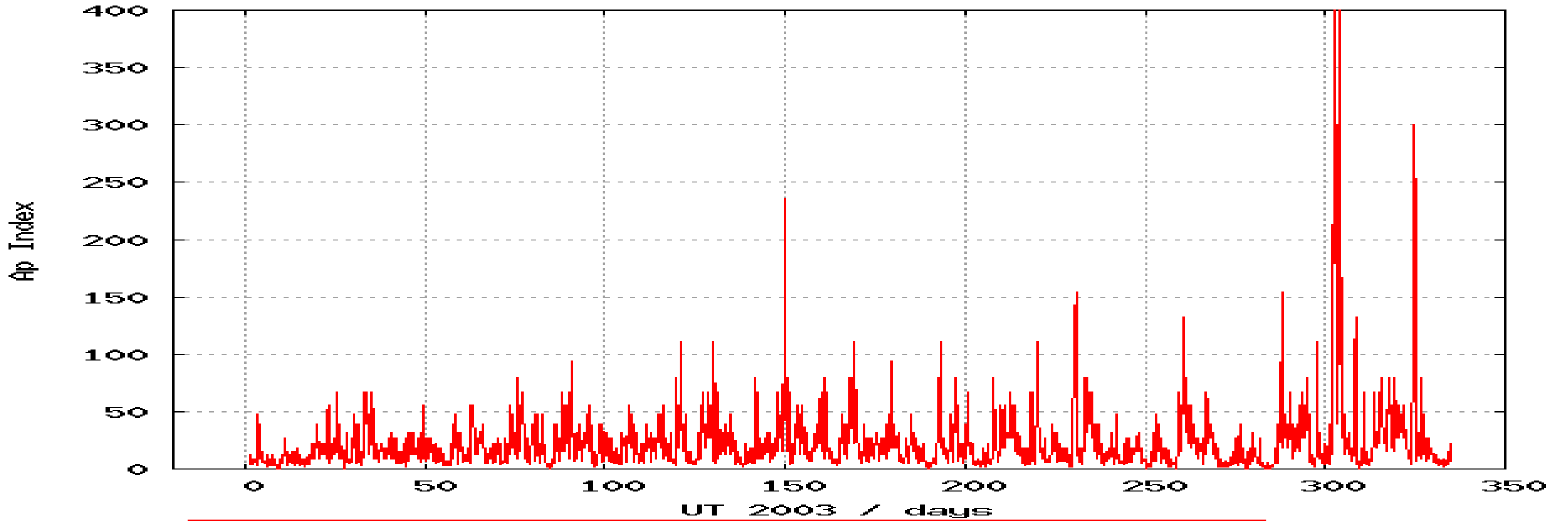

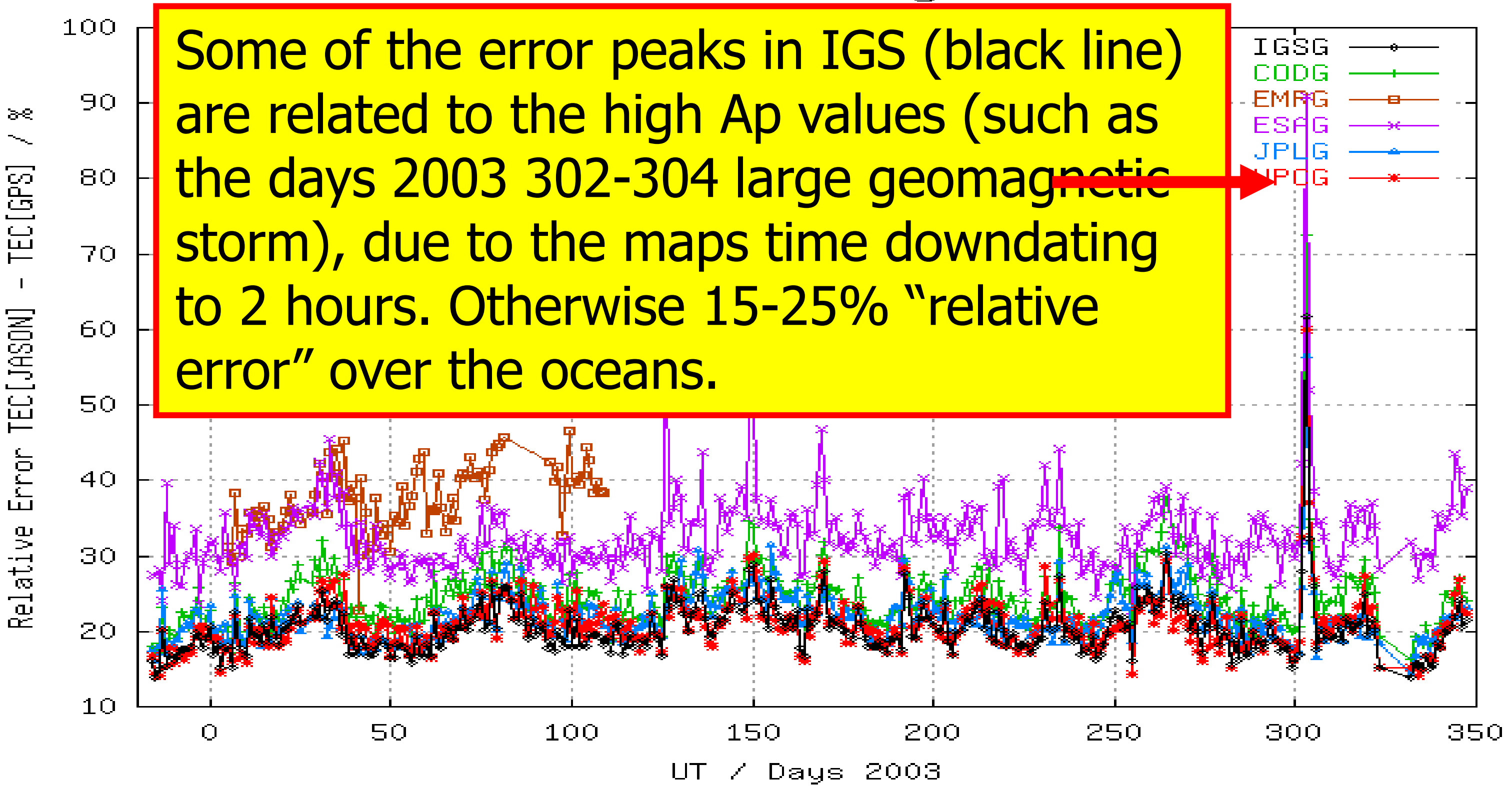

Some of the error peaks in IGS (black line) are related to the high Ap values (such as the days 2003 302-304 large geomagnetic storm), due to the maps time downdating to 2 hours. Otherwise 15-25% "relative error" over the oceans.

Std.Dev vs. JASON (gmag.lat.)

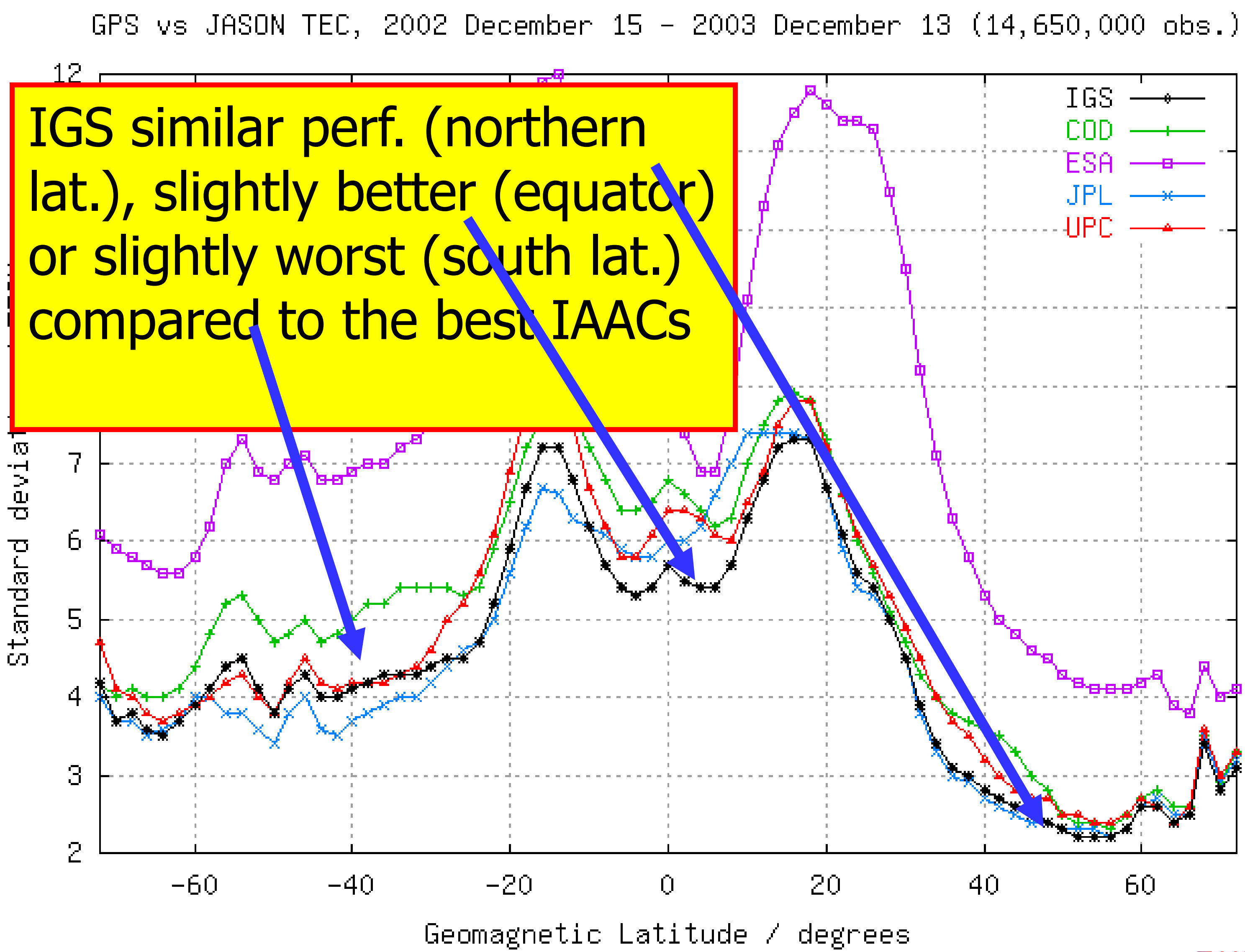

IGS similar perf. (northern lat.), slightly better (equator) or slightly worst (south lat.) compared to the best IAACs

UNIVERSITAT POLITÈCNICA DE CATALUNYA
BARCELONATECH

Bias vs. JASON (gmag.lat.)

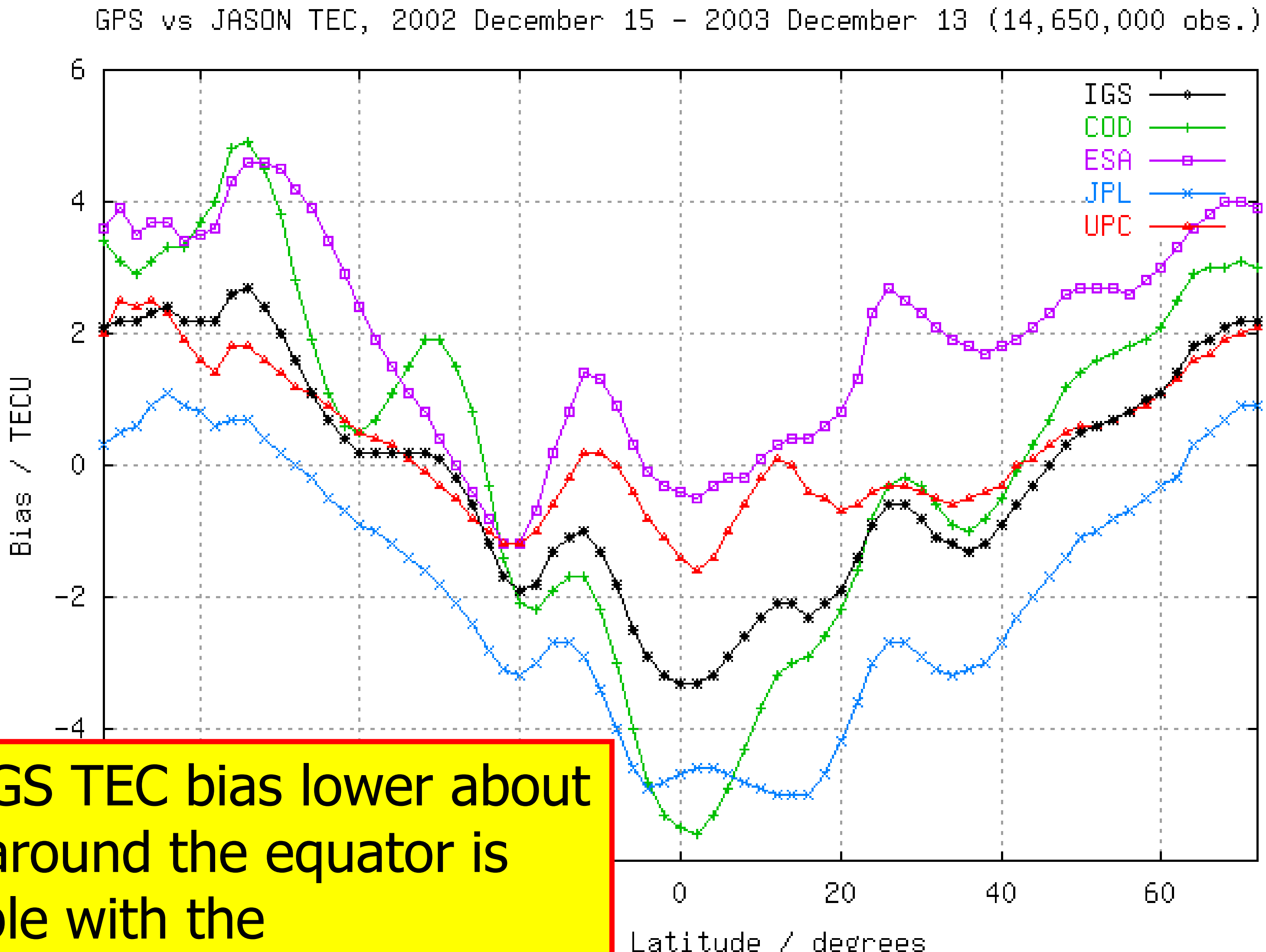

JASON-IGS TEC bias lower about 5 TECU around the equator is compatible with the plasmaspheric component. The absolute bias ref. is still unclear

“Rel. error” vs. TOPEX(gmag.lat.)

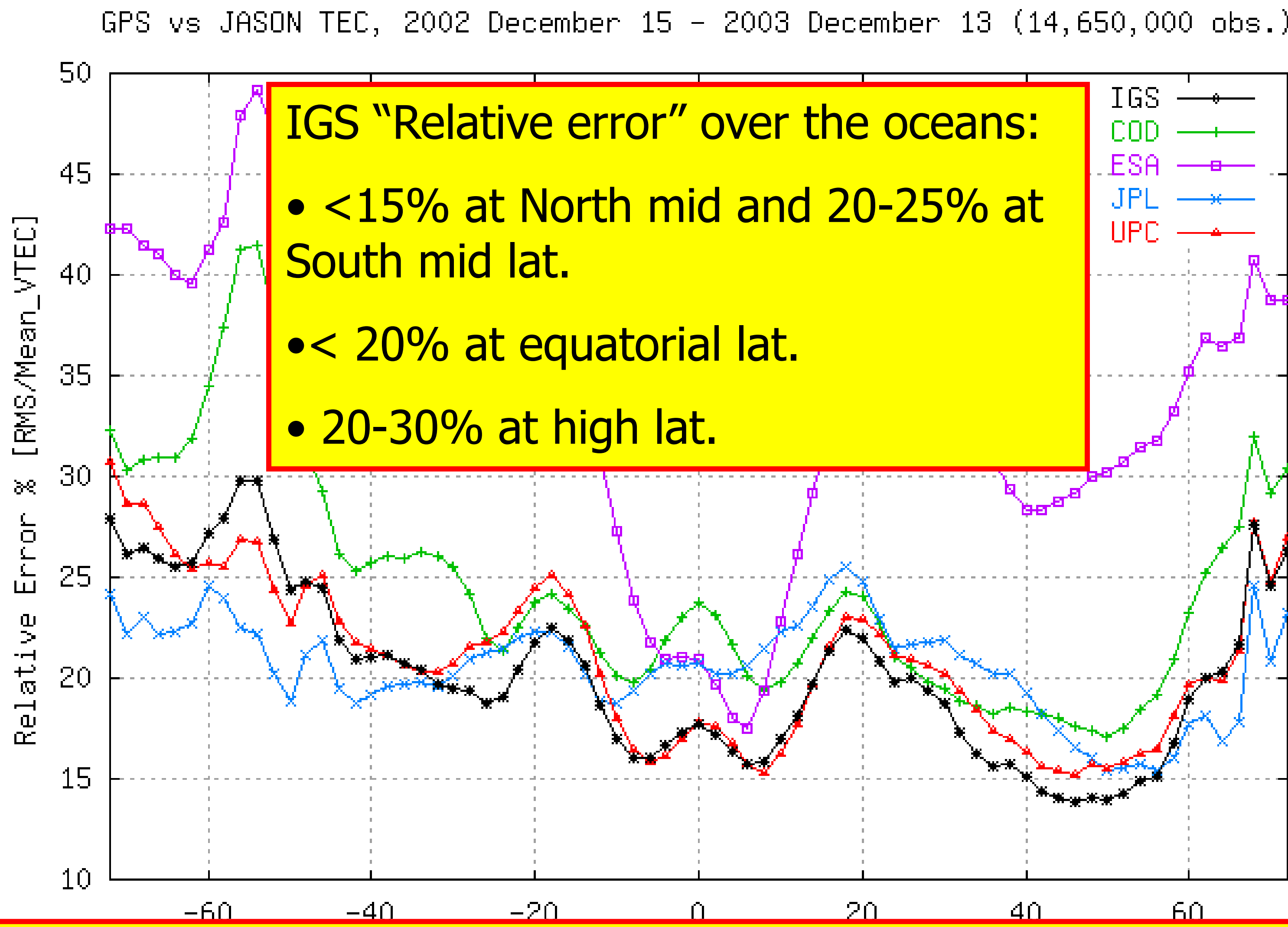

IGS “Relative error” over the oceans:

- <15% at North mid and 20-25% at South mid lat.
- < 20% at equatorial lat.
- 20-30% at high lat.

More performance details of the IGS final product (satellite and receiver DCBs, double dif. STEC, latency, with different data scarcity): **http://maite152.upc.es/~ionex3/doc/IGS_IONO_report_April2003_7.pdf**

Rapid vs Final IGS TEC “Rel.Error”

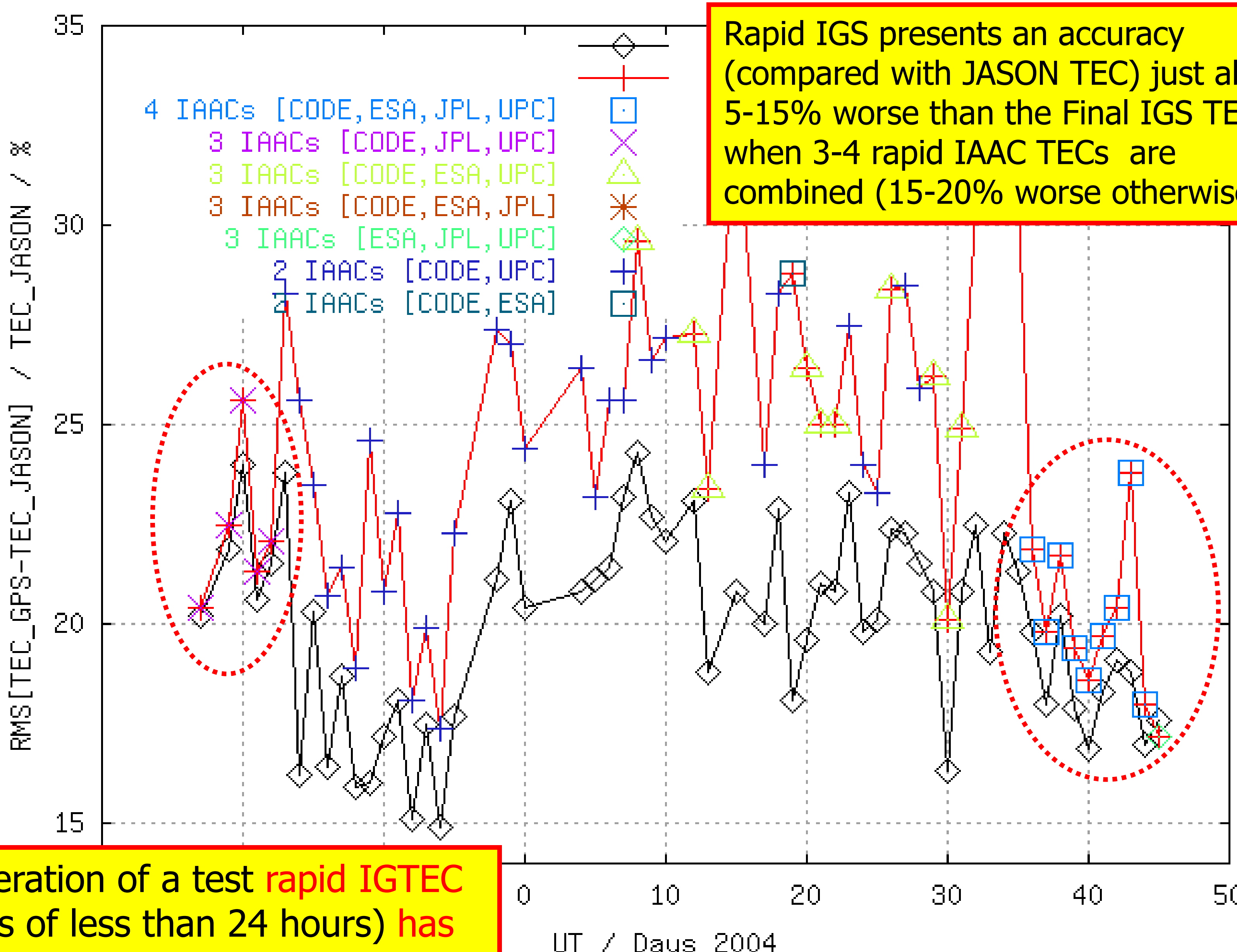

Rapid IGS presents an accuracy (compared with JASON TEC) just about 5-15% worse than the Final IGS TEC when 3-4 rapid IAAC TECs are combined (15-20% worse otherwise).

The generation of a test rapid IGTEC (latencies of less than 24 hours) has started recently (Dec.2003).

Rapid vs Final IGS DCBs

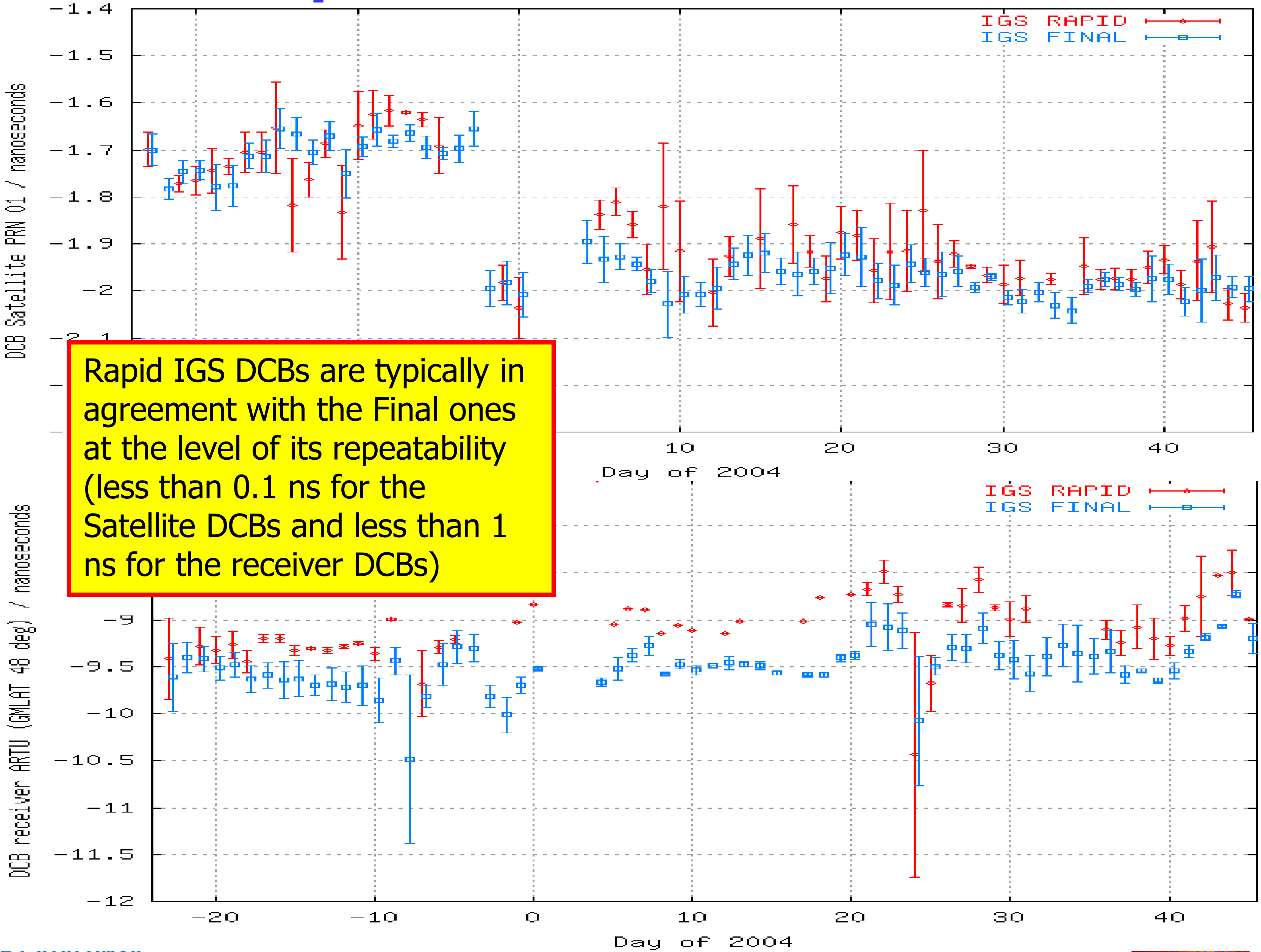

Rapid IGS DCBs are typically in agreement with the Final ones at the level of its repeatability (less than 0.1 ns for the Satellite DCBs and less than 1 ns for the receiver DCBs)

Alternative weighting schemes

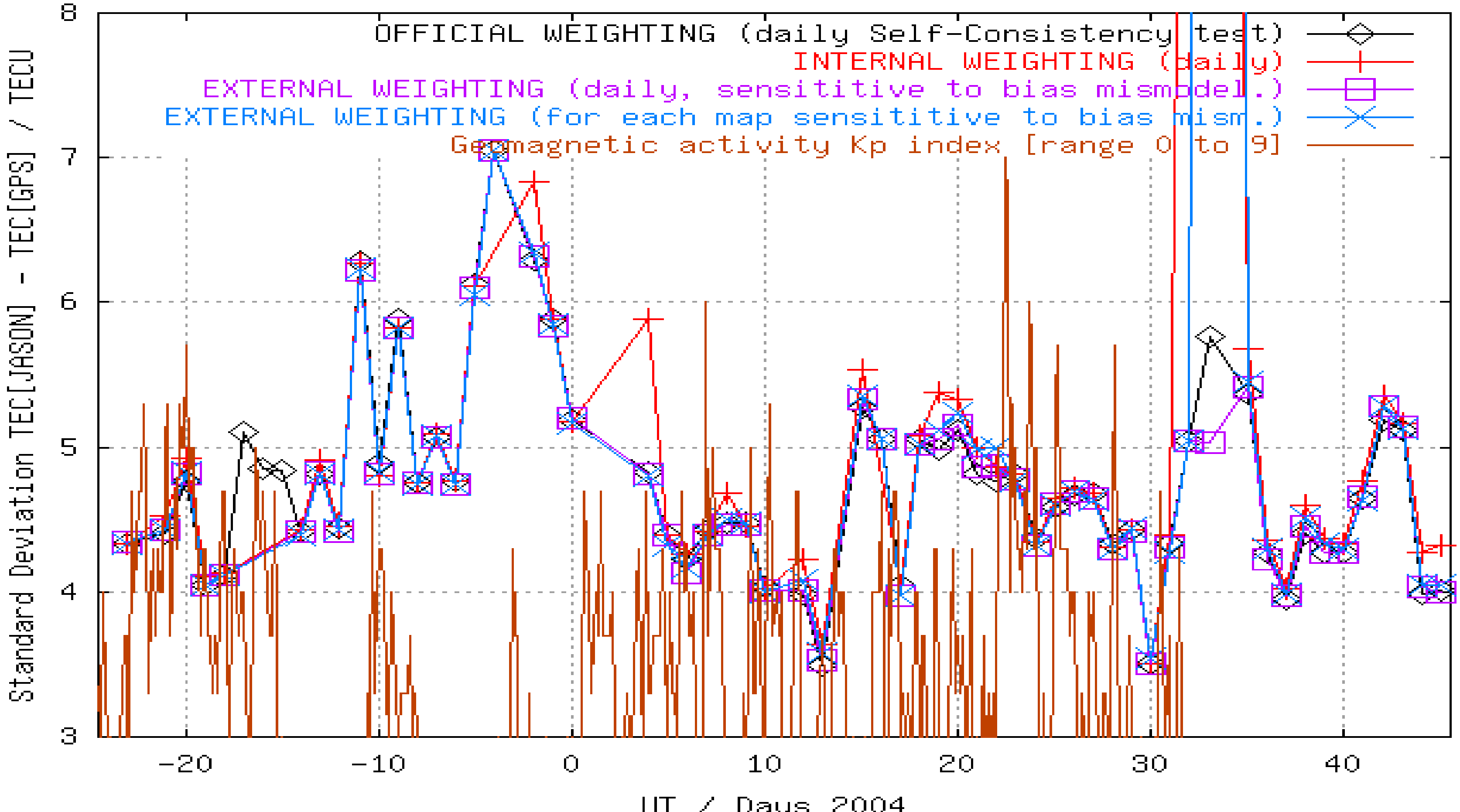

- The performance between daily weighting (magenta squares) and independent map weighting (blue crosses) are very similar, including geomagnetic activity periods (days -23 to -19 and 22 to 28, 2004).
- The performance of the official weighting algorithm (bias insensitive) is very similar to that using a bias-sensitive weighting algorithm (truth: STEC referred to the max. elevation ray STEC, both observed).
- It is confirmed the best performance of external weighting strategies (presently used), compared with the internal weighting, from the deviates to the plain mean of IAAC TEC maps (red crosses).

Alternative weighting schemes (2)

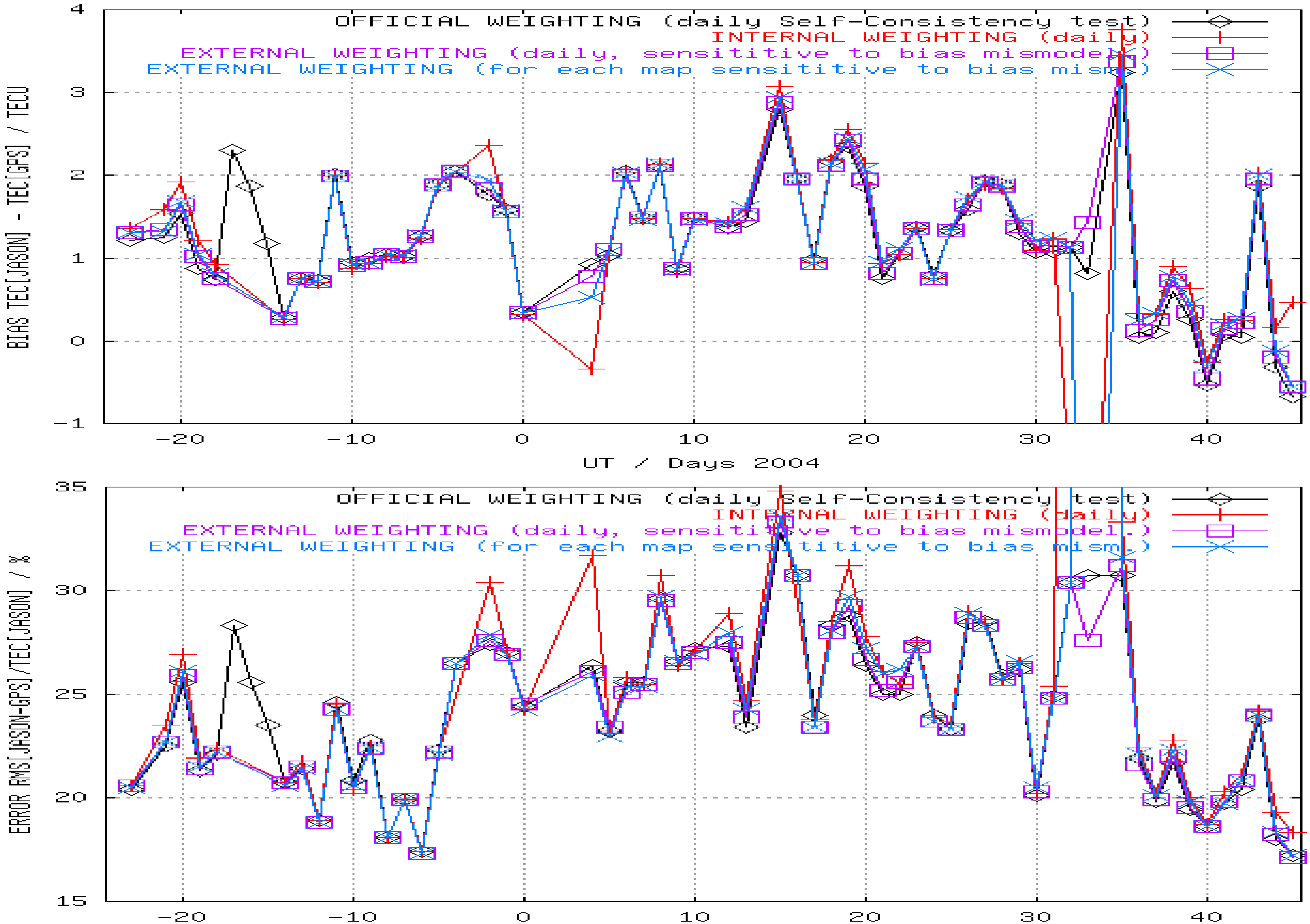

Previous results confirmed with bias and "relative error"

Bias vs. JASON & TOPEX (daily)

*JASON and TOPEX fly at the same orbit with about 60 sec. of difference.

* JASON TEC bias seems about 1 TECU lower than TOPEX TEC bias.

*JASON TEC seems more compatible with IGS TEC than TOPEX TEC.

UNIVERSITAT POLITÈCNICA DE CATALUNYA
BARCELONATECH

TEC performance vs. Distance (1)

Comparison with TOPEX: worst case estimate of performance (far from the GPS sites).

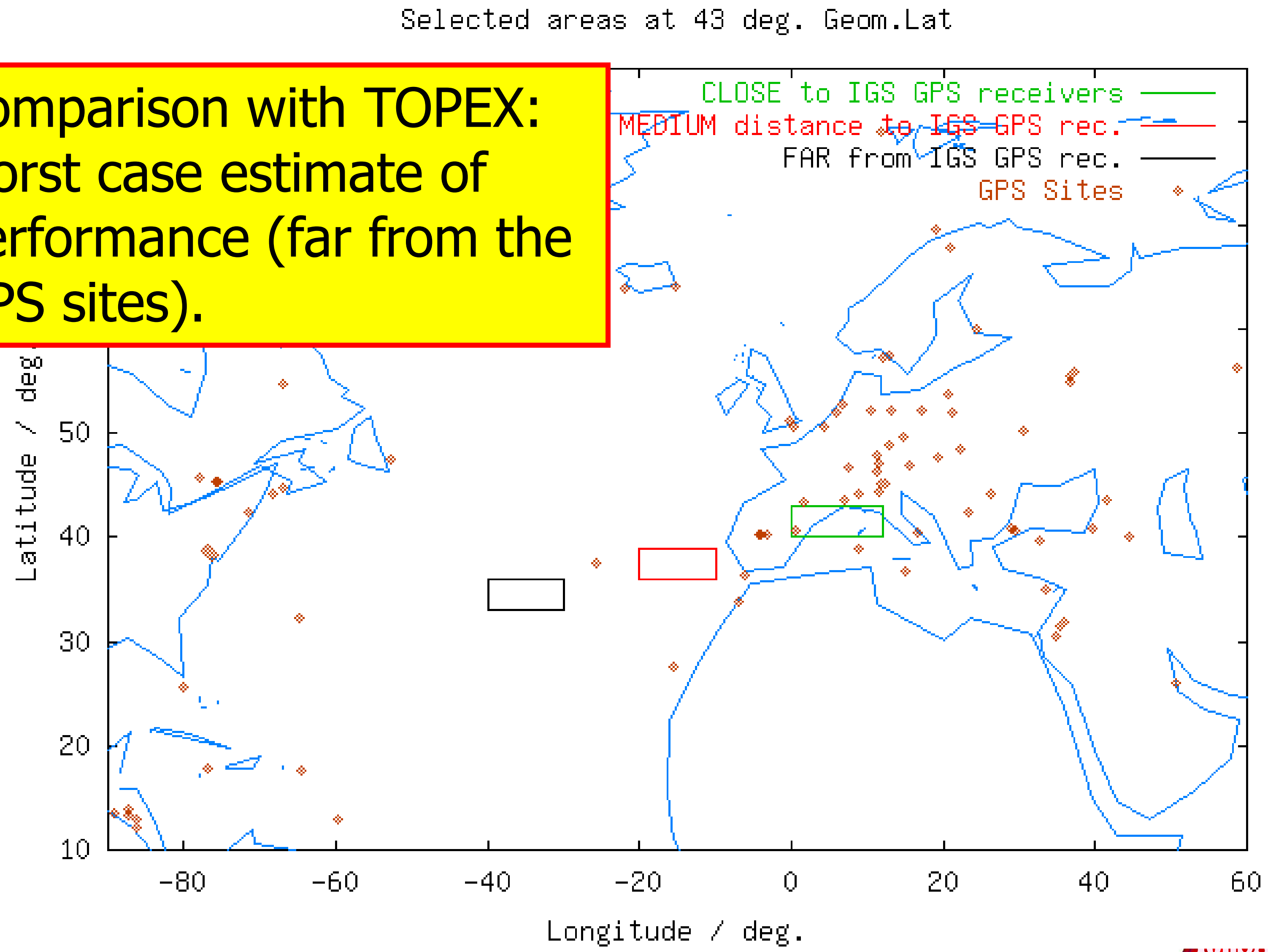

UNIVERSITAT POLITÈCNICA DE CATALUNYA
BARCELONATECH

TEC performance vs. Distance (2)

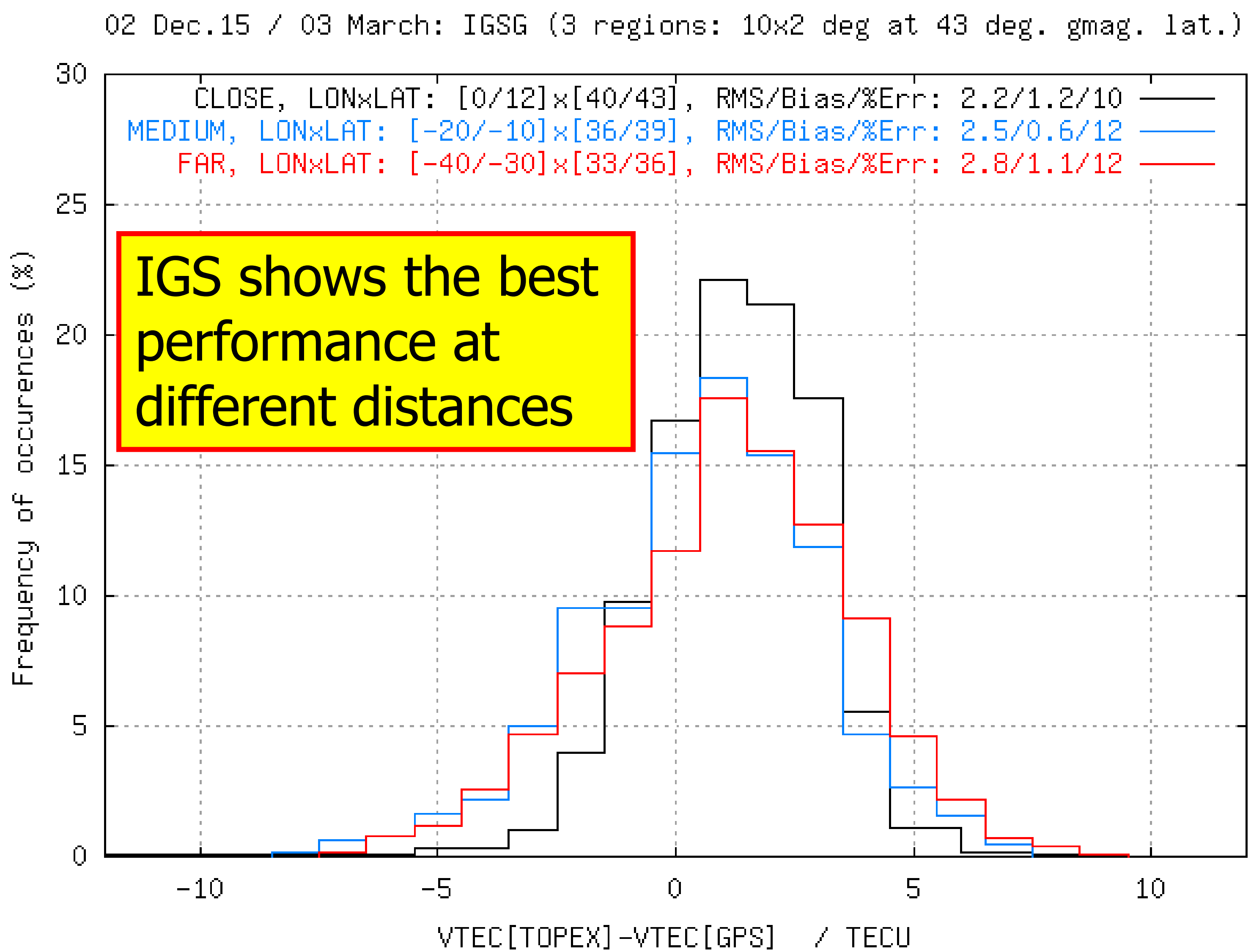

Double Diff. STEC performance

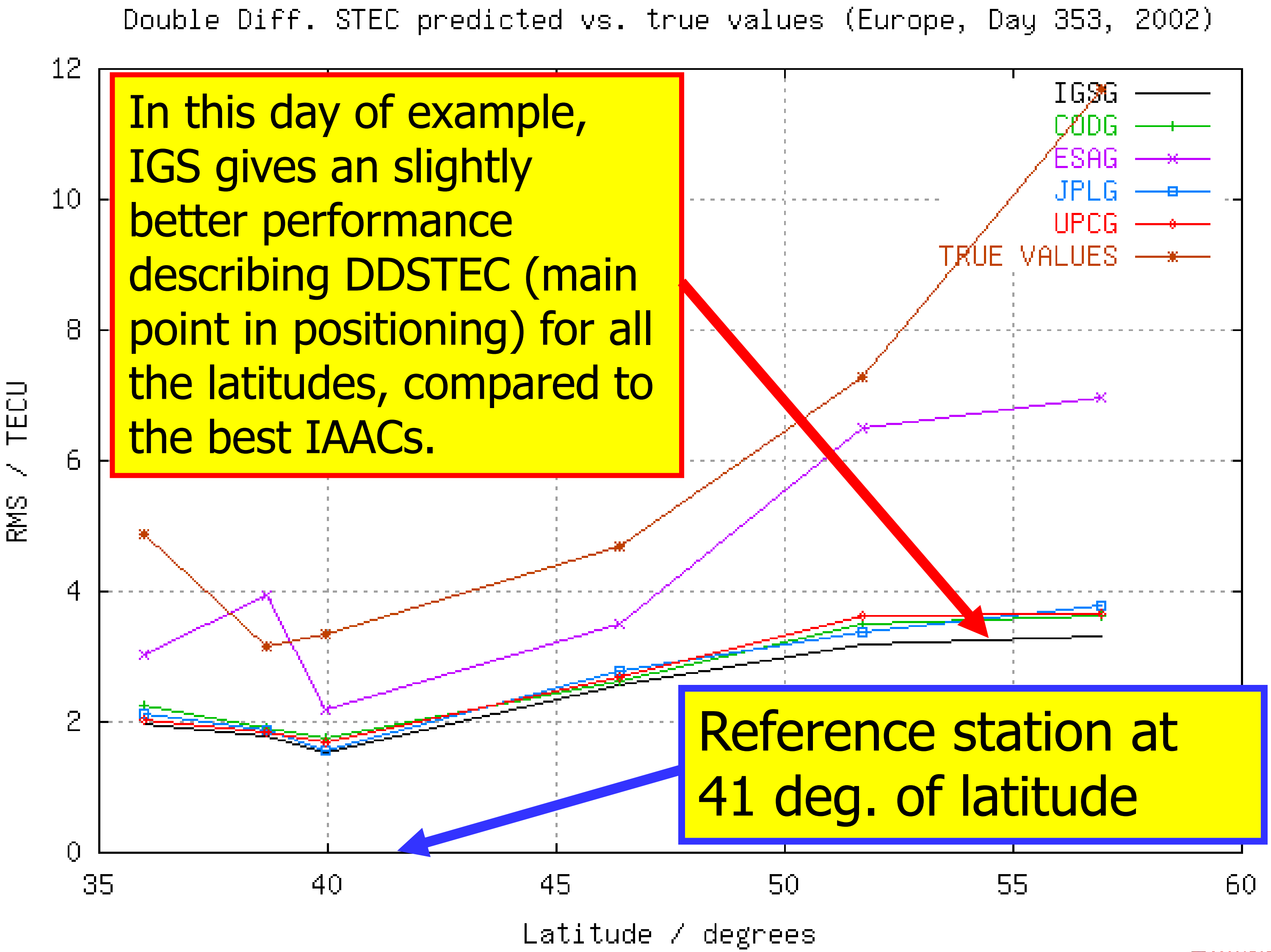

UNIVERSITAT POLITÈCNICA DE CATALUNYA
BARCELONATECH

TOPEX RMS vs Formal Std.Dev.

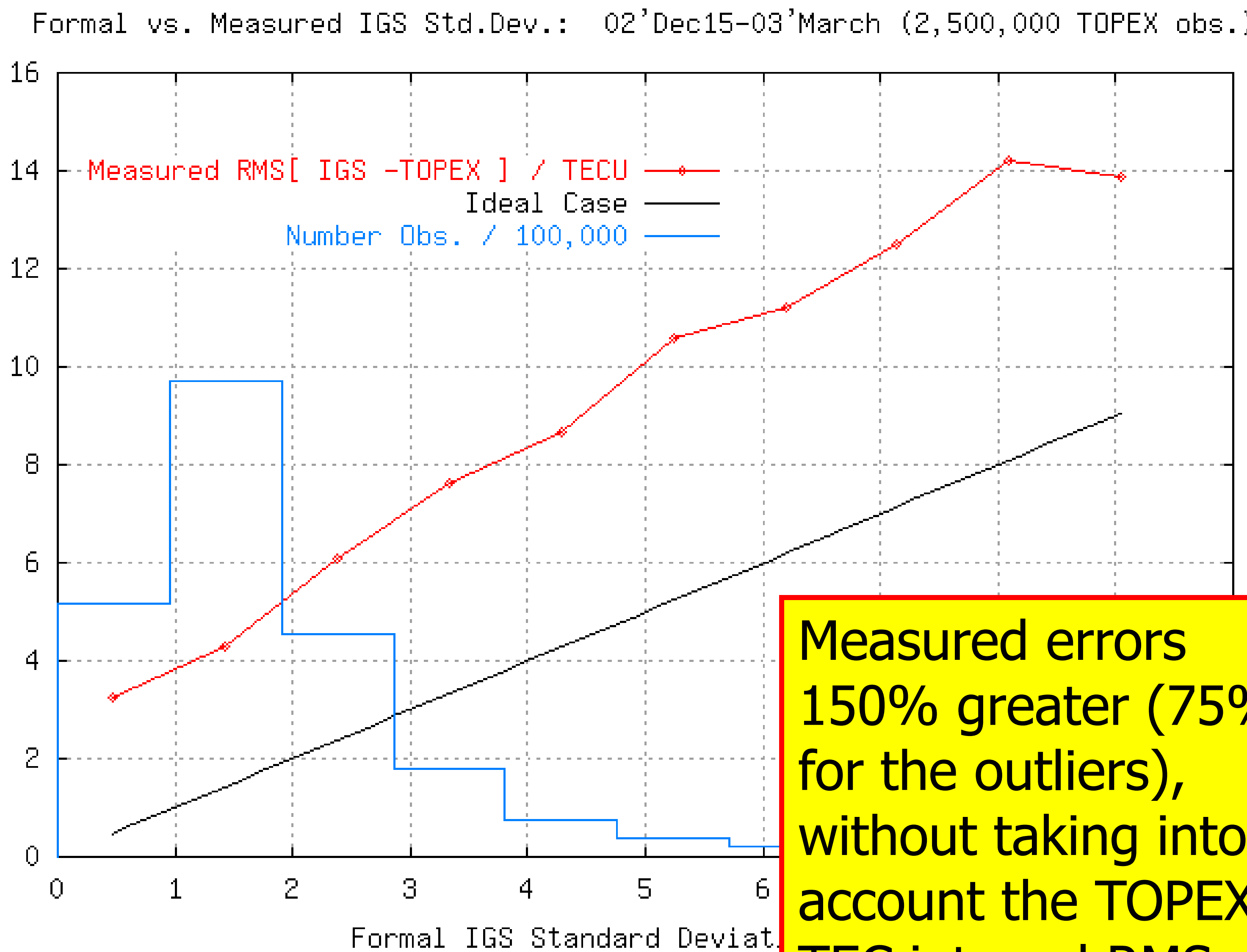

Measured errors 150% greater (75% for the outliers), without taking into account the TOPEX TEC internal RMS.

UNIVERSITAT POLITÈCNICA DE CATALUNYA BARCELONATECH

Satellite DCB's stability

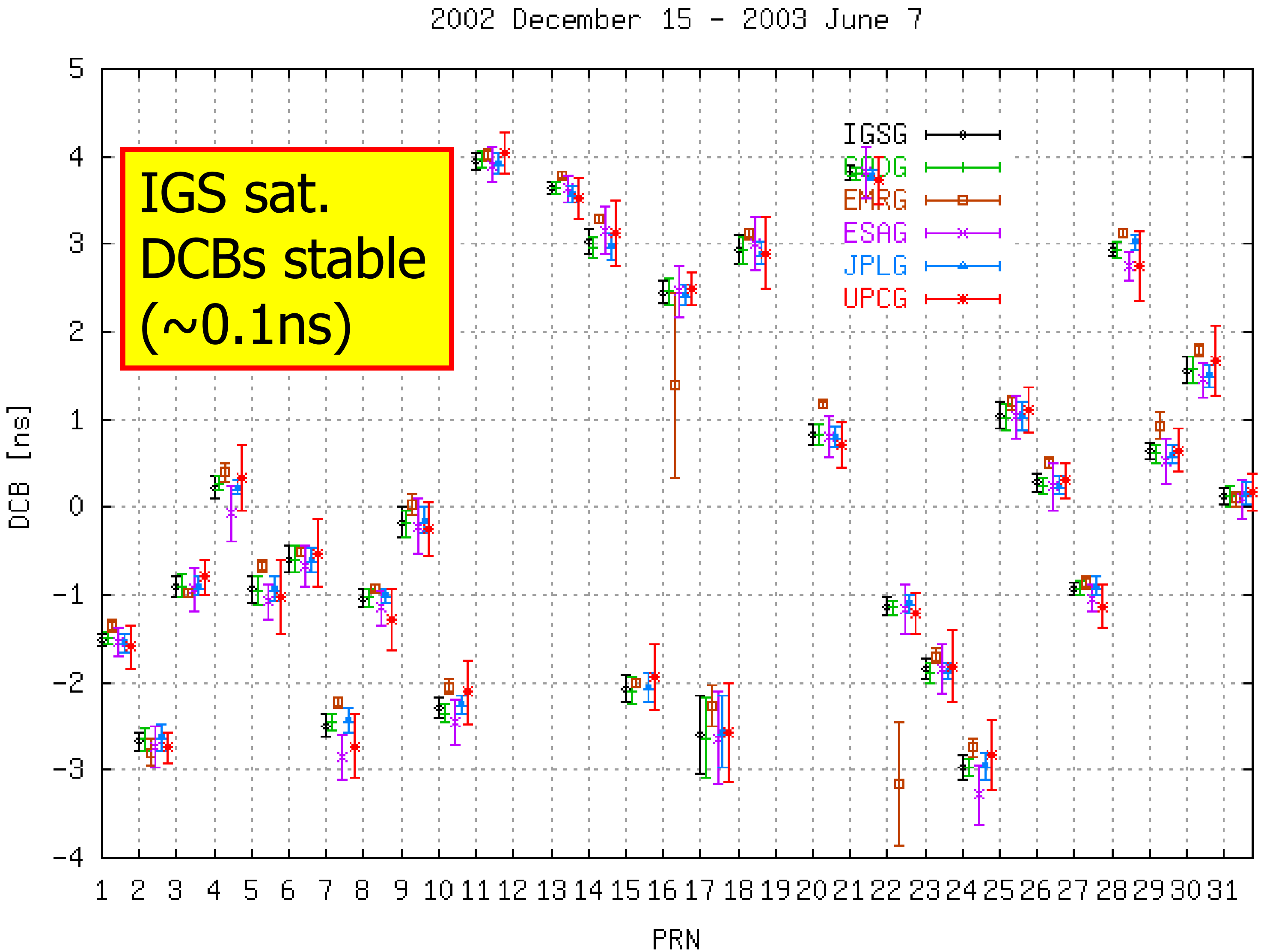

Station DCB's stability

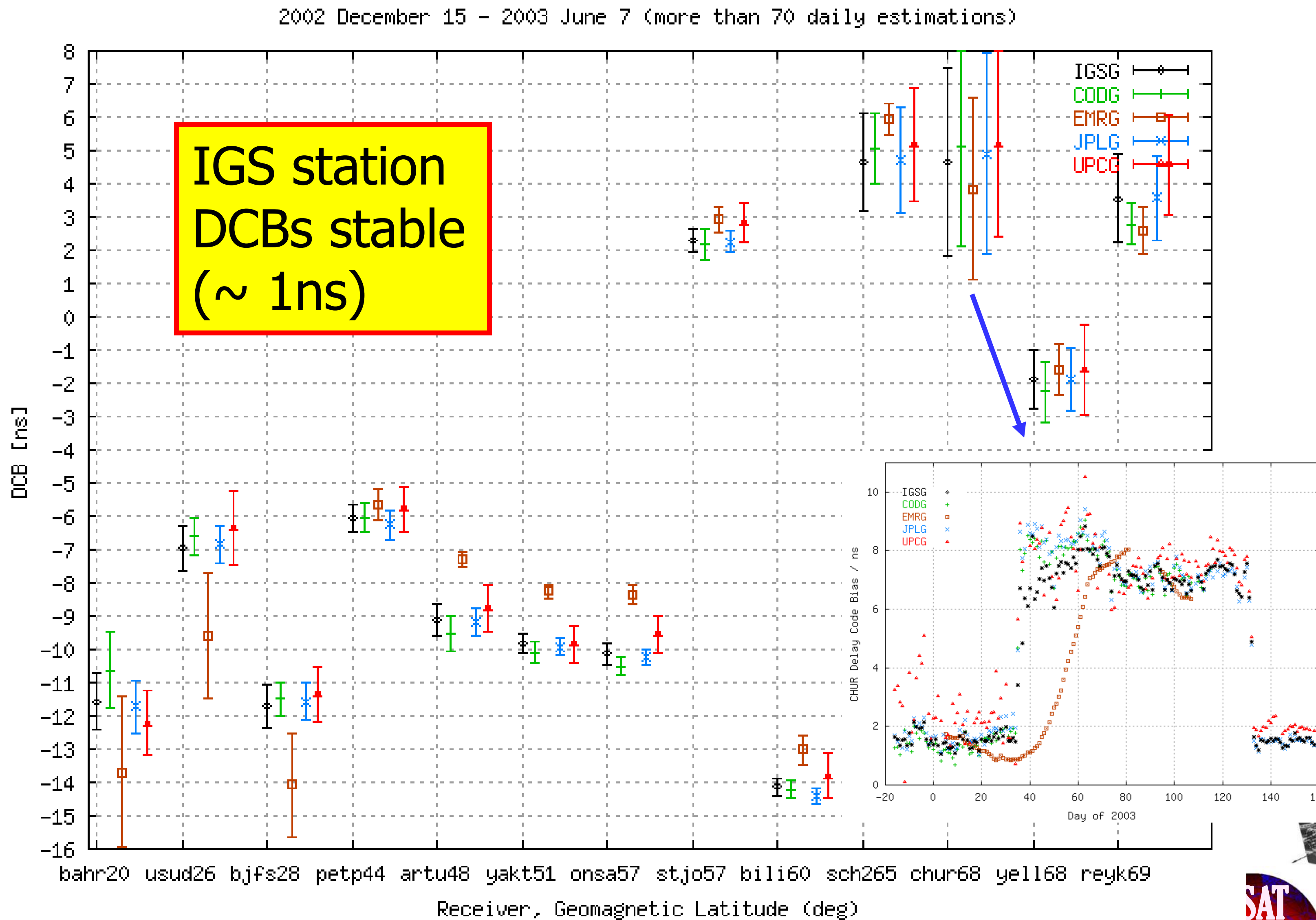

UNIVERSITAT POLITÈCNICA DE CATALUNYA
BARCELONATECH

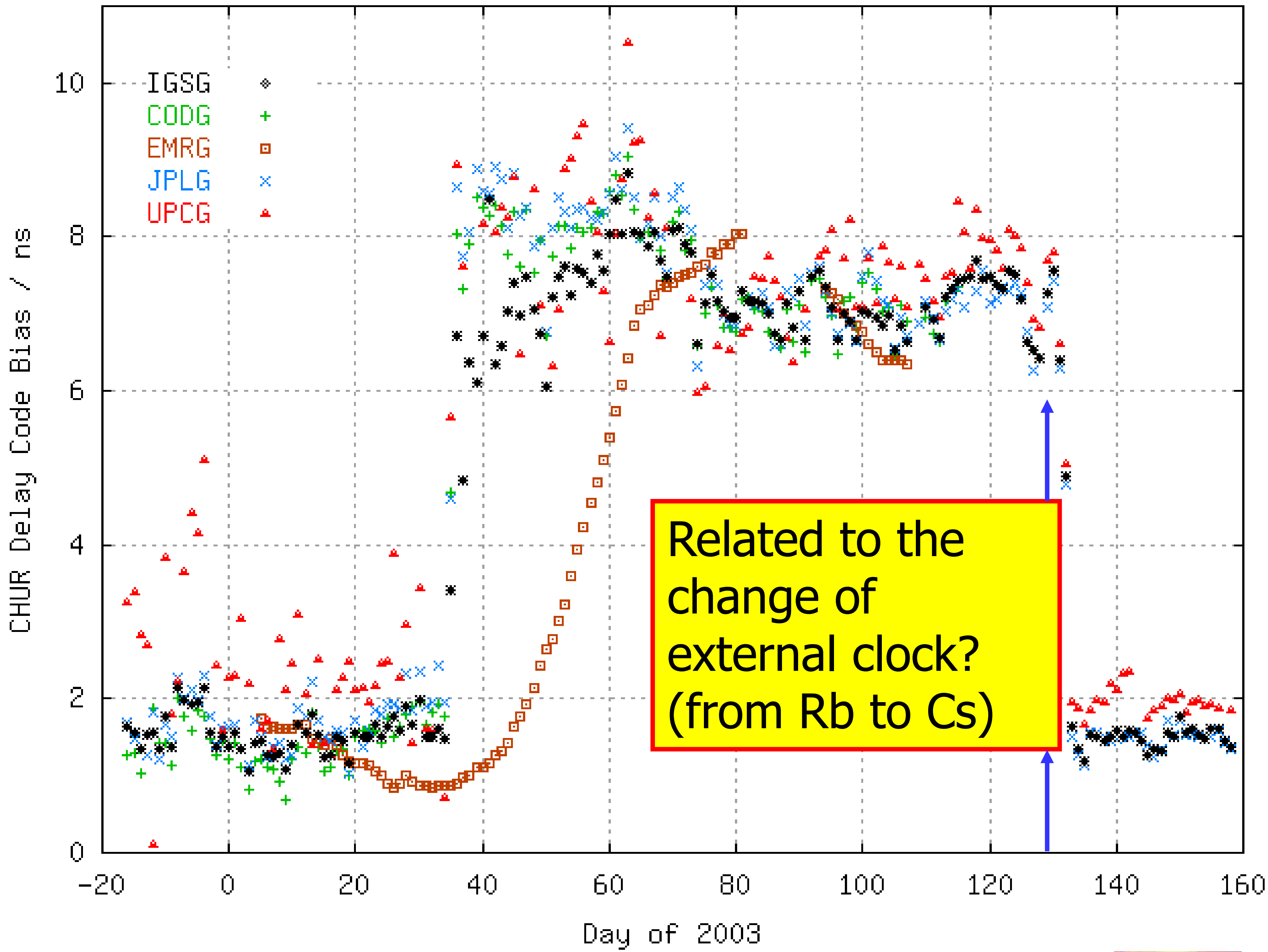

UNIVERSITAT POLITÈCNICA DE CATALUNYA BARCELONATECH

IGS Ionospheric Activities status

- After several improvements performed in the IAACs and IGS Ionosphere Map combination algorithms in 2003, the IGS final combination of TEC maps shows a good performance that is slightly better or even better than the individual IAAC maps, that justified our efforts to start producing the final iono product in April 2003.
- The rapid IGS TEC maps generation started, in testing mode, in December 2003 (latency less than 24 hours, as opposed to 11 days of the final product). The first maps (and DCBs) show a good accuracy (about 10% worse than the final maps) when 3-4 rapid IAACs TEC maps are combined.
- Regarding alternative weighting strategies:
  - The performance of the official weighting algorithm (bias insensitive) is similar to that using a bias-sensitive algorithm.
  - It is confirmed the best performance of external weighting strategies (presently used), compared with the internal weighting.
  - The performance between daily and independent map weighting seems very similar, including geomagnetic activity periods.

UNIVERSITAT POLITÈCNICA DE CATALUNYA BARCELONATECH

IonSAT

Final Ionosphere product use (2003, from cddisa)

- 453 distinct IPs (hosts) downloaded IONEX files in 2003.
- 154,000 files donwloaded.
- 29 countries.
- Top “Non-IAAC” users (60% of files donwloaded from them, E=Education, C=Commercial, G=Government, N=Network):
- APL, US (E), TU, Vienna, Austria (E), NAO, Japan (E), CRL, Japan (G), CABLESPEED, U.S. (C/N), ENST-BRETAGNE, France (E), UWM, Poland (E), WAT, Poland (E), U.TRIESTE, Italy (E), NRAO, U.S. (E), STATE OF TENESSEE, U.S. (G), IGN, France (G), ISP, Russia (N), ALCATEL, France (C), ISP, S.Korea (N), U.MUNICH, Germany (E).
- 68% files donwloaded from “Non-IAAC” users.

Some recommendations (updated from the IGS Iono. WG splinter meeting happened at the IGS Technical Meeting held at Bern, March 2004)

- The use of the final IGS product is quite large. However for the rapid product, started in Dec.2003, very few downloads are registered from its temporarily server at UPC. In this context to promote its use, the next actions items have been adopted:

1. To send a new e-mail to the IGS e-mail list announcing the rapid product.
2. Moving the igs-iono e-mailing list to igscb.
3. Moving rapid product server from UPC to CDDISA.

- After receiving inputs from VLBI, Altimeter and Timing users, it has been decided:

1. To maintain the present generation of both final and rapid IGS TEC maps.
2. To include the list of GPS receivers used for timing in the list of IAAC used stations to compute the ionospheric product, in order to ensure IGS DCB estimations for such receivers.

- There has not been consensus between the IAACs on increasing the temporal, spatial resolution/densification of the present ionospheric products.

IGS Final Ionosphere ionex files at
ftp://cddisa.gsfc.nasa.gov/gps/products/ionex/

Thank you!

UNIVERSITAT POLITÈCNICA DE CATALUNYA
BARCELONATECH

IonSAT

- Application Example: WARTK and WARTK-3

Introduction

- A GNSS navigation service with errors of few centimeters at continental scale will enhance existing applications (civil eng.…) , allowing new ones (real-time mapping…).

- The differential ionospheric refraction limits typically its coverage to baselines <20 km (RTK).

- Until now, the authors had combined an accurate ionospheric model: (1) with RTK in two-frequency systems (GPS: WARTK), and (2) with TCAR in three-frequency systems (Galileo and Modernized GPS: WARTK-3, extending the Local Area Galileo services to continental scales).

- The main goal of this presentation: to show the WARTK/WARTK-3 consolidation and improvement algorithm, WARTK-3 Laboratory campaign data generation and results, taking into account two main improvements:
  - *Improving the integrity of the ionospheric corrections.*
  - *Integration in a navigation filter* (WARTK-3.2).

UNIVERSITAT POLITÈCNICA DE CATALUNYA BARCELONATECH

Why does a GPS user need external ionospheric corrections better than 2.7cm (0.25 TECU) to navigate with sub-decimeter accuracy?

- We can get sub-decimeter accuracy when we are able to convert the precise carrier phases in precise and accurate pseudoranges by estimating and fixing the integer ambiguities. This speeds up very much the convergence and the accuracy by eliminating such ambiguity unknowns.

- One typical dual-frequency user can navigate with ionosphere-free combination of carrier phases (Lc), but the iono-free ambiguity (Bc) is not integer, and cannot be fixed and removed.

- Solution: to estimate accurately a second independent ambiguity, the geometric free one (BI), which is linear combination of both L1 and L2 integer ambiguities, thanks to very accurate external double-differenced ionospheric corrections.

$$\nabla\Delta B_I = \nabla\Delta L_I - \nabla\Delta STEC_{ext}$$

- Then the L1 ambiguity can be estimated (the widelane ambiguity Nw can be estimated from a rough Bc and BI).

$$\nabla\Delta N_1 = \frac{-1}{\lambda_2-\lambda_1}\nabla\Delta B_I + \frac{\lambda_2}{\lambda_2-\lambda_1}\nabla\Delta N_w$$

- And N1 can be fixed and removed if the iono. error is lesser than 2.7cm=0.25TECU

$$\frac{1}{\lambda_2-\lambda_1}\varepsilon[\nabla\Delta B_I] < 0.5\,cycles \quad\Rightarrow\quad \varepsilon[\nabla\Delta B_I] \approx \varepsilon[\nabla\Delta STEC_{ext}] < \frac{\lambda_2-\lambda_1}{2} = 2.7\,cm$$

UNIVERSITAT POLITÈCNICA DE CATALUNYA BARCELONATECH

Vertical Ionospheric Refraction

UPC Global Ionospheric Map: 077 2000, 15UT

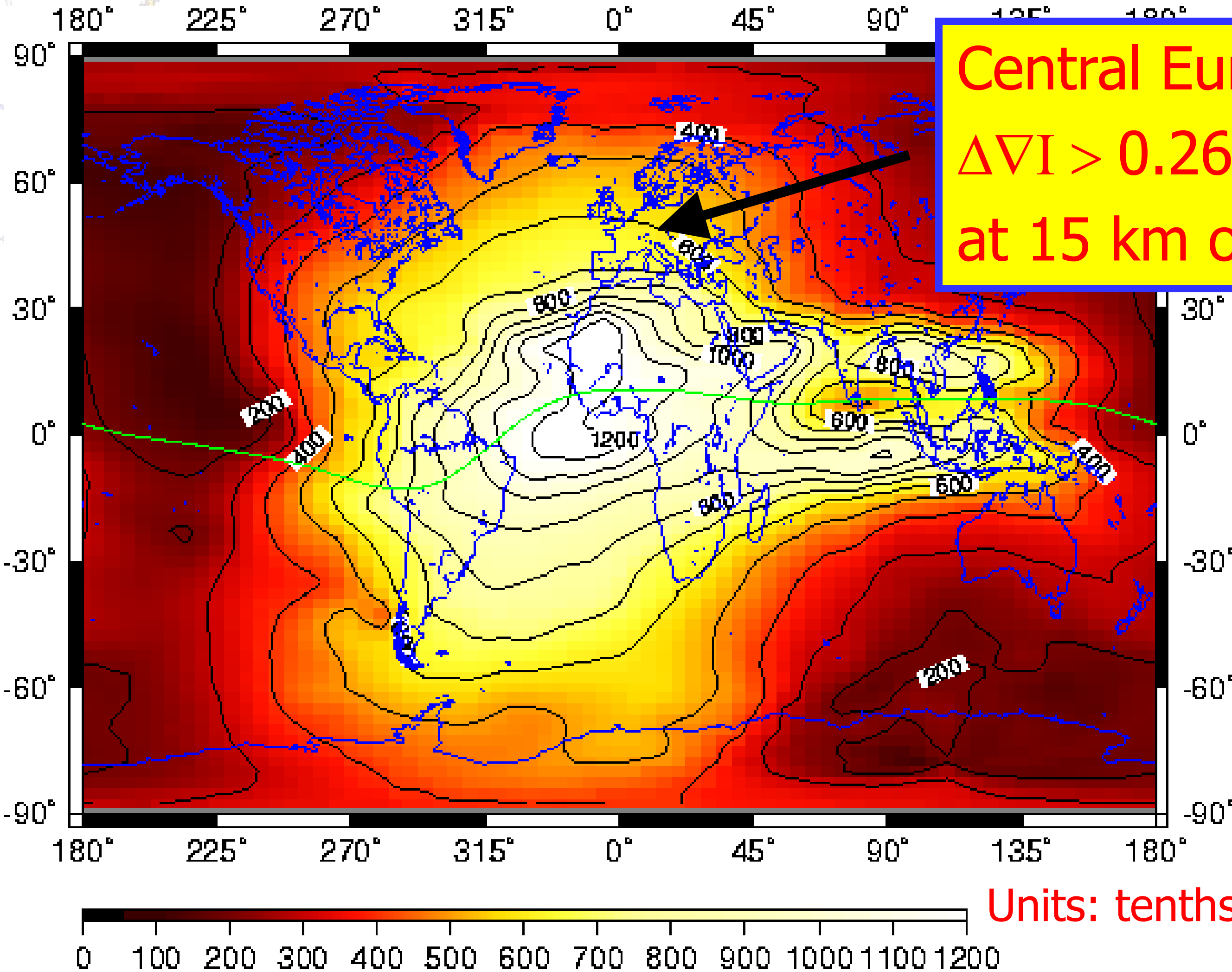

Central Europe:
$\Delta \nabla I > 0.26$TECU
at 15 km or more

Units: tenths of TECU

UNIVERSITAT POLITÈCNICA DE CATALUNYA
BARCELONATECH

IonSAT

WARTK: Combining real-time Ionospheric & Geodetic models

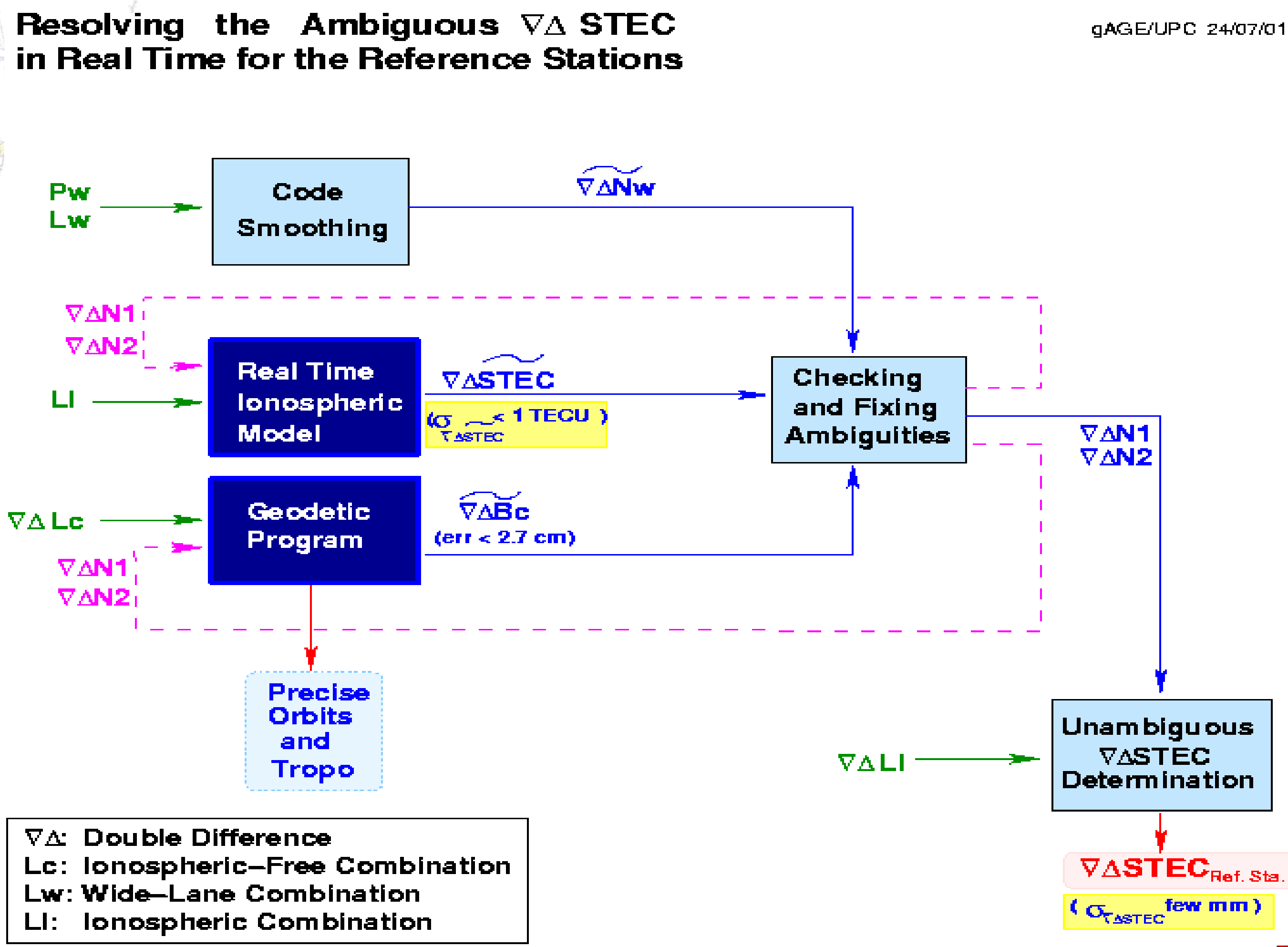

WARTK: Can be based on Wide Area GPS Networks (i.e. EGNOS)

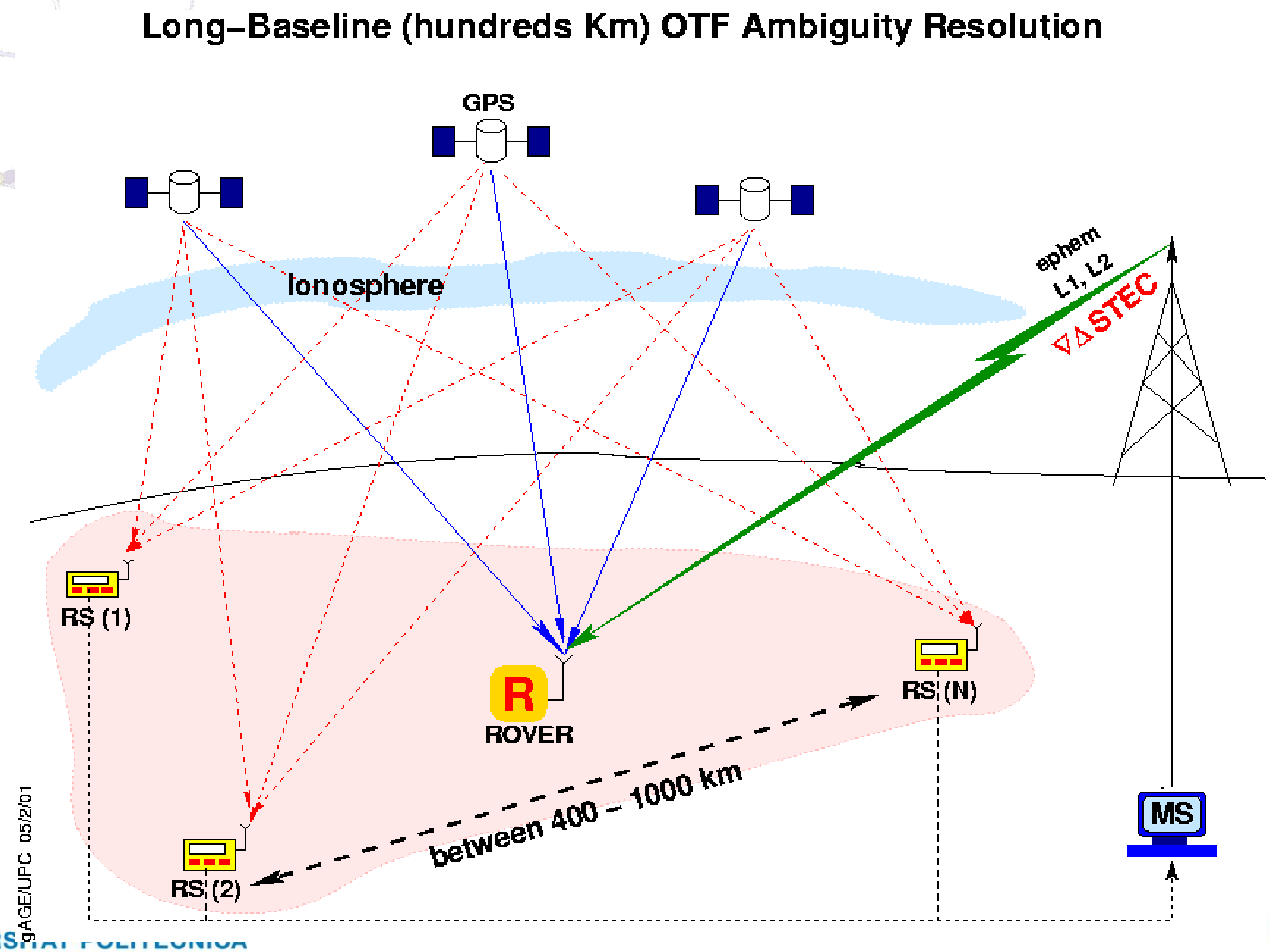

WARTK(GPS): cm-Navigation at hundreds km far

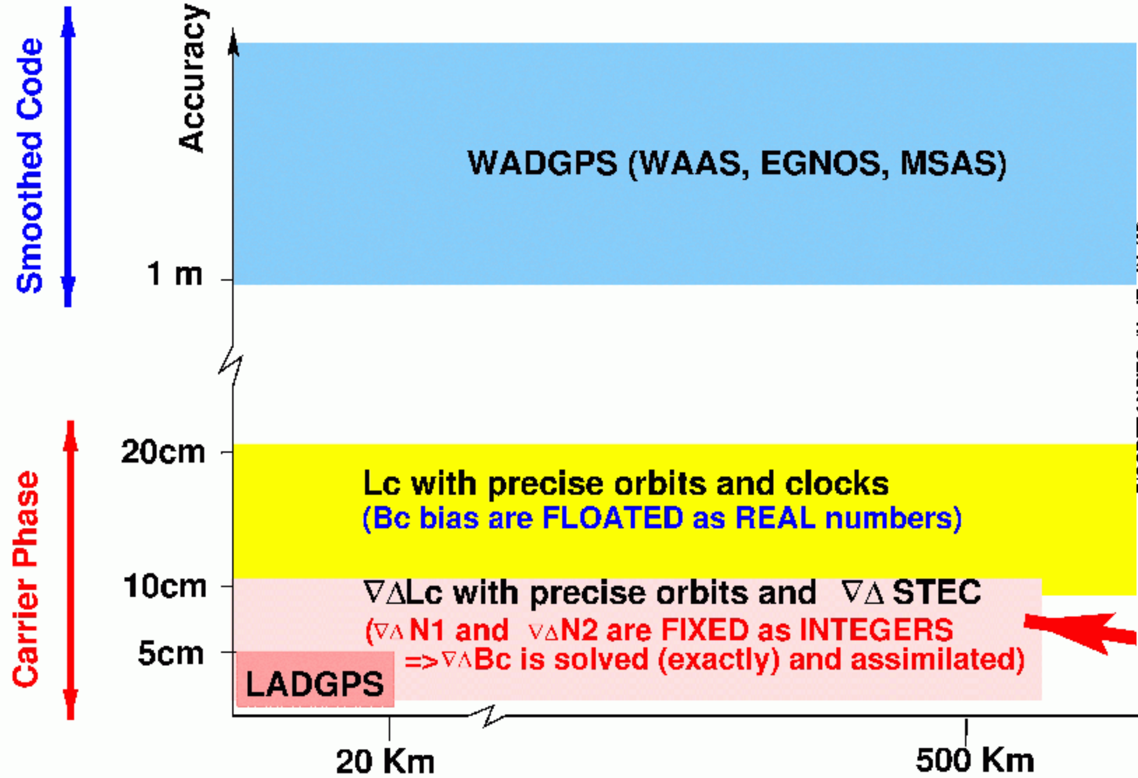

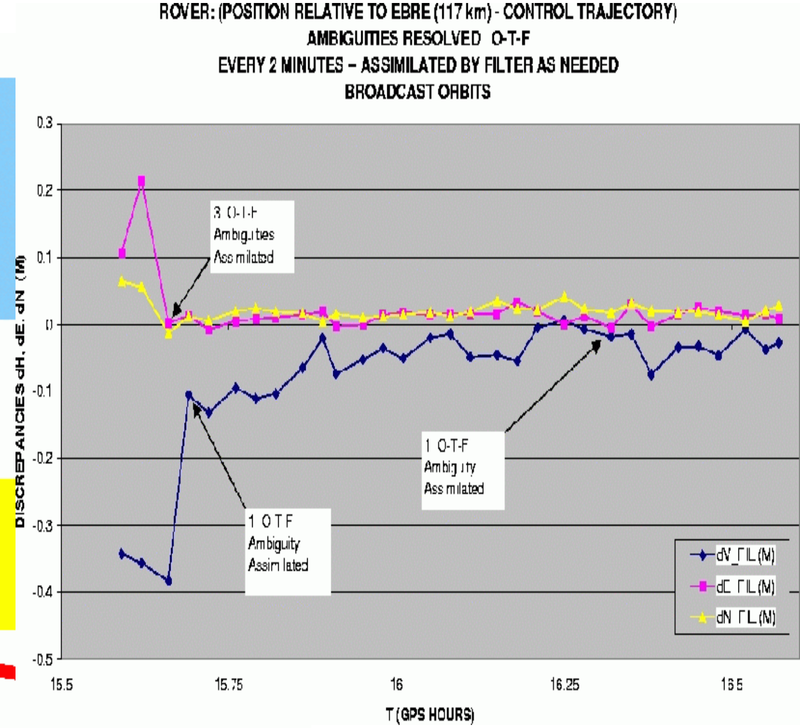

LC: Ionospheric-Free Combination

gAGE/UPC 05/2/01

UNIVERSITAT POLITÈCNICA DE CATALUNYA
BARCELONATECH

IonSAT

WARTK*: experiments & results

Experiment	Shortest baseline/km Rover/Fixed	Ionospheric Activity	Fixed Rec. Ambiguity success %	Roving Rec. Ambiguity success (%	Kind of rover	Region	Dates	Reported in
BellKin99	116 / 286	Mid.Solar Cycle & Quite	97	80-100	4x4 Car	Catalonia, NE Spain	23-03-99	Colombo et al. 99 (ION)
NWPacific1	400/900	Mid Solar Cycle & Active high lat. (Kp=6)	90-100	80	IGS Site	NWCanada-USA	03-05-98	Hernández et al. 00a, Colombo et al. 00 (GRL, PLANS)
NWPacific2	162/900	Mid-Low Solar Cycle & Irreg.	95-100	80-90	IGS Site	NWCanada-USA	28-04 to 01-05-98	Hernández et al. 00b (ION)
SolarMax1	130/500	Solar Maximum	85-95	80	IGS Site	Central Europe	19 to 22-04-00	Hernández et al. 01 (GRL)
SolarMax2	130/500	Solar Max. & Supestorm	50-95	80	IGS Site	Central Europe	12 to 15-07-00	Hernández et al. 00b (ION)
Baltic99	144/285	Travelling Iono. Disturb. (TIDs)	97	83	IGS Site	North Europe	25-08-99	Hernández et al. 01b (ION)
Equator01	1000-3000/.	Solar Max. & Equator & Very Active (Kp to 9)	90	---	IGS Sites	Central Asia to Oceania	06-03 to 02-04-01	Hernández et al. 02 (JGR)
TCARdata (simulated)	130/300	Solar Max.	100	92 (single-epoch)	Sim. car	Central Europe	17-03-00 (noon)	Hernández et al. 03a-b (IEEE TGARS, Navigation)
UNBAR01	70-115/100	Solar Max. & Strong TIDs	100	~80 (with integrity)	Car	Barcelona, NE Spain	11-06-01	This project
WARTK3 Lab.Test 1-2	178-238 /250-600	Solar Max.	100	100	1:Car 2:Air.	Iberian Peninsula	31-03-90 (ionos.)	This project
WARTK3 Lab. Test 3	416/250-600	Solar Max.	100	99	Fixed Site	Iberian Peninsula	31-03-90 (ionos.)	This project

Conclusions

• Different techniques and results summarized in this presentation show the **maturity of the GPS Ionospheric Modelling techniques in order to provide an unique view of the Ionosphere (in terms of temporal and spatial resolution) and to make feasible new applications.**

Thank you!

UNIVERSITAT POLITÈCNICA DE CATALUNYA
BARCELONATECH

IonSAT

References(1)

AGGA Validation, "Test Setup" and "User Manual", Austrian Aerospace under ESA contract No. 12782/98/NL/GD, Doc. No. OCC-TNT-0026-AAE, May 18, 2000.

Bierman, G.J., Factorization Methods for Discrete Sequential Estimation, Vol. 128 in Mathematics in Science and Engineering, Academic Press, New York, 1977.

Billitza D., International Reference Ionosphere 1990, URSI/COSPAR, NSSDC/WDC-A-R&S 90-22, 1990.

Colombo, O.L., M. Hernández-Pajares, J.M. Juan, J. Sanz and J. Talaya, Resolving carrier-phase ambiguities on-the fly, at more than 100 km from nearest site, with the help of ionospheric tomography, ION GPS'99, Nashville, USA, September 1999.

Colombo O.L., Hernández-Pajares M., Juan J.M. and Sanz J., Ionospheric Tomography Helps Resolve GPS Ambiguities On-the-Fly At Distances of Hundreds of Kilometers During High Geomagnetic Activity, Position Location and Navigation Symposium (PLANS 2000 IEEE conference), San Diego (USA), March 2000.

Hernández-Pajares M., J.M. Juan and J. Sanz, New approaches in global ionospheric determination using ground GPS data, Journal of Atmospheric and Solar Terrestrial Physics. Vol 61, 1237-1247, 1999a.

Hernández-Pajares M., J.M. Juan, J. Sanz and O.L. Colombo, Precise ionospheric determination and its application to real-time GPS ambiguity resolution, Institute of Navigation ION GPS'99, Nashville, Tennessee, USA, September 1999b.

Hernández-Pajares, M., J.M. Juan, J. Sanz and O.L. Colombo, Application of ionospheric tomography to real-time GPS carrier-phase ambiguities resolution, at scales of 400-1000 km, and with high geomagnetic activity, Geophysical Research Letters, 27, 2009-2012, 2000a.

Hernández-Pajares, M., J.M. Juan, J. Sanz, O. Colombo, H. Van der Marel, Real-time integrated water vapor determination using OTF carrier-phase ambiguity resolution in WADGPS networks, ION GPS'2000, Salt Lake City, September 2000b.

References(2)

Hernández-Pajares, M., J.M. Juan, J. Sanz, O.L. Colombo, and H. van der Marel, A new strategy for real-time Integrated Water Vapour determination in WADGPS networks, Geophysical Research Letters, 28, 3267-3270, 2001.

Hernández-Pajares, M., J.M. Juan, J. Sanz, O.L. Colombo, Tomographic modeling of GNSS ionospheric corrections: Assessment and real-time applications, ION GPS'2001, Salt Lake, USA, September 2001b.

Hernández-Pajares, M., J.M. Juan, J. Sanz, O.L. Colombo, Improving the real-time ionospheric determination from GPS sites at Very Long Distances over the Equator, Journal of Geophysical Research, in press, 2002.

Jung, J., P.Enge, B.Pervan, Optimization of Cascade Integer Resolution with Three Carrier GPS Frequencies, Proceedings of the ION-GPS 2000.

Laboratory Experiment On Carrier Phase Positioning Techniques for GNSS 2 (TCAR-Test). Technical Note "Familiarization with Test Equipment" and "Generation of Scenarios", Spectra Precision Terrasat GmbH, Germany, under ESA contract No. 12406/77/NL/DS Rider 1, Issue 1, Revision 2, Sept. 2000.

Vollath, U., S. Birnbach, H. Landau, J.M. Fraile-Ordoñez, M. Martin-Neira, Analysis of Three-Carrier Ambiguity Resolution (TCAR) Technique for Precise Relative Positioning in GNSS-2, Proceedings of the ION-GPS 1998.

Vollath, U., E. Roy, Ambiguity Resolution using Three Carriers -Performance Analysis using "Real" Data, GNSS Symposium, Seville, May 2001.